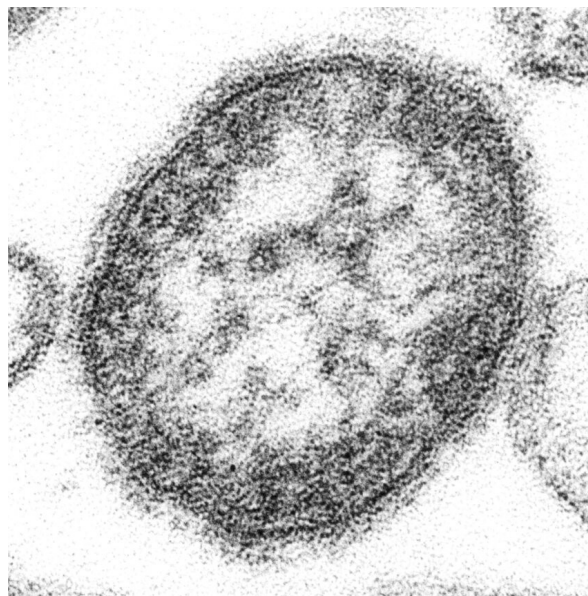


**TESIS DOCTORAL**

**DOLPHIN MORBILLIVIRUS IN STRANDED  
MARINE MAMMALS: DIAGNOSIS AND  
NEUROPATHOLOGICAL CHARACTERIZATION**



**FEDERICA GIORDA**

**DOCTORADO EN SANIDAD ANIMAL Y SEGURIDAD ALIMENTARIA  
LAS PALMAS DE GRAN CANARIA**

**JUNIO 2022**











**TESIS DOCTORAL**

**DOLPHIN MORBILLIVIRUS IN STRANDED MARINE  
MAMMALS: DIAGNOSIS AND NEUROPATHOLOGICAL  
CHARACTERIZATION**

**FEDERICA GIORDA**

**DOCTORADO EN SANIDAD ANIMAL Y SEGURIDAD  
ALIMENTARIA**

**LAS PALMAS DE GRAN CANARIA**

**JUNIO 2022**









A mi hijo Pietro,  
a mi abuelo Alfredo,  
a la belleza







## TABLA DE CONTENIDO

1. Introduction and objectives .....	1
1.1. Summary of papers .....	7
2. Scientific publications .....	11
3. Conclusions .....	75
4. Resumen .....	79
4.1. Introducción y objetivos.....	81
4.2. Publicaciones .....	86
4.3. Conclusiones .....	90
5. Reference List / Lista de Referencias .....	92
6. Acknowledgments / agradecimientos .....	101

# **1. INTRODUCTION AND OBJECTIVES**



Cetacean morbillivirus (CeMV) is a member of the genus *Morbillivirus* (*Paramyxoviridae* family, order *Mononegavirales*), consisting of a single linear molecule of negative-sense single-stranded RNA, whose genome is constituted of six transcription units that encode six structural proteins: the nucleocapsid protein (N), phosphoprotein (P), matrix protein (M), fusion glycoprotein (F), haemagglutinin glycoprotein (H) and the RNA dependent RNA polymerase (L), as well as two virulence factor proteins (C and V).

It's regarded as the natural agent with the greatest impact on cetacean health and conservation worldwide (Di Guardo and Mazzariol 2016; Zinzula et al. 2021).

Two lineages of CeMV have been described so far (Gulland et al. 2018): CeMV-1, which accounts for the well-characterized strains of the northern hemisphere, comprising dolphin morbillivirus (DMV) (Visser et al. 1993), porpoise morbillivirus (PMV) (Visser et al. 1993), pilot-whale morbillivirus (PWMV) (Taubenberger et al. 2000) and beaked-whale morbillivirus (BWMV) (West et al. 2013); and CeMV-2 for three strains more recently identified in the southern hemisphere, precisely in a Guiana dolphin (*Sotalia guianensis*) from Brazil (Groch et al. 2014), in an Indo-Pacific bottlenose dolphins (*Tursiops aduncus*) from Western Australia (Stephens et al. 2014) and, finally, in a Fraser's dolphin (*Lagenodelphis hosei*) stranded in Hawaii and described in 2021 (West et al. 2021).

CeMV has been responsible for several outbreaks and inter-epidemic lethal diseases worldwide (Van Bressemer et al. 2014). The first recognized CeMV epizootic occurred in 1987–88 on the Atlantic coast of the USA, when approximately 50% of the bottlenose dolphin (*Tursiops truncatus*) population died (Lipscomb et al. 1994).

Over the last 30 years, the virus has caused two epizootics in the Mediterranean basin, the first one reported in 1990-91 with more than 1000 striped dolphins (*Stenella coeruleoalba*) stranded (Domingo et al. 1990, 1992), and three unusual mortality events (UMEs) (2011, 2013, 2016) (Rubio-Guerri et al. 2013; Casalone et al. 2014; Pautasso et al. 2019) in addition to single disease descriptions of DMV infection along the Italian coastline reported by the C.Re.Di.Ma. in standard annual mortality rates (CReDiMa 2016, 2017, 2018, 2019, 2020).

Recent phylogenic and phylogeographic analysis (Cerutti et al. 2020) on 16 strains that circulated in the last 30 years in the Mediterranean confirmed a general well-conserved

homology among the strains, with an overall sequence identity >98%. A novel lineage of Atlantic origin, named NE-Atlantic strain because first detected in animals found stranded along the coasts of Galicia and Portugal in 2011–2013, started to replace the Mediterranean strain by late 2015 in Italian waters (Pautasso et al. 2019; Cerutti et al. 2020). The first description of the NE-Atlantic strain in the Mediterranean basin refers to a sperm whale (*Physeter macrocephalus*) found beached on the coast of Vasto (CH) in 2014 (Cerutti et al. 2020) during a mass stranding episode (Mazzariol et al. 2018). The animal may have been responsible for the transmission of the new strain in Italian waters, given the role of spillover host of this species (Jo et al. 2018) and the date of stranding recorded almost 2 years before the first description in small odontocetes inhabiting the same geographical area.

No difference in virulence and disease severity between the two strains had been confirmed to date (Zinzula et al. 2021).

From a diagnostic point of view, isolation of DMV on cell cultures is still regarded as the “gold standard” for definitive diagnosis of infection, though it remains a challenge when attempted from stranded cetaceans. Indeed, very few reports on successful virus isolation are available (Nielsen et al. 2008; Peletto et al. 2018; West et al. 2021).

Reverse transcription polymerase chain reaction (RT-PCR) followed by sequencing the PCR product is a specific and sensitive diagnostic method to get a rapid confirmation of the infection, of paramount importance to promptly confirm new ongoing outbreaks, but also to identify new strains and perform phylogenetic studies (Van Bresseem et al. 2014; Pautasso et al. 2019; Felipe-Jiménez et al. 2022).

Several protocols were developed to discriminate different *Morbillivirus* members, including both End-Point PCR (Frisk et al. 1999; Di Guardo et al. 2010; Sierra et al. 2014; Van Bresseem et al. 2014) and Real-Time PCR (Grant et al. 2009; Rubio-Guerri et al. 2013; Sacristán et al. 2015; Yang et al. 2016; Groch et al. 2020).

The majority of mentioned protocols need specific primers for each *Morbillivirus* member and are followed by sequencing of the reaction products as confirmation of the specificity. This approach requires advanced and expensive instruments and kits and also a considerable amount of time to be performed.

Histology and immunohistochemistry (IHC) should be always carried out to confirm morbillivirus infection (MI) and to obtain information on the stage of the disease. Negative antigen immunolabelling is commonly obtained in subacute-to-chronic or subclinical MI (Amude and Alfieri 2010; Van Bresseem et al. 2014). Since no homologous antibody (Ab) against any CeMV members are commercially available, two Abs prepared against other members of the genus *Morbillivirus* have been used worldwide in the IHC diagnosis. One of them is a monoclonal antibody (MoAb) against the N protein of canine distemper virus (CDV) (Giorda et al. 2017; Pintore et al. 2018; Díaz-Delgado et al. 2019; Cuvertoret-Sanz et al. 2020; Sierra et al. 2020). The other is a poly (polyclonal) Ab raised in rabbits against rinderpest virus (RPV) (Yang et al. 2006; Mazzariol et al. 2016).

Serological investigations are very useful tools for studying CeMV epidemiology, to evaluate the immune status of populations before and after an epidemic and, hopefully, to help in predicting new outbreaks (Van Bresseem et al. 2014; Profeta et al. 2015).

(CeMV)-associated pathology is superimposable to that observed in other *Morbillivirus* infected hosts, included humans (De Vries et al. 2015; da Fontoura Budaszewski and von Messling 2016), with non-suppurative meningoencephalitis and broncho-interstitial pneumonia as main pathological findings described. Furthermore, a severe and generalized lymphoid cell depletion is commonly present in the lymphoid tissues of infected animals, proving the prominent immunosuppressive role of this agent. Consequently, the individuals affected tend to develop a large number of secondary viral, bacterial, fungal, protozoan and parasitic infections (Di Guardo and Mazzariol 2016; Díaz-Delgado et al. 2017; Giorda et al. 2017; Sierra et al. 2018, 2020; Garofolo et al. 2020).

Among opportunistic protozoan infections, there is a large literature reporting *Toxoplasma gondii* in marine mammals inhabiting the Mediterranean basin (Di Guardo et al. 2010; Giorda et al. 2017; Pintore et al. 2018), but scant data are available in this geographical area for other protozoa known to affect these species in other seas (Miller et al. 2009; Gulland et al. 2018).

Neuropathological changes due to MI include demyelination, which is largely reported in both marine and terrestrial species and is commonly associated with canine and phocine distemper virus infection (Vandeveldel and Zurbriggen 2005; Duignan et al. 2014; Ulrich et al. 2014), probably due to the well documented high phylogenetic correlation between CDV and Phocine distemper virus (Duignan et al. 2014). A few descriptions of myelin changes have been reported in cetaceans affected by CeMV infections so far (Duignan et al. 1992; Domingo et al. 1995; Soto et al. 2011; Pautasso et al. 2019), in some cases confirmed through Luxol Fast Blue staining that not always proved effective in showing demyelination (Díaz-Delgado et al. 2019).

The present research was developed to broaden the available knowledge on CeMV and to design new diagnostic tools for this infectious agent. Its specific objectives were to:

- 1- Develop and provide a novel end-point PCR RFLP technique to detect, differentiate and characterize different Morbillivirus strains, easily applicable also in limited resource laboratories
- 2- Compare the diagnostic performances of the two heterologous antibodies used worldwide, anti-CDV MoAb and anti-RPV poly ab, for: positivity detection, labelling quality and neuroanatomical distribution of the staining in IHC
- 3- Deepen the immunosuppressive role of CeMV through the description of a novel secondary protozoal infection in the Mediterranean basin
- 4- Compare the two latest DMV variants circulating in the Italian waters, named “Mediterranean” and “NE-Atlantic”, in terms of neurotropic potential
- 5- Confirm myelin damage, through a specific biomarker applied in indirect immunofluorescence (IF) staining, in the brains of cetaceans affected by systemic CeMV
- 6- Characterize areas of myelinopathy, revealing cell changes and viral colonization by means of double IF staining

## 1.1. SUMMARY OF PAPERS

To achieve the aims of this PhD thesis, the following investigations, resulting in four publications indexed in the Journal of Citation Reports, were carried out:

### **Publication I:**

Reverse transcription-PCR (RT-PCR) followed by sequencing represents a sensitive and specific biomolecular tool for the diagnosis of morbilliviruses.

The majority of protocols used to detect Morbillivirus infection need specific primers for the different *Morbillivirus* species, to first amplify the target genetic portion and to sequence the reaction products, as confirmation of the specificity. This approach requires advanced and expensive instruments and kits and also a considerable amount of time to be performed.

Fourteen target frozen tissues from 4 dogs (*Canis canis*), 1 fox (*Vulpes vulpes*) and 3 striped dolphin (*Stenella coeruleoalba*) presenting evidence of morbillivirus infection were employed to develop a RT-PCR restriction fragment length polymorphism (RFLP) essay, using degenerate primers targeting a 287bp fragment of a conserved portion of the N gene, to detect, differentiate and characterize both canine distemper virus and dolphin morbillivirus, without the need of sequencing.



**Publication II:**

Confirmation and staging of morbillivirus infections rely on histology and immunohistochemistry (IHC), following molecular detection. As at the present time no specific antibodies (Abs) against DMV are available, two heterologous Abs, known to cross-react with DMV, have been used worldwide for the examinations of morbillivirus infections of cetaceans. One is a monoclonal Ab (MoAb) prepared against the N protein of canine distemper virus (CDV), whereas the other is a polyclonal Ab raised in rabbits against rinderpest virus (RPV).

Aim of this study was comparing the performance of these two Abs related to: positivity detection, labelling quality and neuroanatomical distribution of staining.

Serial sections of the target organs from ten free-ranging stranded cetaceans, previously diagnosed as being infected with DMV by PCR and/or serology, were subjected to IHC. The brain, lungs and lymph nodes of one animal were found to be positive with both Abs. From two other animals, the brain and the spleen, respectively, tested positive only with the polyclonal Ab.

In the positive brain tissues, multifocal immunostaining was observed, with similar staining location and extent, with the two antibodies tested.

**Publication III:**

CeMV is known to be an immunosuppressant agent, able to cause also opportunistic protozoan infections. Despite a large literature reporting *Toxoplasma gondii* in marine mammals inhabiting the Mediterranean basin, scant data are available in this geographical area for other protozoa of the *Sarcocystidae* family known to affect these species in other seas.

In this study we report the first description of a *Sarcocystis*-like infection in muscle tissue of dolphins from the Mediterranean basin along with the first report of *Sarcocystis*-like tissue cysts in the brain of stranded cetaceans. These two animals presented a subclinical and a systemic CeMV co-infection, respectively. The unknown organisms were genetically similar to *Sarcocystis* species infecting the *Bovidae* family.

**Publication IV:**

A novel dolphin morbillivirus lineage of Atlantic origin circulating in Italian waters replaced the previous Mediterranean strain in late 2015; however, differences in virulence and pathogenesis between the two strains have not yet been documented.

There is abundant literature reporting demyelination in dogs and pinnipeds affected by morbillivirus infection, but myelinopathy is poorly investigated in stranded cetaceans affected with the virus. Also, the neuropathogenesis of cetacean morbillivirus infection has not been fully clarified, leaving questions on cell tropism unanswered.

This study describes neuropathological findings in the brain tissue of 31 cetaceans found stranded along the Italian coastline and positive for DMV infection on molecular testing. Cell changes in the areas of myelinopathy were revealed by double indirect immunofluorescence. The most frequent DMV-associated lesions were astro-microgliosis, neuronal necrosis, spongiosis, malacia, and non-suppurative meningoencephalitis. Myelin reduction and areas of demyelination were revealed by means of a specific myelin biomarker. Morbilliviral antigen immunolabelling was mainly observed in neurons and microglial cells, in association with a marked activation of microglia and astrocytes. Molecular and immunohistochemical analysis suggested a higher neurotropic affinity of the novel circulating strain.

## **2. SCIENTIFIC PUBLICATIONS**





ELSEVIER

Contents lists available at [ScienceDirect](#)

## Journal of Virological Methods

journal homepage: [www.elsevier.com/locate/jviromet](http://www.elsevier.com/locate/jviromet)



### Corrigendum

## Corrigendum to “Detection of morbillivirus infection by RT-PCR RFLP analysis in cetaceans and carnivores” [Journal of Virological Methods 247 (2017) 22–27]



Federica Verna<sup>a,1</sup>, Federica Giorda<sup>a,b,1</sup>, Ilaria Miceli<sup>a</sup>, Giovanna Rizzo<sup>a</sup>, Alessandra Pautasso<sup>a</sup>, Angelo Romano<sup>a</sup>, Barbara Iulini<sup>a</sup>, Maria Domenica Pintore<sup>a</sup>, Walter Mignone<sup>c</sup>, Carla Grattarola<sup>a</sup>, Elena Bozzetta<sup>a</sup>, Katia Varello<sup>a</sup>, Alessandro Dondo<sup>a</sup>, Cristina Casalone<sup>a</sup>, Maria Goria<sup>a,\*</sup>

<sup>a</sup> Istituto Zooprofilattico Sperimentale del Piemonte, Liguria e Valle d'Aosta, Turin, Italy

<sup>b</sup> Institute for Animal Health and Food Security (IUSA), Veterinary School, University of Las Palmas de Gran Canaria, Canary Islands, Spain

<sup>c</sup> Istituto Zooprofilattico Sperimentale del Piemonte, Liguria e Valle d'Aosta, Imperia, Italy

The authors regret that some errors in their affiliations were published in the above article. The correct affiliation is now corrected in this corrigendum.

The authors would like to apologise for any inconvenience caused.  
DOI of original article: <http://dx.doi.org/10.1016/j.jviromet.2017.05.009>

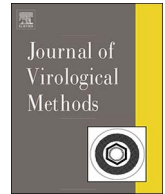
DOI of original article: <https://doi.org/10.1016/j.jviromet.2017.05.009>

\* Corresponding author.

<sup>1</sup> These authors have equally contributed to this work.

E-mail address: [maria.goria@izsto.it](mailto:maria.goria@izsto.it) (M. Goria).

<https://doi.org/10.1016/j.jviromet.2018.10.012>



## Detection of morbillivirus infection by RT-PCR RFLP analysis in cetaceans and carnivores



Federica Verna<sup>a,1</sup>, Federica Giorda<sup>a,1</sup>, Ilaria Miceli<sup>a</sup>, Giovanna Rizzo<sup>a</sup>, Alessandra Pautasso<sup>a</sup>, Angelo Romano<sup>a</sup>, Barbara Iulini<sup>a</sup>, Maria Domenica Pintore<sup>a</sup>, Walter Mignone<sup>b</sup>, Carla Grattarola<sup>a</sup>, Elena Bozzetta<sup>a</sup>, Katia Varello<sup>a</sup>, Alessandro Dondo<sup>a</sup>, Cristina Casalone<sup>a</sup>, Maria Goria<sup>a,\*</sup>

<sup>a</sup> Istituto Zooprofilattico Sperimentale del Piemonte, Liguria e Valle d'Aosta, Turin, Italy

<sup>b</sup> Istituto Zooprofilattico Sperimentale del Piemonte, Liguria e Valle d'Aosta, Imperia, Italy

### ARTICLE INFO

#### Keywords:

Dolphin morbillivirus  
Canine distemper virus  
RT-PCR  
RFLP  
Carnivore  
Cetacean

### ABSTRACT

Morbillivirus genus comprises several members related to specific hosts, such as canine distemper virus (CDV) and cetacean morbillivirus (CeMV) in which the dolphin morbillivirus (DMV) is included. Both CDV and DMV are able to cause serious outbreak associated with high morbidity and mortality representing an important conservation threat for terrestrial and aquatic mammalian species. This paper describes a new RT-PCR RFLP technique based on a RT-PCR with degenerate primers targeting a 287 bp fragment located on the conserved N terminus of the morbillivirus NP gene, followed by MseI RFLP, in order both to confirm the detection of the virus and to distinguish DMV from CDV. Both carnivores and cetaceans tissues (brain, lung and lymph node) presenting evidence of morbillivirus infection (MI) were analyzed. RT-PCR positive samples were typed by RFLP analysis and then sequenced to confirm the RFLP results. This method was applied during the last morbillivirus cetacean die-off occurred in the Mediterranean basin in 2013, when there was the urgent need of a rapid and economic method to investigate among causes of death on stranded cetaceans. This new technique has proved to be a valuable, reliable, simple and relatively inexpensive diagnostic tool easily applicable also in limited-resource laboratories.

### 1. Introduction

Morbillivirus genus (subfamily Paramyxovirinae, family Paramyxoviridae, order Mononegavirales) comprises several members related to specific hosts: measles virus (MeV), canine distemper virus (CDV), rinderpest virus (RPV), peste-des-petits-ruminants virus (PPRV), phocine distemper virus (PDV) and cetacean morbillivirus (CeMV) (De Vries et al., 2015), which includes the porpoise morbillivirus (PMV), the dolphin morbillivirus (DMV), the pilot whale morbillivirus (PMMV) (Van Bressems et al., 2014), the Longman's beaked whale morbillivirus (West et al., 2013) and 2 novel CeMV sequences in the Southern Hemisphere (Groch et al., 2014; Stephens et al., 2014). In general, these viruses are known to be highly infectious and immunosuppressant, to spread *via* respiratory route and to be able to cause serious outbreaks associated with high morbidity and mortality (De Vries et al., 2015). Since in the last 25 years at least 10 dramatic morbilliviral epidemics have occurred among free ranging pinniped and cetacean species and population worldwide (Di Guardo and Mazzariol, 2014). Similarly, CDV has global distribution and high pathogenic potential for several

domestic and wild carnivores (Origi et al., 2012) and it represents an important conservation threat, having contributing to the population decline of numerous wild mammalian species. (Murray et al., 1999; Kennedy et al., 2000). Most morbilliviruses are lymphotropic and epitheliotropic and central nervous system (CNS) complications are common both for CDV and CeMV infections (Delpout et al., 2014; Van Bressems et al., 2014).

Viral isolation and identification are considered the “gold standard” for definitive diagnosis of morbilliviruses (Van Bressems et al., 2014), but this is often a challenging issue given the poor preservation of virus-targeted tissues when dealing with wild animals.

Currently, to overcome these limitations, reverse transcription-PCR (RT-PCR) followed by sequencing represents a sensitive and specific biomolecular tool for the diagnosis of morbilliviruses. Several protocols, have been developed by using different pairs of primers for differentiating between species of viruses including both End-Point PCR (Barrett et al., 1993; Di Guardo et al., 2010; Frisk et al., 1999; Sierra et al., 2014; Van Bressems et al., 2014) and Real-Time PCR (Grant et al., 2009; Rubio-Guerri et al., 2013). Recently, two specific protocols

\* Corresponding author.

E-mail address: [maria.goria@izsto.it](mailto:maria.goria@izsto.it) (M. Goria).

<sup>1</sup> These authors have equally contributed to this work.

for the diagnosis of CeMV, in which detection and genotyping are both based on melting temperature with no sequencing needed, have been published (Sacristán et al. 2015; Yang et al., 2016).

The majority of mentioned protocols need specific primers for the different *Morbillivirus* species to first amplify target genetic portion and to sequence reaction products as confirmation of the specificity. This approach requires advanced and expensive instruments and kits and also a considerable amount of time to be performed.

A PCR analysis designed with degenerate primers promises to be more sensitive than a PCR with specific primers due to the increased probability of finding unknown divergent variants of a sequence family (Iserte et al., 2013).

Moreover, a PCR-restriction fragment length polymorphism (RFLP)-based analysis is a popular cost effective assay useful for assuring specificity and genotyping as well. Setting up of a PCR RFLP test requires several separate steps, including design of primers, identification of an appropriate restriction enzyme, optimization of amplification conditions and enzyme restriction analysis of amplified products resolving restriction fragments by mean of gel electrophoresis. Generally, RFLP PCR analysis has been applied for the detection of intraspecies as well as interspecies variation and it can be used to identify and/or characterize different virus genotypes saving additional sequencing procedures (Botelho-Souza et al., 2015; Kawachi et al., 2015).

This paper aims at describing the development of an improved RT-PCR RFLP assay to detect, differentiate and characterize both CDV and DMV as rapid and basic detection pathway, easily applicable also in limited-resource laboratories. This method has proved to be a valuable tool during the last morbillivirus cetacean die-off occurred in the Mediterranean basin in 2013 (Casalone et al., 2014), when there was the urgent need to have available a rapid, effective and economic method to investigate among causes of death on stranded cetaceans.

## 2. Methods

### 2.1. Tissue sampling

In order to develop an RT-PCR RFLP protocol for morbillivirus detection to be applied both to carnivores and cetaceans, 14 target frozen tissues (brain, lung and lymph node) from 5 terrestrial (4 dogs-*Canis canis*, and 1 fox-*Vulpes vulpes*) and 3 marine mammals (striped dolphin-*Stenella coeruleoalba*) presenting classical associated microscopic lesions and/or immunohistochemistry (IHC) (Di Guardo et al., 2010; Mazzariol et al., 2012) and/or immunofluorescence (IF) (Caruso et al., 2014) evidence of morbillivirus infection (MI) were selected. In addition a panel of 5 tissues, sampled from 1 *C. canis*, 1 *V. vulpes* and 1 *S. coeruleoalba*, all negative at the aforementioned analysis and with no lesions suggestive of MI, were also used as negative process control. RT-PCR positive samples were typed by RFLP analysis and then sequenced to confirm the RFLP results (Table 1).

Later, the RT-PCR followed by RFLP (without the sequencing confirmation) was routinely carried out on 33 tissues belonging to 15 cetaceans (13 *S. coeruleoalba*, 1 long-finned pilot whale-*Globicephala melas* and 1 bottlenose dolphin-*Tursiops truncatus*, included tissues from cetaceans died during the last Mediterranean morbillivirus epidemic in 2013), 1 *C. canis* and 6 *V. vulpes*, naturally died in the period 2012–2015 and submitted for necropsy at the Istituto Zooprofilattico Sperimentale del Piemonte, Liguria e Valle d'Aosta. All the aforementioned animals had been regarded as suspected of MI on the basis of IHC and/or IF and/or microscopic evidence suggestive of virus infection (Table 2).

### 2.2. Molecular analyses

For total RNA extraction, tissue samples from different areas of the same organ were pooled (30–50 mg) and homogenized using the

TissueLyser II (QIAGEN) by high speed shaking in Eppendorf tubes with stainless steel beads (5 mm diameter, QIAGEN). Homogenates were centrifuged at 14,000 rpm for 3 min to remove the suspended solids, without removing beads. Supernatants were submitted to RNA extraction with AllPrep DNA/RNA Mini kit (QIAGEN), according to the manufacturer's instructions.

For each sample, RNA was eluted from the QIAGEN columns in a final volume of 100 µl of elution buffer and was stored at –80 °C until analyzed.

A RT-PCR protocol was developed to detect a 287 bp sequence of a highly-conserved region of the CDV nucleoprotein (NP) (Frisks et al., 1999), which shows great homology with slight differences among morbilliviruses (Diallo et al., 1994; Rima et al., 1995; Rozenblatt et al., 1985; Sidhu et al., 1993).

Considering the polymorphisms of the NP gene in carnivores and cetacean species, Frisk's primers were redesigned through an *in silico* analysis. The new primers MvF (5'-ACAGGATTGCKGAGGACCTAT-3') and MvR (5'-VARGATAACCATGTACGGTGC-3') were degenerated in position 779 (forward primer) and 1055 and 1053 (reverse primer) respectively.

Reverse transcription and amplification were simultaneously performed in a RT-PCR method using the QIAGEN OneStep RT-PCR Kit (Qiagen) on all samples listed in Tables 1 and 2.

The reaction mixture consisted of a total volume of 50 µl containing: 10 µl of 5X buffer (final MgCl<sub>2</sub> concentration 2.5 mM), 2 µl of dNTP Mix (400 µM of each dNTP), 0.2 µM of the appropriate forward and reverse primers, 2 µl of enzyme mix (containing Omniscript™ and Sensiscript™ Reverse Transcriptases and HotStarTaq™ DNA polymerase), 30 µl of RNase-free water and 5 µl of template RNA. The reaction was performed in a 9700GeneAmp PCR System (ABI) with the following RT-PCR conditions: 30 min at 50 °C; 15 min at 95 °C; 40 cycles of 30 s at 95 °C, 30 s at 59.5 °C, 1 min at 72 °C; 10 min at 72 °C.

The amplification products were analyzed by electrophoresis, in a GelRed (Biotium) staining 2% agarose gel, visualized under UV light transillumination (Gel-Doc UV transilluminator system Bio-Rad) and then identified by their molecular weights.

The NP gene segment was analyzed *in silico* to select an appropriate enzyme to confirm specificity of PCR products. *In silico* analysis were performed by using on line tools NEB cutter V2.0 (<http://tools.neb.com/NEBcutter2/>; Vincze et al., 2003), on both complete genome sequences available from GenBank (Table 3) and sequences obtained on field samples and DNA sequences were cut *in silico* with *MseI* enzyme to generate restriction fragments. This allowed to identify that TTAA sites located into the 287 bp NP gene fragment, cleaved by the restriction enzyme *MseI*, are useful not only to PCR specificity confirmation, but also to differentiate DMV from CDV and to characterize differences in DMV genotypes and CDV genotypes.

Then *MseI* restriction enzyme was selected and used according to the manufacturer's instructions. The digested DNA was resolved by electrophoresis through a 3% agarose gel and was visualized after staining with GelRed (Biotium).

Following restriction analysis, to further confirm specificity, DMV and CDV RT-PCR amplicons were purified and sequenced by using Big Dye Terminator Sequence Kit (version 3.1, Applied Biosystems) and 3500 DNA Analyzer (Applied Biosystems).

Chromatograms were manually evaluated and consensus sequences were generated using BioEdit software (version 7.0.9.0, Hall, 1999) to perform a basic local alignment search tool (BLAST) in the GenBank library.

## 3. Results

The results of the RT-PCR RFLP detection protocol applied on selected field samples to develop the method are shown in Table 1. The NP gene region specific amplification products were demonstrated in all the 14 samples, with bands corresponding to the expected molecular



**Table 1**  
Reference samples applied to RT-PCR RFLP assay setting.

Animal code	Species	Tissue sample	Microscopic lesions	IHC	IF	RT-PCR	MseI RFLP
CC#1	<i>Canis canis</i>	Brain	+	+	+	+	CDV, domestic carnivore genotype
		Lung	+	n.p.	n.p.	+	CDV, domestic carnivore genotype
		Lymph node	+	n.p.	n.p.	+	CDV, domestic carnivore genotype
CC#2	<i>Canis canis</i>	Brain	+	+	+	CDV, domestic carnivore genotype	
CC#3	<i>Canis canis</i>	Brain	+	+	+	CDV, domestic carnivore genotype	
CC#4	<i>Canis canis</i>	Lung	+	n.p.	n.p.	+	CDV, domestic carnivore genotype
		Brain	+	+	+	+	CDV, domestic carnivore genotype
VV#1	<i>Vulpes vulpes</i>	Brain	–	+	+	+	CDV, wild carnivore genotype
SC#1	<i>Stenella coeruleoalba</i>	Brain	+	+	n.p.	+	DMV, Mediterranean genotype
		Lung	+	n.p.	n.p.	+	DMV, Mediterranean genotype
SC#2	<i>Stenella coeruleoalba</i>	Brain	–	+	n.p.	+	DMV, Mediterranean genotype
		Lung	+	n.p.	n.p.	+	DMV, Mediterranean genotype
SC#3	<i>Stenella coeruleoalba</i>	Brain	–	+	n.p.	+	DMV, Mediterranean genotype
CC#5	<i>Canis canis</i>	Brain	–	n.p.	–	–	n.a.
		Lung	–	n.p.	–	–	n.a.
VV#2	<i>Vulpes vulpes</i>	Brain	–	–	–	–	n.a.
		Lung	–	n.p.	n.p.	–	n.a.
SC#4	<i>Stenella coeruleoalba</i>	Brain	–	–	n.p.	–	n.a.

–: Negative sample; +: Positive sample; n.p. not performed; n.a. = not applicable.

weight of 287 bp (Fig. 1). *MseI* enzyme digestion of specific amplicons confirmed *in silico* analysis generating respectively: 2 fragments (217 and 70 bp, dog pattern) on the suspected CDV dog samples, 4 fragments (105 bp, 70–67 bp and 45 bp) on the suspected DMV samples, and 3 fragment (150 bp and 70–67 bp, fox pattern) on the suspected CDV/DMV genotypes. Results showed in Table 3 demonstrated that the

enzyme restricted in the same way all CDV genomes from different wild animals and differentiated them respect to those from domestic animals and DMV from dolphins.

Moreover, *in silico* analysis showed that *MseI* restriction analysis potentially allowed to reveal and to discriminate among different DMV genotypes, i.e. DMV from Mediterranean Sea cetaceans (Bellière et al., 2011) and DMV reported from North Sea cetaceans (Wohlsein et al.,

**Table 2**  
Field samples submitted to Morbillivirus NP gene RT-PCR RFLP protocol.

Animal code.	Species.	Year of death.	Tissue sample.	Microscopic lesions.	IHC.	IF.	RT-PCR.	MseI RFLP.
.CC#6	<i>Canis canis</i> .	2012	Brain.	+	+	–	+	CDV, domestic carnivore genotype.
			Lung	+	n.p.	n.p.	–	n.a.
VV#3	<i>Vulpes vulpes</i>	2014	Brain	–	+	–	+	CDV, wild carnivore genotype
VV#4	<i>Vulpes vulpes</i>	2014	Brain	–	+	–	+	CDV wild carnivore genotype
VV#5	<i>Vulpes vulpes</i>	2014	Brain	–	n.p.	+	+	CDV, wild carnivore genotype
VV#6	<i>Vulpes vulpes</i>	2014	Brain	+	n.p.	–	+	CDV, wild carnivore genotype
VV#7	<i>Vulpes vulpes</i>	2014	Brain	+	n.p.	–	+	CDV, wild carnivore genotype
VV#8	<i>Vulpes vulpes</i>	2014	Brain	+	n.p.	–	+	CDV, wild carnivore genotype
VV#9	<i>Vulpes vulpes</i>	2014	Brain	+	n.p.	–	–	n.a.
VV#10	<i>Vulpes vulpes</i>	2014	Brain	+	n.p.	–	+	CDV, wild carnivore genotype
VV#11	<i>Vulpes vulpes</i>	2014	Brain	+	n.p.	–	+	CDV, wild carnivore genotype
SC#5	<i>Stenella coeruleoalba</i>	2012	Brain	+	–	n.p.	+	DMV, Mediterranean genotype
			Lung	+	–	n.p.	–	n.a.
SC#6	<i>Stenella coeruleoalba</i>	2013	Brain	+	–	n.p.	–	n.a.
			Lung	+	n.p.	n.p.	+	DMV, Mediterranean genotype
SC#7	<i>Stenella coeruleoalba</i>	2013	Brain	+	n.p.	n.p.	+	DMV, Mediterranean genotype
SC#8	<i>Stenella coeruleoalba</i>	2013	Brain	+	n.p.	n.p.	+	DMV, Mediterranean genotype
SC#9	<i>Stenella coeruleoalba</i>	2013	Lung	+	n.p.	n.p.	+	DMV, Mediterranean genotype
SC#10	<i>Stenella coeruleoalba</i>	2013	Spleen	+	n.p.	n.p.	+	DMV, Mediterranean genotype
SC#11	<i>Stenella coeruleoalba</i>	2013	Brain	–	+	n.p.	+	DMV, Mediterranean genotype
SC#12	<i>Stenella coeruleoalba</i>	2013	Spleen	+	n.p.	n.p.	+	DMV, Mediterranean genotype
SC#13	<i>Stenella coeruleoalba</i>	2013	Brain	+	n.p.	n.p.	+	DMV, Mediterranean genotype
			Lung	+	n.p.	n.p.	+	DMV, Mediterranean genotype
SC#14	<i>Stenella coeruleoalba</i>	2013	Brain	+	–	n.p.	+	DMV, Mediterranean genotype
SC#15	<i>Stenella coeruleoalba</i>	2013	Lung	+	n.p.	n.p.	+	DMV, Mediterranean genotype
SC#16	<i>Stenella coeruleoalba</i>	2014	Brain	+	–	n.p.	–	n.a.
SC#17	<i>Stenella coeruleoalba</i>	2015	Brain	+	–	n.p.	+	DMV, Mediterranean genotype
			Lung	+	–	n.p.	–	n.a.
SC#18	<i>Stenella coeruleoalba</i>	2015	Brain	+	–	n.p.	–	n.a.
			Lung	+	–	n.p.	+	DMV, Mediterranean genotype
SC#19	<i>Stenella coeruleoalba</i>	2015	Brain	+	–	n.p.	–	n.a.
GM#1	<i>Globicephala melas</i>	2013	Brain	+	–	n.p.	+	DMV, Mediterranean genotype
TT#1	<i>Tursiops truncatus</i>	2013	Brain	+	–	n.p.	+	DMV, Mediterranean genotype

–: Negative sample; +: Positive sample; n.p. not performed; n.a. = not applicable.

**Table 3**  
Morbillivirus sequences (complete genome of 15690 bp, in NCBI GenBank) included in in silico RFLP analysis by *MseI* on 287 bp fragment NP gene. <sup>(1)</sup> Genome of 15559 bp.

Origin	Source	Accession Number/ (year of submission)	<i>MseI</i> RFLP profile on 287 bp fragment NP gene	
			Fragment Length	Genotype
Raccoon Dog	CDV SY isolate	KJ466106/ (2014)	2 clivage sites: 150 bp 67 bp 70 bp	Wild
Giant Panda	CDV isolate/SX/ 2014	KP793921/ (2016)	2 clivage sites: 150 bp 67 bp 70 bp	Wild
Fox	CDV599/2016 isolate, partial genome <sup>(1)</sup>	KX545421/ (2016)	2 clivage sites: 150 bp 67 bp 70 bp	Wild
Wild dog	CDV isolate 171391-513	KU578253/ (2016)	2 clivage sites: 150 bp 67 bp 70 bp	Wild
Golden jackal	CDV isolate SE/2011	KU578254/ (2016)	2 clivage sites: 150 bp 67 bp 70 bp	Wild
Ferret	CDV strain 5804	AY386315/ (2003)	2 clivage sites: 150 bp 67 bp 70 bp	Wild
Dog	CDV isolate CDV2784/2013	KF914669/ (2014)	1 clivage site: 217 bp 70 bp	Dog
Striped dolphin	Dolphin morbillivirus isolate DMV_Sc/2007, partial coding sequence	HQ829973/ (2011)	3 clivage sites: 105 bp 70 bp 67 bp 45 bp	DMV (Mediterranean Sea)
White-beaked dolphin	Dolphin morbillivirus isolate DE/2007, N gene, partial coding sequence	EF469546/ (2016)	2 clivage sites: 172 bp 70 bp 45 bp	DMV (North Sea)

2007): this NP gene segment showed in facts only two restriction enzyme cleavage sites for TTAA as drawn in Fig. 3.

Amplicons sequences from samples showing a digestion pattern referring to DMV, were aligned, with an identity equal to 99%, to DMV NP gene sequence (accession nr: HQ829973) in NCBI-BLASTN Genbank and the sequences of amplicons showing a digestion pattern referring to CDV were all respectively aligned to CDV NP gene sequence, with an identity equal to 99%, for dog samples (accession nr. AF014953, dog genotype) and for fox samples (accession nr. KX545421 for fox genotype).

The results of RT-PCR RFLP analyses obtained from 33 field samples suspected of MI on the basis of IHC and/or IF and/or microscopic evidence, are shown in Table 2. Twenty-five samples were positive to RT-PCR and all generated restriction patterns corresponding to the expected one with no restriction profile variation. Eight samples, selected on the basis of microscopic lesions, were negative by RT-PCR.

Taking into account all the results of this paper (Tables 1 and 2) among the tissues suspected of morbillivirus (i.e. excluding the negative

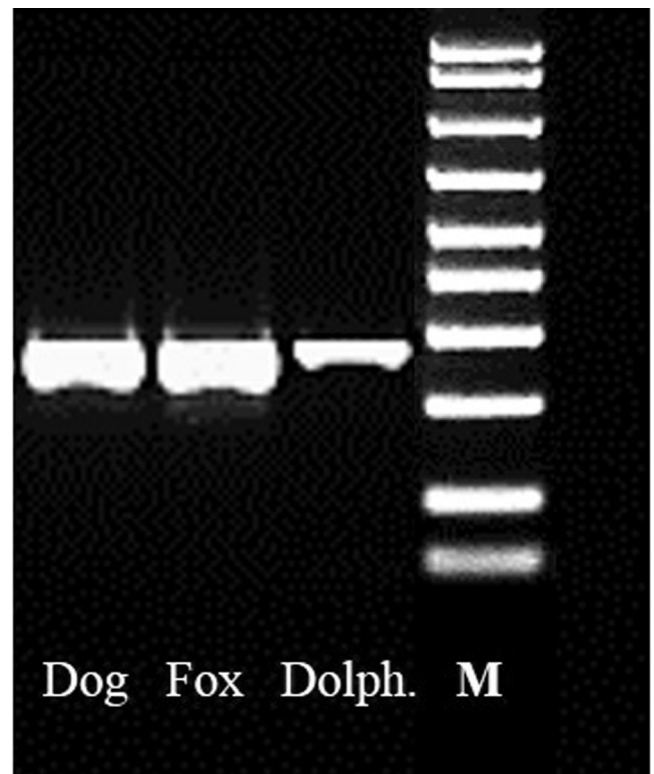


Fig. 1. NP gene region RT-PCR amplification products: specific bands at the expected molecular weight of 287 bp in samples from dog (lane 1), fox (lane 2) and dolphin (lane 3) with suspected MI; [M: 50–2000 bp Ladder, Biorad].

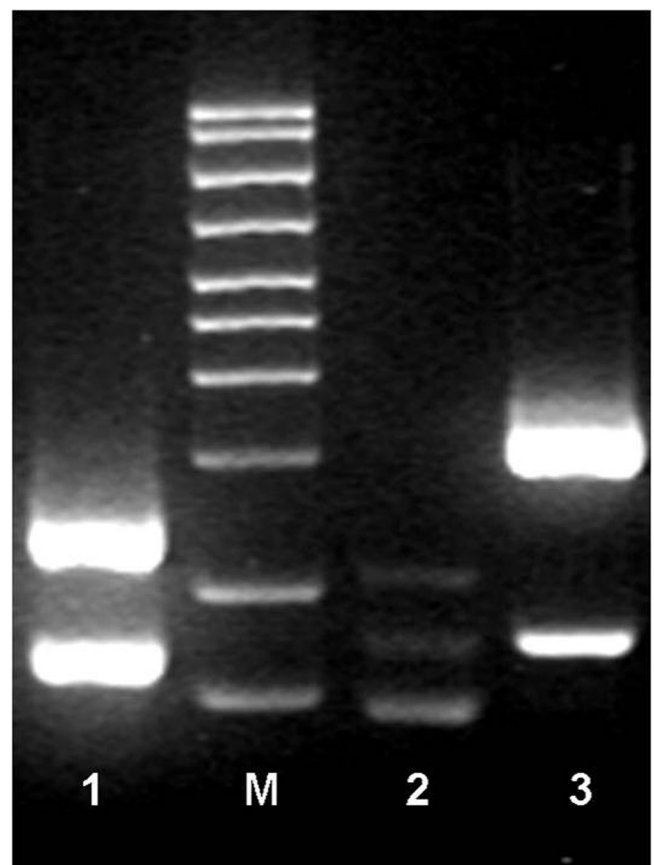


Fig. 2. RFLP patterns by enzymatic digestion with *MseI* of amplicons generated by RT-PCR of Morbillivirus NP gene: CDV wild carnivore genotype (lane 1); DMV Mediterranean sea (lane 2) CDV domestic carnivore genotype (lane 3); [M: 50–2000 bp Ladder, Biorad].

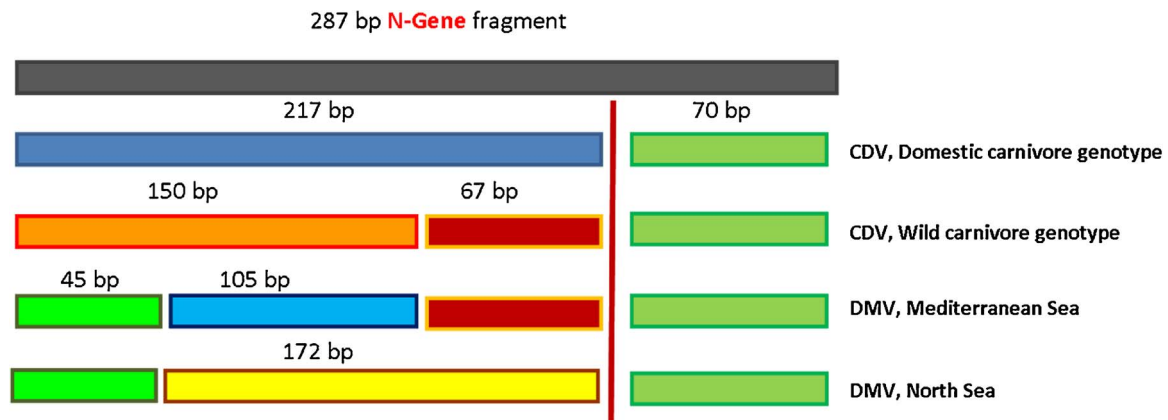


Fig. 3. *In silico* restriction analysis for the highly conserved region of NP gene belonging to *Morbillivirus* genus.

controls), by comparing PCR and IHC, 18 out of 26 tissues tested by both the methods resulted positive in PCR, while 12 in IHC. Comparing PCR and IF, 14 out of 17 were positive in PCR and 6 in IF.

#### 4. Discussion and conclusions

The RT-PCR RFLP method described has proved to be a valuable, reliable, simple and relatively inexpensive diagnostic tool for the diagnosis and identification of several genotypes of morbillivirus.

In brief, the protocol is based on a RT-PCR targeting a fragment of 287 bp located on the conserved N *terminus* of the morbillivirus NP gene, followed by *MseI* RFLP, in order both to confirm the detection of the virus and to distinguish DMV genotypes from CDV genotypes. In addition, this protocol could be particularly useful in routine diagnostic laboratories allowing to discriminate between different genotypes of DMV and CDV without sequencing, providing new insights into the epidemiology of morbillivirus in both terrestrial and aquatic animals.

The use of degenerate primers leads to amplify with equal selectiveness the same 287 bp fragment both in CDV and DMV and the resulting fragments restriction allows to define the specific genotype without sequencing.

During the protocol development, different specific restriction patterns were observed, confirmed by sequencing, and all patterns were re-obtained without variation during the following routine analysis.

The DMV genotype and CDV fox genotype restriction patterns on agarose gel could apparently be in discordance with the *in silico* analysis, that respectively predicted 4 fragments (105 bp, 70–67 bp and 45 bp) in DMV genotype and 3 fragments (150 bp and 70–67 bp) in CDV fox genotype: this is due to the low resolution power of agarose gels to separate segments that only differ in length for 3 bp: the two smallest fragments of 67 bp and 70 bp are detectable just as a single small fragment at approximately 70 bp. This deficiency is primarily caused by the same speed diffusion rate of small molecules in the weak agarose matrix, even when high agarose concentrations (e.g., 3–4%) are employed (Sanderson et al., 2014). Moreover, during the RT-PCR RFLP developing procedure the sequence analysis of each 287 bp amplicons confirms the presence of all cleavage sites.

Evaluated this, no doubts are raised in the interpretation of the results obtained.

Considering that a reliable diagnostic approach should be based on RT-PCR for a rapid confirmation of MI and the use of IHC or IF concurrently to confirm the molecular diagnosis and further exploring the pathogenesis of the infection (Van Bressen et al., 2014), we compared results obtained by PCR, IHC and IF. The RT-PCR RFLP method allowed to detect more positive tissues with respect to IHC or IF. This is not surprising, considering the multifocal pattern of MI.

Indeed, samples used for PCR analysis derived from homogenized tissue from different areas of the same organ/tissue pooled together, increasing the probability of virus detection, whereas in IHC or IF only some organs' sections were analyzed.

The sampling could thus be considered the focus point of these discrepancies, confirming the need of performing a multiple sampling in case of suspected MI.

Eight samples showed negative PCR results despite of microscopic lesions typical of viral infection. The pathological features observed could be referred to viral agents other than Morbillivirus.

Important advantages of the RT-PCR RFLP technique include its low cost, the minimal hands-on time required and the possibility of being performed also in absence of advanced instruments (i.e. sequencer). In addition, the design of PCR RFLP analyses generally is easy and can be accomplished using public available programs. In this specific case, it doesn't require a method designed *ad hoc* for each species of *Morbillivirus* to be detected, being able to identify different genotypes of DMV and CDV, also thanks to the advantage of using degenerate primers, as previously suggested by Frisk et al. (1999).

Considering the contagious nature and the high mortality rates of CDV that make necessary to speed up the diagnostic procedure in order to quarantine infected dogs and start appropriate treatments early (Elia et al., 2006) and in a perspective of a future cetacean die-off, given the cyclic trend of this infection among cetaceans' populations (Van Bressems et al., 2014), this protocol will allow to obtain a rapid detection of MI, bypassing the sequencing step and saving time and money.

The possibility of rapidly distinguishing between different genotypes of DMV (the North Sea and the Mediterranean Sea genotypes) could be also useful to obtain rapid information about geographic and host population distribution of cetacean morbillivirus worldwide as well as about its current epidemiological *status* in cetacean populations. These factors may be particularly crucial for the management of the populations suffering the pressure from human activities (Van Bressems et al., 2001) and for their conservation in general.

Further studies will be conducted in order to extensively evaluate the sensitivity of this new technique, performing an analysis of low-titer dilution series of both CDV and DMV. In addition, considering the lack of resolution that agarose gels showed, we will test the use of other technique (i.e. polyacrylamide gel electrophoresis) to improve the resolution of small molecules.

Future perspectives may consist in testing the method developed with other *Morbillivirus* genera, included the two other well-characterized genotypes of CeMV (PMV and PWMV), as already proposed by Sacristán et al. (2015), as well as comparing our protocol with other morbillivirus molecular diagnosis References

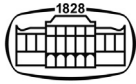
## Acknowledgments

This study was funded by the Italian Ministry of Health.

Authors thank colleagues of IIZZSS Mezzogiorno and Sicilia for their availability in sharing the samples used in this study.

## References

- Barrett, T., Visser, I.K., Mamaev, L., Goatley, L., van Bresse, M.F., Osterhaust, A.D., 1993. Dolphin and porpoise morbilliviruses are genetically distinct from phocine distemper virus. *Virology* 193 (2), 1010–1012.
- Bellièrre, E.N., Esperón, F., Sánchez-Vizcaíno, J.M., 2011. Genetic comparison among dolphin morbillivirus in the 1990–1992 and 2006–2008 Mediterranean outbreaks. *Infect. Genet. Evol.* 11, 1913–1920.
- Botelho-Souza, L.F., Souza Vieira, D., de Oliveira Dos Santos, A., Cunha Pereira, A.V., Villalobos-Salcedo, J.M., 2015. Characterization of the genotypic profile of hepatitis delta virus: isolation of HDV genotype-1 in the western amazon region of Brazil. *Intervirology* 58, 166–171.
- Casalone, C., Mazzariol, S., Pautasso, A., Di Guardo, G., Di Nocera, F., Lucifora, G., Ligios, C., Franco, A., Fichi, G., Cocumelli, C., Cersini, A., Guercio, A., Puleio, R., Gorla, M., Podestà, M., Marsili, L., Pavan, G., Pintore, A., De Carlo, E., Eleni, C., Caracappa, S., 2014. Cetacean strandings in Italy: an unusual mortality event along the Tyrrhenian Sea coast in 2013. *Dis. Aquat. Organ.* 109, 81–86.
- De Vries, R.D., Duprex, W.P., de Swart, R.L., 2015. Morbillivirus infections: an introduction. *Viruses* 7, 699–706.
- Delpout, S., Noyce, R.S., Richardson, C.D., 2014. The tumor-associated marker, PVRL4 (nectin-4), is the epithelial receptor for morbilliviruses. *Viruses* 6, 2268–2286.
- Di Guardo, G., Mazzariol, S., 2014. Cetacean morbillivirus in northern and southern hemispheres. *Front. Microbiol.* 5, 211.
- Di Guardo, G., Proietto, U., Di Francesco, C.E., Marsilio, F., Zaccaroni, A., Scaravelli, D., Mignone, W., Garibaldi, F., Kennedy, S., Forster, F., Iulini, B., Bozzetta, E., Casalone, C., 2010. Cerebral toxoplasmosis in striped dolphins (*Stenella coeruleoalba*) stranded along the Ligurian Sea coast of Italy. *Vet. Pathol.* 47 (2), 245–253.
- Diallo, A., Barrett, T., Barbron, M., Meyer, G., Lefevre, P.C., 1994. Cloning of the nucleocapsid protein gene of peste-des-petits-ruminants virus: relationship to other morbilliviruses. *J. Gen. Virol.* 75, 233–237.
- Elia, G., Decaro, N., Martella, V., Cirone, F., Lucente, M.S., Lorusso, E., Di Trani, L., Buonavoglia, C., 2006. Detection of canine distemper virus in dogs by real-time RT-PCR. *J. Virol. Methods* 136 (1), 171–176.
- Frisk, A.L., König, M., Moritz, A., Baumgärtner, W., 1999. Detection of Canine Distemper Virus Nucleoprotein RNA by reverse-transcription-PCR using serum, whole blood, and cerebrospinal fluid from Dogs with Distemper. *J. Clin. Microbiol.* 37, 3634–3643.
- Grant, R.J., Banyard, A.C., Barrett, T., Saliki, J.T., Romero, C.H., 2009. Real-time RT-PCR assays for the rapid and differential detection of dolphin and porpoise morbilliviruses. *J. Virol. Methods* 156 (1–2), 117–123.
- Groch, K.R., Colosio, A.C., Marcondes, M.C., Zucca, D., Díaz-Delgado, J., Niemeyer, C., Marigo, J., Brandão, P.E., Fernández, A., Luiz Catão-Dias, J., 2014. Novel cetacean morbillivirus in Guiana dolphin. *Braz. Emerg. Infect. Dis.* 20, 511–513.
- Hall, T.A., 1999. BioEdit: a user-friendly biological sequence alignment editor and analysis program for Windows 95/98/NT. *Nucl. Acids. Symp. Ser.* 41, 95–98.
- Iserte, J.A., Stephan, B.I., Goñi, S.E., Borio, C.S., Ghiringhelli, P.D., Lozano, M.E., 2013. Family-specific degenerate primer design: a tool to design consensus degenerated oligonucleotides. *Biotechnol. Res. Int.* 2013, 383646.
- Kawauchi, K., Takahashi, C., Ishihara, R., Hatama, S., 2015. Development of a novel PCR-RFLP assay for improved detection and typing of bovine papillomaviruses. *J. Virol. Methods.* 218, 23–26.
- Kennedy, S., Kuiken, T., Jepson, P.D., Deaville, R., Forsyth, M., Barrett, T., Van de Bildt, M.W.G., Osterhaus, A., Eybatov, T., Duck, C., Kydyr-Manov, A., Mitrofanov, I., Wilson, S., 2000. Mass die-off of Caspian seals caused by canine distemper virus. *Emerg. Infect. Dis.* 6, 637–639.
- Mazzariol, S., Marcer, F., Mignone, W., Serracca, L., Gorla, M., Marsili, L., Di Guardo, G., Casalone, C., 2012. Dolphin Morbillivirus and *Toxoplasma gondii* coinfection in a Mediterranean fin whale (*Balaenoptera physalus*). *BMC Vet. Res.* 8, 20.
- Murray, D.L., Kapke, C.A., Everman, J.J., Fuller, T.K., 1999. Infectious disease and the conservation of free-ranging large carnivores. *Anim. Conserv.* 2, 154–241.
- Origi, F.C., Plattet, P., Sattler, U., Robert, N., Casaubon, J., Mavrot, F., Pewsner, M., Wu, N., Giovannini, S., Oevermann, A., Stoffel, M.H., Gaschen, V., Segner, H., Ryser-Degorgis, M.P., 2012. Emergence of canine distemper virus genotypes with modified molecular signature and enhanced neuronal tropism leading to high mortality in wild carnivores. *Vet. Pathol.* 49, 913–929.
- Rima, B.K., Wishaupt, R.G., Welsh, M.J., Earle, J.A., 1995. The evolution of morbilliviruses: a comparison of nucleocapsid gene sequences including a porpoise morbillivirus. *Vet. Microbiol.* 44, 127–134.
- Rozenblatt, S., Eizenberg, O., Ben-Levy, R., Lavie, V., Bellini, W.J., 1985. Sequence homology within the morbilliviruses. *J. Virol.* 53, 684–690.
- Rubio-Guerri, C., Melero, M., Rivera-Arroyo, B., Belliere, E.N., Crespo, J.L., Parraga, D.G., Esperon, F., Sanchez-Vizcaino, J.M., 2013. Simultaneous diagnosis of Cetacean morbillivirus infection in dolphins stranded in the Spanish Mediterranean sea in 2011 using a novel Universal Probe Library (UPL) RT-PCR assay. *Vet. Microbiol.* 9, 106–114.
- Sacristán, C., Carballo, M., Muñoz, M.J., Bellière, E.N., Neves, E., Nugal, V., Esperón, F.J., 2015. Diagnosis of Cetacean morbillivirus: a sensitive one step real time RT fast-PCR method based on SYBR<sup>®</sup> Green. *Virol. Methods* 15 (December(226)), 25–30.
- Sanderson, B.A., Araki, N., Lilley, J.L., Guerrero, G., Lewis, L.K., 2014. Modification of gel architecture and TBE/TAE buffer composition to minimize heating during agarose gel electrophoresis. *Anal. Biochem.* 454, 44–52.
- Sidhu, M.S., Husar, W., Cook, S.D., Dowling, P.C., Udem, S.A., 1993. Canine distemper terminal and intergenic non-protein coding nucleotide sequences: completion of the entire CDV genome sequence. *Virology* 193, 66–72.
- Sierra, E., Sanchez, S., Saliki, J.T., Blas-Machado, U., Arbelo, M., Zucca, D., Fernandez, A., 2014. Retrospective study of etiologic agents associated with nonsuppurative meningoencephalitis in stranded cetaceans in the Canary Islands. *J. Clin. Microbiol.* 52, 2390–2397.
- Stephens, N., Duignan, P.J., Wang, J., Bingham, J., Finn, H., Bejder, L., Patterson, A.P., Holyoake, C., 2014. Cetacean morbillivirus in coastal Indo-Pacific bottlenose dolphins, Western Australia. *Emerg. Infect. Dis.* 20, 666–670.
- Van Bresse, M.F., Van Waerebeek, K., Jepson, P.D., Raga, J.A., Duignan, P.J., Nielsen, O., Di Benedetto, A.P., Siciliano, S., Ramos, R., Kant, W., Peddemors, V., Kinoshita, R., Ross, P.S., López-Fernandez, A., Evans, K., Crespo, E., Barrett, T., 2001. An insight into the epidemiology of dolphin morbillivirus worldwide. *Vet. Microbiol.* 81, 287–304.
- Van Bresse, M.F., Duignan, P.J., Banyard, A., Barbieri, M., Colegrove, K.M., De Guise, S., Di Guardo, G., Dobson, A., Domingo, M., Fauquier, D., Fernandez, A., Goldstein, T., Grenfell, B., Groch, K.R., Gulland, F., Jensen, B.A., Jepson, P.D., Hall, A., Kuiken, T., Mazzariol, S., Morris, S.E., Nielsen, O., Raga, J.A., Rowles, T.K., Saliki, J., Sierra, E., Stephens, N., Stone, B., Tomo, I., Wang, J., Waltzek, T., Wellehan, J.F., 2014. Cetacean morbillivirus: current knowledge and future directions. *Viruses* 6 (12), 5145–5181.
- Vincze, T., Posfai, J., Roberts, R.J., 2003. NEBcutter: a program to cleave DNA with restriction enzymes. *Nucleic Acids Res.* 31, 3688–3691.
- West, K.L., Sanchez, S., Rotstein, D., Robertson, K.M., Dennison, S., Levine, G., Davis, N., Schofield, D., Potter, C.W., Jensen, B., 2013. A Longman's beaked whale (*Indopacetus pacificus*) strands in Maui Hawaii, with first case of morbillivirus in the central Pacific. *Mar. Mam. Sci.* 29, 767–776.
- Wohlsein, P., Puff, C., Kreutzer, M., Siebert, U., Baumgärtner, W., 2007. Distemper in a dolphin. *Emerg. Infect. Dis.* 13, 1959–1961.
- Yang, W.C., Wu, B.J., Sierra, E., Fernández, A., Groch, K.R., Catão-Dias, J.L., West, K., Chan, K.W., 2016. A simultaneous diagnosis and genotyping method for global surveillance of cetacean morbillivirus. *Sci. Rep.* 3 (August(6)), 30625.



AKADÉMIAI KIADÓ


Acta Veterinaria  
Hungarica

DOI:  
10.1556/004.2021.00028  
© 2021 Akadémiai Kiadó, Budapest

SHORT  
COMMUNICATION



# Retrospective immunohistochemical investigation on dolphin morbillivirus infection by comparing the performance of heterologous monoclonal and polyclonal antibodies – Short communication

FEDERICA GIORDA<sup>1,2</sup>, GIOVANNI DI GUARDO<sup>3</sup>,  
KATIA VARELLO<sup>1</sup>, ALESSANDRA PAUTASSO<sup>4</sup>, EVA SIERRA<sup>2</sup>,  
MARIA DOMENICA PINTORE<sup>5</sup>, CARLA GRATTAROLA<sup>1</sup>,  
ERIKA MOLICA COLELLA<sup>6</sup>, ENRICA BERIO<sup>1</sup>, MARIA GORIA<sup>1</sup>,  
ELENA BOZZETTA<sup>1</sup>, CRISTINA CASALONE<sup>1</sup> and  
BARBARA IULINI<sup>1\*</sup> 

<sup>1</sup> Istituto Zooprofilattico Sperimentale del Piemonte, Liguria e Valle D'Aosta, via Bologna 148, 10154, Torino, Italy

<sup>2</sup> Institute of Animal Health, University of Las Palmas de Gran Canaria, Arucas, Las Palmas, Spain

<sup>3</sup> Faculty of Veterinary Medicine, University of Teramo, Teramo, Italy

<sup>4</sup> Department of Prevention, Local Veterinary Services (ASL1 Imperiese), Bussana di Sanremo, Imperia, Italy

<sup>5</sup> Department of Prevention, Local Veterinary Services (ASL VCO), Domodossola (VB), Italy

<sup>6</sup> Istituto Zooprofilattico Sperimentale della Lombardia e dell'Emilia Romagna, Brescia, Italy

Received: 1 November 2020 • Accepted: 27 May 2021

## ABSTRACT

Dolphin morbillivirus (DMV) is a pathogen of great concern in free-ranging cetaceans. Confirmation and staging of morbillivirus infections rely on histology and immunohistochemistry (IHC), following molecular detection. As at the present time no specific antibodies (Abs) against DMV are available, two heterologous Abs have been used worldwide for the examinations of morbillivirus infections of cetaceans. One is a monoclonal Ab (MoAb) prepared against the N protein of canine distemper virus (CDV), whereas the other is a polyclonal Ab raised in rabbits against rinderpest virus (RPV). Both Abs are known to show cross-reactivity with DMV. In this study we compared the labelling quality and the neuroanatomical distribution of staining with these two Abs by means of IHC analysis. To this end, serial sections of the target organs from ten free-ranging stranded cetaceans, previously diagnosed as being infected with DMV by PCR and/or serology, were subjected to IHC. The brain, lungs and lymph nodes of one animal were found to be positive with both Abs. From two other animals, the brain and the spleen, respectively, tested positive only with the polyclonal Ab. In the positive brain tissues, multifocal immunostaining was observed, with similar staining location and extent, with the two antibodies tested. Our results suggest that the polyclonal anti-RPV Ab might have a stronger binding activity to DMV than the anti-CDV MoAb. Nevertheless, the elaboration and use of specific anti-DMV Abs might be essential to guarantee conclusive results in diagnostic and pathogenetic investigations.

\*Corresponding author. Tel.: (+39)  
011-2686311.  
E-mail: [barbara.iulini@izsto.it](mailto:barbara.iulini@izsto.it)

## KEYWORDS

cetaceans, dolphin morbillivirus, immunohistochemistry, monoclonal antibody, polyclonal antibody





Dolphin morbillivirus (DMV), officially classified into the virus species *Cetacean morbillivirus* within the genus *Morbillivirus*, causes infection and disease in different cetacean animals. The pathogen has been found to be responsible for several epizootic and enzootic outbreaks worldwide. Over the last 30 years, the virus has caused two epizootics and three unusual mortality events in the Mediterranean basin, the most recent along the Italian coastline in 2016 (Pautasso et al., 2019).

The gold standard for the diagnosis remains virus isolation, which can be challenging when dealing with stranded animals. Indeed, very few reports on successful virus isolation are available (Peletto et al., 2018). Reverse transcription polymerase chain reaction (RT-PCR) followed by sequencing the PCR product is a specific and sensitive diagnostic method; however, histology and immunohistochemistry (IHC) should be performed to confirm morbillivirus infection (MI) and to obtain information on the stage of the disease. Negative antigen immunolabelling is commonly obtained in subacute-to-chronic or subclinical MI (Van Bresseem et al., 2014).

Since no homologous antibody (Ab) against DMV is available, two Abs prepared against other members of the genus *Morbillivirus* have been used worldwide in the IHC diagnosis. One of them is a monoclonal antibody (MoAb) against the N protein of canine distemper virus (CDV). The other is a polyclonal Ab raised in rabbits against rinderpest virus (RPV) (Van Bresseem et al., 2014). In the present study, we performed IHC analysis of cetacean tissue samples from animals that had been found DMV positive by other techniques, such as PCR and/or serology. We compared the performance of the two Abs for positivity detection, labelling quality, and the neuroanatomical distribution of the staining.

The study was performed in 2016 (the serum against RPV is no longer available due to the recent OIE procedures for RPV eradication) on 122 formalin-fixed target tissue samples (brain, lung, spleen, lymph nodes) from seven striped dolphins (*Stenella coeruleoalba*), two bottlenose dolphins (*Tursiops truncatus*), and a pilot whale (*Globicephala melas*). The samples were selected on the basis of the presence of suggestive microscopic lesions and/or molecular (Verna et al., 2017) and/or serological (Di Guardo et al., 2010) evidence of MI. In addition, a panel of 10 tissues sampled from two striped dolphins (ID 11 and 12), all found negative with PCR or serology and without histological lesions suggestive of MI, served as negative control (Table 1). All the animals included in this study were free-ranging cetaceans stranded along the Italian coast of the Pelagos Sanctuary (between 43°47'4"N, 7°31'49"E and 43°45'24"N, 10°16'25"E) in the period 2008–2015 and submitted to complete postmortem examination at the C.Re.Di.Ma. (Italian National Reference Centre for Diagnostic Activities in Stranded Marine Mammals) following standard procedures (Geraci and Lounsbury, 2005). The results obtained on a few specimens included in this study have also been published previously (Giorda et al., 2017).

In detail, lung, spleen, lymph nodes (prescapular, tracheobronchial, and mesenteric, according to tissue

availability) and nine anatomic areas from the brain (basal nuclei, thalamus, mesencephalon, pons, obex, frontal, parietal, occipital and cerebellar cortex) were sampled and examined. Serial formalin-fixed, paraffin-embedded sections were processed by IHC alternately with an anti-CDV-NP MoAb (provided by VMRD, Pullman, WA, USA) (Stanton et al., 2004) and an anti-RPV polyclonal Ab (provided by the Pirbright Institute, Pirbright, UK) (Yang et al., 2006). Two biotinylated antibodies (Vectastain ABC method, provided by Vector Laboratories, Burlingame, CA, USA) were used as secondary antibodies, namely a horse anti-mouse IgG for the MoAb and a goat anti-rabbit IgG for the polyclonal Ab. Negative internal controls were employed in which the primary antibody was replaced with a non-immune homologous serum.

Two pathologists independently reviewed all the slides and identified each tissue as negative or positive by the MoAb and/or polyclonal Ab staining. Tissue samples that tested positive by only one of the two Abs underwent additional evaluation by a board-certified pathologist. The results reported here are thus to be intended as an agreement reached by two or three pathologists. Moreover, the type(s) of cells that showed positive staining in each organ was/were recorded. Kappa statistic was calculated using the EpiTools epidemiological calculator to test agreement between the two IHC protocols (Sergeant, 2018): if at least one organ was positive, the animal was classified as positive for DMV by IHC with the MoAb and/or the polyclonal Ab.

Only three out of the ten cetaceans showed positive IHC staining. These included ID1 (striped dolphin), ID 6 (bottlenose dolphin), and ID 8 (pilot whale). In detail, the brain, the lung and the tracheobronchial lymph node from ID1 tested positive with both Abs, whereas the brain of ID6 and the spleen of ID8 tested positive with the anti-RPV polyclonal Ab. Among the tissues testing positive with both Abs, labelling of morbillivirus antigen was demonstrated in the same types of cells, including astrocytes, neurons (soma and processes), meningeal and endothelial cells and mononuclear cells in the perivascular cuffs and the meninges in the brain; type I and II pneumocytes and multinucleated giant cells/syncytia (MGCS) in the lung; follicular lymphocytes and MGCS in the lymph nodes, and macrophages in the spleen. The brain of ID6 showed focal immunoreactivity in the inflamed meninges of the parietal cortex, with limited staining of mononuclear and meningeal cells (Fig. 1a), while scattered labelling of macrophages was evident in the spleen of ID8 (Fig. 1b). The lung of ID3 was not evaluable due to postmortem autolysis.

There was a similar pattern of immunoreactivity for both Abs characterised by diffuse or fine granular dark cytoplasmic and nuclear immunostaining. Generally, the MoAb showed a stronger staining intensity, free of non-specific signal. Differently, the polyclonal Ab showed strong, diffuse background labelling. In addition, the bradyzoites, belonging to multiple *Toxoplasma gondii* cysts, stained positive with this Ab in ID1 that presented a co-infection with this protozoan (data not shown). Such non-specific labelling was not observed in any section of the internal controls.



Table 1. Data of the stranded cetaceans involved in this study, along with the results of the histopathological, molecular, serological and immunohistochemical (IHC) analyses. IHC was performed by using an anti-canine distemper virus (CDV) monoclonal antibody (MoAb) or an anti-rinderpest virus (RPV) polyclonal antibody on selected tissue samples as shown

ID animal – YS	Species	Age	NuS	DC	Tissues	Microscopic lesions suggestive of MI	RT-PCR	Anti-CDV Abs in serum	IHC results	
									anti-CDV MoAb	anti-RPV polyclonal Ab
1–2008	Striped dolphin	Adult	Poor	2	Brain	NS meningoencephalitis	+	-	+	+
					Lung	Bronchointerstitial pneumonia	+		+	+
					Spleen	Lymphoid depletion	n. p.		-	-
					Tracheobronchial LN	Lymphoid depletion	n. p.		+	+
2–2011	Striped dolphin	Adult	Poor	4	Brain	NS meningoencephalitis	-	1:16	-	-
					Lung	-	-		NVA	NVA
					Spleen	Germinal centre hyperplasia	-		-	-
					Prescapular LN	Lymphoid depletion	n. p.		-	-
3–2012	Striped dolphin	Adult	Good	4	Brain	NS meningoencephalitis	+	-	-	-
					Lung	-	-		-	-
					Spleen	-	+		-	-
4–2012	Striped dolphin	Adult	Good	2	Brain	NS meningoencephalitis	-	1:8	-	-
					Lung	-	-		-	-
					Spleen	-	n. p.		-	-
					Prescapular LN	-	-		-	-
					Tracheobronchial LN	-	-		-	-
5–2012	Striped dolphin	Adult	Good	3	Brain	NS meningoencephalitis	-	1:32	-	-
					Lung	Bronchointerstitial pneumonia	-		-	-
					Spleen	-	-		-	-
					Prescapular LN	-	-		-	-
					Tracheobronchial LN	-	-		-	-
					Brain	NS meningoencephalitis	-	1:32	-	+
6–2012	Bottlenose dolphin	Juvenile – subadult	Good	3	Spleen	-	-	-	-	-
					Tracheobronchial LN	-	-		-	-
					Brain	-	-		1:8	-
7–2013	Bottlenose dolphin	Juvenile – subadult	Good	3	Lung	-	-	-	-	-
					Spleen	Germinal centre hyperplasia	-		-	-
					Tracheobronchial LN	Germinal centre hyperplasia	-		-	-
					Mesenteric LN	Germinal centre hyperplasia	-		-	-

(continued)





**Table 1. Continued**

ID animal – YS	Species	Age	NuS	DC	Tissues	Microscopic lesions suggestive of MI	RT-PCR	Anti-CDV Abs in serum	IHC results					
									anti-CDV MoAb	anti-RPV polyclonal Ab				
8–2013	Pilot whale	Juvenile – subadult	Good	3	Brain	Mild and focal NS encephalitis	-	1:8	-	-				
					Lung	-	-		-					
					Spleen	Germinal centre hyperplasia and hyalinosis	n. p.		-	+				
					Prescapular LN	Hyperplastic lymphadenitis	n. p.		-	-				
					Tracheobronchial LN	-	n. p.		-	-				
9–2015	Striped dolphin	Adult	Good	2	Mesenteric LN	-	n. p.	-	-					
					Brain	NS encephalitis	+	1:32	-	-				
					Lung	Bronchointerstitial pneumonia	-		-	-				
					Spleen	Lymphoid depletion	-		-	-				
					Prescapular LN	-	+		-	-				
10 –2015	Striped dolphin	Adult	Poor	3	Brain	NS meningoencephalitis	-		-	-				
					Lung	Interstitial pneumonia	+	-	-					
					Spleen	Lymphoid depletion	-	-	-					
					11–2008 NC	Striped dolphin	Adult	Poor	3	Brain	-	-	n. p.	-
										Lung	NVA	-	-	-
Spleen	-	-	-	-										
Prescapular LN	-	-	-	-										
Tracheobronchial LN	-	-	-	-										
12–2008 NC	Striped dolphin	Juvenile – subadult	Good	2	Brain	-	-	n. p.	-					
					Lung	-	-	-	-					
					Spleen	-	-	-	-					
					Prescapular LN	-	-	-	-					
					Tracheobronchial LN	-	-	-	-					

*Legend:* YS: year of stranding; NuS: nutritional status; DC: decomposition code (2: fresh; 3: moderate autolysis; 4: decomposed); Abs: antibodies; MI: morbillivirus infection; -: Negative sample; +: Positive sample; n. p.: not performed; LN: lymph node; NS: non-suppurative; NVA: not evaluable due to autolysis; NC: negative control



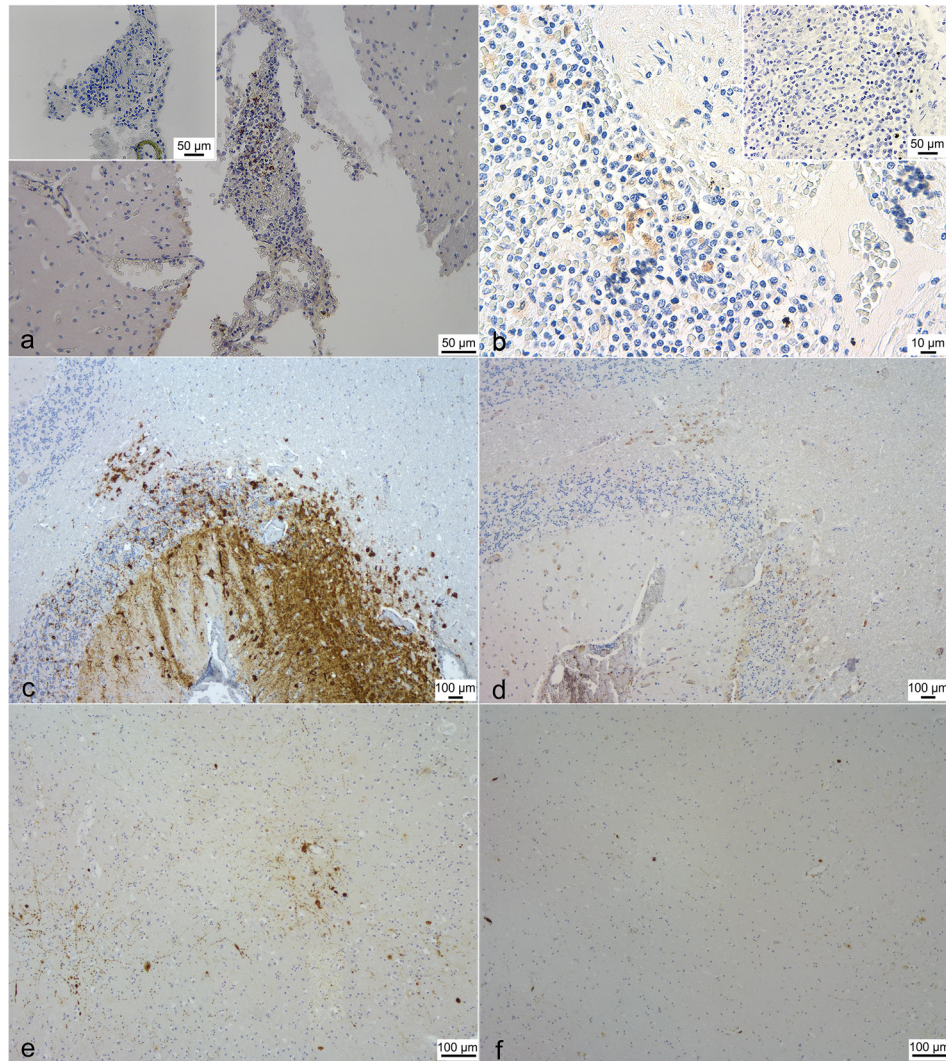


*Fig. 1. a)* Meninges of the parietal cortex (ID6). Positive labelling in mononuclear and meningeal cells. Anti-RPV polyclonal Ab. Upper left inset: meninges of the parietal cortex (ID6). Absence of staining (minimal unspecific signal in a blood vessel). Anti-CDV MoAb. *b)* Spleen (ID8). Positive labelling in macrophages. Anti-RPV polyclonal Ab. Upper right inset: Spleen (ID8). Absence of staining. Anti-CDV MoAb. *c)* Cerebellar cortex (ID1). Intense and extensive positive labelling of Purkinje cells, molecular and granular layers, and endothelial cells. Anti-CDV MoAb. *d)* Cerebellar cortex (ID1). Positive staining of molecular and granular layers and scattered endothelial and Purkinje cells. Anti-RPV polyclonal Ab. *e)* Occipital cortex (ID1). Intense immunoreaction of neurons (soma and processes) and glia cells. Anti-CDV MoAb. *f)* Positive labelling of scattered neurons (soma and processes), glia and endothelial cells. Anti-RPV polyclonal Ab

The neuroanatomical localisation of the staining by the two Abs could be compared only in ID1, since the brain of this animal was the only tissue from the nervous system that tested positive with both Abs. Histologically, there was a mild, multifocal non-suppurative sub-acute meningoencephalitis with minimal demyelination, without MGCS or inclusion bodies. Multifocal immunostaining was present with both Abs in all the neuroanatomical areas examined, including both the grey and the white matter, and generally involving scattered cells. The areas most affected were the mesencephalon and the cerebral and cerebellar cortex. The extent and location of the regions of immunostaining were similar, except for the cerebellum and the occipital cortex, in which positivity with the MoAb was more intense and

widespread compared to the polyclonal Ab (Figs. 1c, 1d, 1e and 1f).

The agreement between the two IHC techniques was moderate (Cohen's kappa = 0.4118, SE for non-zero kappa = 0.2557). Of particular interest is that fewer tissues tested positive with the MoAb compared to the polyclonal Ab (4 vs. 6). This difference may have stemmed from the relatively small amount of antigen detected within the sections that stained positive only with the polyclonal Ab (brain of ID6 and spleen of ID8), as reported in a similar study of West Nile infection (Smedley et al., 2007). Furthermore, since the MoAb is directed against a single epitope of the N protein, its binding with the antigen may be influenced by the formalin fixation, the heat retrieval and the autolysis.

These conditions might exert less effect on the results obtained with the polyclonal Ab, which targets different epitopes of multiple structural proteins of the virus. Finally, Amude et al. (2010) has found that the chronicity of infections in CDV brain lesions may lead to antigen (N protein) clearance from the lesions and, as a consequence, to negative staining. Such aspects may explain the lower sensitivity of the MoAb compared to the polyclonal Ab in our study. We have no plausible explication for the more marked staining obtained with the MoAb in the cerebellum and the occipital cortex; additional positive tissues would be necessary to analyse this feature. Unlike Amude et al. (2010), we observed no non-specific intra-neuronal immunoreaction with the MoAb, but a minimal unspecific signal was present in the blood vessels (Fig. 1a, inset).

Interestingly, the MI of the two animals that tested positive by the polyclonal Ab only, was not confirmed by molecular methods previously. The RT-PCR test of the young bottlenose dolphin (ID6) was negative, whereas in the pilot whale (ID) the PCR was not performed. A similar situation has been reported before (Díaz-Delgado et al., 2017). In the animals examined by us, the diagnosis of MI was based on DMV-related microscopic lesions associated with the presence of specific serum antibodies (Di Guardo et al., 2010).

Our results suggest that a polyclonal Ab is more efficient than a MoAb in detecting DMV by IHC, though the staining quality is overall enhanced with the MoAb. Within this framework, future studies should be aimed at evaluating the cross-reactivity of the MoAb and polyclonal antibodies, raised against additional members of the genus *Morbillivirus*, with DMV-specific epitopes. Finally, because IHC should always be associated with RT-PCR and because this technique is essential for staging DMV infection (Van Bressemer et al., 2014; Díaz-Delgado et al., 2019), considering that the use of both antibodies is not able to ensure conclusive results, the next step would be to produce a MoAb specific for DMV proteins, which would be fundamental for increasing the accuracy of diagnostic and pathogenetic investigations.

## ACKNOWLEDGEMENTS

This research was funded by the Italian Ministry of Health (Ricerca Corrente 2014 IZS PLV 08/14 RC). The authors are grateful to C. E. Di Francesco for her support in serological analysis, to R. Desiato and F. Ingravalle for their help in statistical analysis and to M. Giorda for his assistance with the microscopic images.

## REFERENCES

- Amude, A. M., Alfieri, A. F. and Alfieri, A. A. (2010): Use of immunohistochemistry and molecular assays such as RT-PCR for precise post mortem diagnosis of distemper-related encephalitis. In: Méndez-Vilas, A. (ed.) Current Research, Technology and Education Topics in Applied Microbiology and Microbial Biotechnology, Formatex, Spain. pp. 1539–1545.
- Di Guardo, G., Proietto, U., Di Francesco, C. E., Marsilio, F., Zaccaroni, A., Scaravelli, D., Mignone, W., Garibaldi, F., Kennedy, S., Forster, F., Iulini, B., Bozzetta, E. and Casalone, C. (2010): Cerebral toxoplasmosis in striped dolphins (*Stenella coeruleoalba*) stranded along the Ligurian Sea coast of Italy. *Vet. Pathol.* **47**, 245–253.
- Díaz-Delgado, J., Groch, K. R., Sierra, E., Sacchini, S., Zucca, D., Quesada-Canales, Ó., Arbelo, M., Fernández, A., Santos, E., Ikeda, J., Carvalho, R., Azevedo, A. F., Lailson-Brito, J. Jr., Flach, L., Ressio, R., Kanamura, C. T., Sansone, M., Favero, C., Porter, B. F., Centelleghé, C., Mazzariol, S., Di Renzo, L., Di Francesco, G., Di Guardo, G. and Catão-Dias, J. L. (2019): Comparative histopathologic and viral immunohistochemical studies on CeMV infection among Western Mediterranean, Northeast-Central, and Southwestern Atlantic cetaceans. *PLoS One* **14**, 1–21.
- Díaz-Delgado, J., Sierra, E., Vela, A. I., Arbelo, M., Zucca, D., Groch, K. R. and Fernández, A. (2017): Coinfection by *Streptococcus phocae* and cetacean morbillivirus in a short-beaked common dolphin *Delphinus delphis*. *Dis. Aquat. Org.* **124**, 247–252.
- Geraci, J. R. and Lounsbury, V. J. (2005): *Marine Mammals Ashore: A Field Guide for Strandings*. 2<sup>nd</sup> ed. National Aquarium in Baltimore, Baltimore, MD. 382 pp.
- Giorda, F., Ballardini, M., Di Guardo, G., Pintore, M. D., Grattarola, C., Iulini, B., Mignone, W., Gorla, M., Serracca, L., Varello, K., Dondo, A., Acutis, P. L., Garibaldi, F., Scaglione, F. E., Gustinelli, A., Mazzariol, S., Di Francesco, C. E., Tittarelli, C., Casalone, C. and Pautasso, A. (2017): Postmortem findings in cetaceans found stranded in the Pelagos sanctuary, Italy, 2007–14. *J. Wildl. Dis.* **53**, 795–803.
- Pautasso, A., Iulini, B., Grattarola, C., Giorda, F., Gorla, M., Peletto, S., Masoero, L., Mignone, W., Varello, K., Petrella, A., Carbone, A., Pintore, A., Denurra, D., Scholl, F., Cersini, A., Puleio, R., Purpari, G., Lucifora, G., Fusco, G., Di Guardo, G., Mazzariol, S. and Casalone, C. (2019): Novel dolphin morbillivirus (DMV) outbreak among Mediterranean striped dolphins *Stenella coeruleoalba* in Italian waters. *Dis. Aquat. Org.* **132**, 215–220.
- Peletto, S., Caruso, C., Cerutti, F., Modesto, P., Biolatti, C., Pautasso, A., Grattarola, C., Giorda, F., Mazzariol, S., Mignone, W., Masoero, L., Casalone, C. and Acutis, P. L. (2018): Efficient isolation on Vero-DogSLAMtag cells and full genome characterization of Dolphin Morbillivirus (DMV) by next generation sequencing. *Sci. Rep.* **8**, 1–8.
- Sergeant, E. S. G. (2018): *Epitools Epidemiological Calculators*, Ausvet Pty Ltd. Available from: <http://epitools.ausvet.com.au>.
- Smedley, R. C., Patterson, J. S., Miller, R., Massey, J. P., Wise, A. G., Maes, R. K., Wu, P., Kaneene, J. B. and Kiupel, M. (2007): Sensitivity and specificity of monoclonal and polyclonal immunohistochemical staining for West Nile virus in various organs from American crows (*Corvus brachyrhynchos*). *BMC Infect. Dis.* **7**, 1–9.
- Stanton, J. B., Brown, C. C., Poet, S., Lipscomb, T. P., Saliki, J. and Frasca, S., Jr. (2004): Retrospective differentiation of canine distemper virus and phocine distemper virus in phocids. *J. Wildl. Dis.* **40**, 53–59.









- Van Bresse, M. F., Duignan, P. J., Banyard, A., Barbieri, M., Colegrove, K. M., De Guise, S., Di Guardo, G., Dobson, A., Domingo, M., Fauquier, D., Fernandez, A., Goldstein, T., Grenfell, B., Groch, K. R., Gulland, F., Jensen, B. A., Jepson, P. D., Hall, A., Kuiken, T., Mazzariol, S., Morris, S. E., Nielsen, O., Raga, J. A., Rowles, T. K., Saliki, J., Sierra, E., Stephens, N., Stone, B., Tomo, I., Wang, J., Waltzek, T. and Wellehan, J. F. (2014): Cetacean morbillivirus: current knowledge and future directions. *Viruses* **6**, 5145–5181.
- Verna, F., Giorda, F., Miceli, I., Rizzo, G., Pautasso, A., Romano, A., Iulini, B., Pintore, M. D., Mignone, W., Grattarola, C., Bozzetta, E., Varello, K., Dondo, A., Casalone, C. and Gorla, M. (2017): Detection of morbillivirus infection by RT-PCR RFLP analysis in cetaceans and carnivores. *J. Virol. Methods* **247**, 22–27.
- Yang, W. C., Pang, V. F., Jeng, C. R., Chou, L. S. and Chueh, L. L. (2006): Morbilliviral infection in a pygmy sperm whale (*Kogia breviceps*) from Taiwanese waters. *Vet. Microbiol.* **116**, 69–76.



## Article

# Evidence for Unknown *Sarcocystis*-Like Infection in Stranded Striped Dolphins (*Stenella coeruleoalba*) from the Ligurian Sea, Italy

Federica Giorda <sup>1,2,†</sup>, Umberto Romani-Cremaschi <sup>3,†</sup>, Antoinette E. Marsh <sup>4</sup>, Carla Grattarola <sup>1</sup>, Barbara Iulini <sup>1</sup>, Alessandra Pautasso <sup>5</sup>, Katia Varello <sup>1</sup> , Enrica Berio <sup>1</sup>, Paola Gazzuola <sup>1</sup>, Letizia Marsili <sup>6</sup> , Cristina E. Di Francesco <sup>7</sup> , Maria Gorla <sup>1</sup>, Federica Verna <sup>8</sup>, Tania Audino <sup>1</sup>, Simone Peletto <sup>1</sup> , Maria Caramelli <sup>1</sup>, Mercedes Fernández-Escobar <sup>9</sup>, Eva Sierra <sup>2</sup>, Antonio Fernández <sup>2</sup> , Rafael Calero-Bernal <sup>9</sup>  and Cristina Casalone <sup>1,\*</sup>

<sup>1</sup> Istituto Zooprofilattico Sperimentale del Piemonte, Liguria e Valle d'Aosta, 10154 Torino, Italy; federica.giorda@izsto.it (F.G.); carla.grattarola@izsto.it (C.G.); barbara.iulini@izsto.it (B.I.); katia.varello@izsto.it (K.V.); enrica.berio@izsto.it (E.B.); paola.gazzuola@izsto.it (P.G.); maria.gorla@izsto.it (M.G.); tania.audino@izsto.it (T.A.); simone.peletto@izsto.it (S.P.); maria.caramelli@izsto.it (M.C.)

<sup>2</sup> Institute for Animal Health and Food Safety (IUSA), Veterinary School, University of Las Palmas de Gran Canaria, Las Palmas de Gran Canaria, 35416 Canary Islands, Spain; eva.sierra@ulpgc.es (E.S.); antonio.fernandez@ulpgc.es (A.F.)

<sup>3</sup> Veterinary Department, Mundomar, Calle Sierra Helada s/n, 03503 Benidorm, Spain; umberto.romanicremaschi@gmail.com

<sup>4</sup> Department of Veterinary Preventive Medicine, College of Veterinary Medicine, The Ohio State University, 1920 Coffey Road, Columbus, OH 43210, USA; marsh.2061@osu.edu

<sup>5</sup> Department of Prevention, Local Veterinary Services (ASL1 Imperiese), Via Aurelia Ponente 97, Bussana di Sanremo, 18038 Imperia, Italy; a.pautasso@asl1.liguria.it

<sup>6</sup> Dipartimento di Scienze Fisiche, della Terra e dell'Ambiente, University of Siena, Via Mattioli 4, 53100 Siena, Italy; letizia.marsili@unisi.it

<sup>7</sup> Faculty of Veterinary Medicine, University of Teramo, Strada Provinciale 18 Località Piano d'Accio, 64100 Teramo, Italy; cedifrancesco@unite.it

<sup>8</sup> Department of Prevention, Local Veterinary Services, Via Conte Verde 125, 35040 Asti, Italy; fverna@asl.at.it

<sup>9</sup> SALUVET, Department of Animal Health, Faculty of Veterinary, Complutense University of Madrid, 28040 Madrid, Spain; merfer02@ucm.es (M.F.-E.); r.calero@ucm.es (R.C.-B.)

\* Correspondence: cristina.casalone@izsto.it

† These authors have equally contributed to this work.



**Citation:** Giorda, F.; Romani-Cremaschi, U.; Marsh, A.E.; Grattarola, C.; Iulini, B.; Pautasso, A.; Varello, K.; Berio, E.; Gazzuola, P.; Marsili, L.; et al. Evidence for Unknown *Sarcocystis*-Like Infection in Stranded Striped Dolphins (*Stenella coeruleoalba*) from the Ligurian Sea, Italy. *Animals* **2021**, *11*, 1201. <https://doi.org/10.3390/ani11051201>

Academic Editor: Pablo Diaz

Received: 20 March 2021

Accepted: 20 April 2021

Published: 22 April 2021

**Publisher's Note:** MDPI stays neutral with regard to jurisdictional claims in published maps and institutional affiliations.



**Copyright:** © 2021 by the authors. Licensee MDPI, Basel, Switzerland. This article is an open access article distributed under the terms and conditions of the Creative Commons Attribution (CC BY) license (<https://creativecommons.org/licenses/by/4.0/>).

**Simple Summary:** Two stranded striped dolphins presented meningoencephalitic lesions associated with the presence of unknown protozoan tissue cysts. The present study aimed at fully characterizing these previously undescribed parasites. Light microscopy re-examination of affected CNS areas showed high numbers of tissue cysts with morphological features resembling those of *Sarcocystis* species. Tissue cyst bradyzoites positively stained when labeled with polyclonal antisera but cross-reactivity could not be precluded. *Sarcocystis* sp. sequences with high homology to species infecting livestock were amplified by means of PCR from myocardial and muscle tissues. This is the first report of *Sarcocystis*-like tissue cysts in the cerebral tissue of stranded cetaceans with muscular sarcocystosis in Mediterranean dolphins. The obtained results may suggest a land-to-sea cycling of Apicomplexan parasites in this region and the need for further investigations in order to foster marine mammal conservation.

**Abstract:** Two striped dolphins (SD1, SD2), stranded along the Ligurian coast of Italy, were diagnosed with a nonsuppurative meningoencephalitis associated with previously undescribed protozoan tissue cysts. As tissue cysts were morphologically different from those of *Toxoplasma gondii*, additional histopathological, immunohistochemical, ultrastructural, and biomolecular investigations were performed, aiming to fully characterize the organism. Histopathology revealed the presence of large *Sarcocystis*-like tissue cysts, associated with limited inflammatory lesions in all CNS areas studied. IHC was inconclusive, as positive staining with polyclonal antisera did not preclude cross-reaction with other Sarcocystidae coccidia. Applied to each animal, 11 different PCR protocols

precluded a neural infection by *Sarcocystis neurona*, *Sarcocystis falcatula*, *Hammondia hammondi*, and *Neospora caninum*. *T. gondii* coinfection was confirmed only in dolphin SD2. *Sarcocystis* sp. sequences, showing the highest homology to species infecting the Bovidae family, were amplified from SD1 myocardium and SD2 skeletal muscle. The present study represents the first report of *Sarcocystis*-like tissue cysts in the brain of stranded cetaceans along with the first description of *Sarcocystis* sp. infection in muscle tissue of dolphins from the Mediterranean basin.

**Keywords:** striped dolphin; tissue cysts; neuropathology; *Toxoplasma gondii*; *Sarcocystis*-like; genotype

## 1. Introduction

Tissue cyst-forming coccidia from the genera *Toxoplasma*, *Sarcocystis*, and *Neospora* (Apicomplexa) are capable of infecting several species of marine mammals and are responsible for either chronic diseases or acute mortality [1]. While *Neospora caninum* does not seem to pose a major threat to marine wildlife, *Toxoplasma gondii* and *Sarcocystis neurona* are the two coccidian parasites most widely reported in North American marine mammals [1], especially in coastal species that are more likely to be overexposed to immunosuppressant chemical pollutants and to high concentrations of land-derived oocysts [2–4]. The most probable exposure route in these animals is through ingestion of environmentally resistant oocysts or sporocysts shed on land by the definitive hosts and passed into the sea through freshwater runoffs or the release of contaminated ship waters. Eventually, protozoal infectious stages may then accumulate in marine invertebrates, bivalve mollusks, or fish on which intermediate hosts prey [5]. In the Mediterranean basin, *T. gondii* is a frequent finding in stranded odontocetes, and it is often associated with protozoal meningoencephalitis [6,7].

On the other hand, neither muscular nor neural sarcocystosis has ever been officially reported in this geographical area, to the authors' best knowledge. However, a fatal case of hepatic sarcocystosis [8], caused by an unknown species, is the only account of a *Sarcocystis* sp. infection in a Mediterranean cetacean.

In this study, we provide evidence of an infection sustained by a *Sarcocystis*-like organism in two striped dolphins (*Stenella coeruleoalba*) stranded along the Ligurian coast of Italy, in the marine protected area of the Pelagos Sanctuary, in 2011 and 2017.

## 2. Materials and Methods

### 2.1. Naturally Infected Dolphins

The cases, SD1 and SD2, included in the present study were diagnosed during routine pathological and cause-of-death assessment in stranded cetaceans at the Istituto Zooprofilattico Sperimentale del Piemonte, Liguria e Valle d'Aosta. The two striped dolphins (*Stenella coeruleoalba*), stranded along the Ligurian Sea coast in 2011 (SD1) and 2017 (SD2) (Figure 1), were submitted for a complete postmortem examination, according to standard protocols [9]. Dolphin SD1 was a 206 cm (total length, TL) adult male, in a poor nutritional status and in a postmortem condition code 3 (moderately decomposed). Dolphin SD2 was a 177 cm (TL) juvenile male, in a moderate nutritional status and in postmortem condition code 2 (fresh). Neither animals displayed any evidence of interaction with fishing activities, and the stomach chambers were devoid of intake. Initially, postmortem findings from SD1 and SD2 were previously published [10,11] and, for the present study, these two cases were re-examined with the focus on neurotrophic causes of inflammation, CNS, and tissue protozoal cysts, parasite identification, and distribution.

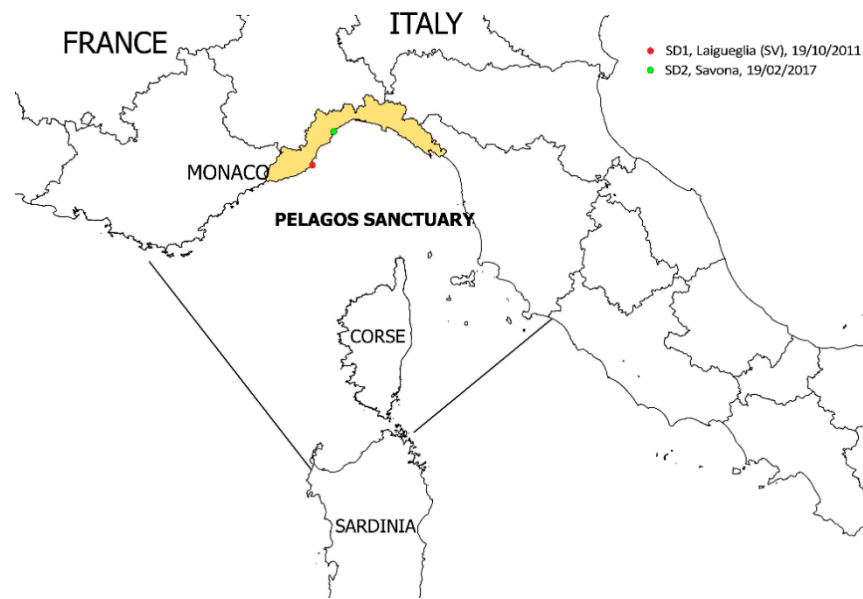


**Figure 1.** Map of the study area (Ligurian coastline), displaying the stranding locations (red and green dots) of the two striped dolphins infected by Sarcocystidae organisms. The map was created by A.P. with QGIS (QGIS Development Team (2018). QGIS Geographic Information System. Open Source Geospatial Foundation Project. <http://qgis.osgeo.org>, accessed on 17 August 20).

During necropsy, the tissue samples of all the major organs and lesions were collected and split into aliquots for subsequent analyses: one was kept frozen at  $-20\text{ }^{\circ}\text{C}$  for microbiological and toxicological investigations, one was kept frozen at  $-80\text{ }^{\circ}\text{C}$  for biomolecular analyses, and the other was preserved in 10% buffered formalin for histological and immunohistochemical (IHC) investigations. Blood serum, aqueous humor, and cerebrospinal fluid (CSF) were collected, when available, and kept frozen at  $-20\text{ }^{\circ}\text{C}$  for serological investigations.

## 2.2. Histology and Immunohistochemistry

Representative tissues from SD1 (brain, lung, heart, liver, spleen, kidney, prescapular lymph node, urinary bladder, and reproductive system) and from SD2 (brain, tonsils, lung, prescapular and tracheobronchial lymph nodes, heart, liver, spleen, pancreas, intestine, skeletal muscle, skin, kidney, urinary bladder, adrenal gland, tongue lesion, and reproductive system) were collected and fixed in 10% neutral buffered formalin, embedded in paraffin, sectioned at  $4 \pm 2\text{ }\mu\text{m}$ , stained with hematoxylin and eosin (H&E), and examined through a light microscope.

Nine different areas from the brain were sampled and examined, including basal nuclei, thalamus, mesencephalon, pons, obex, and frontal, parietal, occipital, and cerebellar cortex. Immunohistochemistry (IHC) for *Morbillivirus* was performed on tissue sections from SD1 (brain) and from SD2 (brain, tonsils, lung, prescapular and pulmonary lymph nodes, spleen, kidney, urinary bladder, liver, skin, and muscle), using a monoclonal anti-*Canine distemper virus* (CDV) antibody (VMRD, Pullman, WA, USA) [6]. *Toxoplasma gondii* IHC was carried out on the nine aforementioned brain tissues of each case, using a polyclonal serum of caprine origin (VMRD, Pullman, WA, USA) [6].

## 2.3. PCR and Sequence Analysis

Molecular detection of *Dolphin morbillivirus* (DMV) [12], *Herpesvirus* (HV) [13], *T. gondii* [14], and *Brucella* spp. [15] was routinely achieved on target tissues available from each case, consisting of brain, lung, tonsils, lymph nodes, liver, spleen, kidney, bladder, and blood for DMV, brain, lung, lymph nodes, spleen, and kidney for HV, brain, lymph nodes, liver,

spleen, heart, and muscle for *T. gondii*, and brain, lung, tonsils, lymph nodes, liver, spleen, kidney, and blood for *Brucella* spp.

For DMV assays, amplicons were directly sequenced using PCR primers on a 3130XL Genetic Analyzer (Thermo Fisher Scientific Inc., Waltham, MA, USA). Sequences were aligned using the SeqMan software (Lasergene package, DNASTAR Inc., Madison, WI, USA) to obtain a consensus sequence and compared with available sequences retrieved from the National Center for Biotechnology Information (NCBI) database through the BLAST tool (<http://blast.ncbi.nlm.nih.gov/Blast.cgi>, accessed on 20 February 2021).

#### 2.4. Serological, Toxicological, and Microbiological Analyses

Serological investigations to screen for the presence of specific antibodies against DMV and *T. gondii* were performed [6] on serum, CSF, and aqueous humor, when these samples were available from SD1 and SD2. These same samples were also tested by rapid serum agglutination (Rose Bengal plate test, RBT) using RBT antigen produced from *B. abortus* strain S99 [6,16] to detect anti-smooth *Brucella* spp. antibodies.

Toxicological investigations were carried out only in SD2. The toxicological analysis did not include tissues from SD1 as they were collected before implementing a sampling protocol that included contaminant analyses. Polychlorinated biphenyls (PCBs), hexachlorobenzene (HCB), and dichlorodiphenyltrichloroethanes (DDTs) were measured in blubber. Measurements were made according to Environmental Protection Agency method 8081/8082, with modifications [17], and toxicological stress was evaluated using a theoretical model [18].

Tissue samples including brain, lung, lymph nodes, liver, spleen, and kidney (SD1 and SD2) were processed for standard aerobic, anaerobic, and microaerobic (5% CO<sub>2</sub>) bacterial culture and identification, using biochemical and/or molecular analyses. Following international recommendations [19], samples from target tissues underwent specific bacteriological procedures to screen for *Salmonella* spp., *Listeria* spp., and *Brucella* spp.

#### 2.5. Light Microscopy Re-Examination for Parasite Characterization: Histology and Immunohistochemistry

CNS and heart sections from both SD1 and SD2 and skeletal muscle tissue only from SD2 were hematoxylin and eosin (H&E)-stained for light microscopy re-examination. For each organ and the aforementioned CNS areas studied, nine additional 5 µm thick sections were cut in series from stored paraffin blocks. Sections n° 1, 4, and 7 were stained with H&E for light microscopy examination. For IHC, only sections adjacent to the H&E slides presenting tissue cysts which were clearly distinct from *T. gondii* tissue cysts were used (well-defined cyst wall and >8 µm long bradyzoites). The IHC protocols included *S. neurona* polyclonal antibodies (PoAb Rabbit 1 R81, [20]), *S. falcatula* polyclonal antibodies (PoAb Rabbit 2 R-anti SF, [20]), and *S. neurona* monoclonal antibody (MAb 2G5, [21]). The IHC analyses were performed as previously described [21,22]. *Sarcocystis neurona*-infected and noninfected murine brains from interferon gamma (IFN-γ) knockout B6.129S7-Ifngtm1Ts (*Mus musculus*) (Jackson Laboratories, Bar Harbor, ME, USA) mice [23] were used, respectively, as positive and negative controls for the polyclonal antibodies, whereas *S. neurona*-infected opossum (*Didelphis virginiana*) intestine tissues and the brain of a bottlenose dolphin (*Tursiops truncatus*) foetus born under human care were used, respectively, as positive and negative control for the monoclonal antibody.

#### 2.6. Electron Microscopy Examination

Transmission electron microscopy (TEM) was performed on CNS samples of both specimens at the Spanish National Center for Electron Microscopy (Complutense University of Madrid). For each animal, two cysts were excised from the paraffin block and samples were prepared for TEM as previously described [24]. Ultra-thin sections were cut on a Leica UC6 ultramicrotome (Leica Microsystems GmbH, Wetzlar, Germany), mounted onto TEM grids, and stained with 6% saturated uranyl acetate and 3% lead citrate. Sections were

examined with a JEOL JEM 1400 Plus (JEOL USA Inc., Peabody, MA, USA) transmission electron microscope operated at 80 kV.

### 2.7. Molecular Analyses: Parasite Detection, Identification, and Characterization

Genomic DNA was extracted from CNS, myocardium, and skeletal muscle tissue samples from SD1 and SD2 and screened for the presence of tissue-cyst forming coccidia (*Sarcocystis* spp., *T. gondii* and *N. caninum*) DNA using 11 different PCR protocols, detailed in Supplementary material Table S1. DNA extraction from frozen samples was achieved using a “four-step” method, namely, ReliaPrep™ gDNA Tissue Miniprep System (Promega Italia S.r.l. Milan, Italy), whereas DNA extraction from paraffin-embedded samples, previously purified using the QIAamp DNA FFPE Tissue Kit, was achieved using QIAamp® DNA Mini Kit (QIAGEN, Hilden, Germany).

For each positive PCR result, amplicons of the expected size were sequenced using the BigDye® Terminator kit v 3.1 (Applied Biosystems, Foster City, CA, USA) and analyzed on an ABI 3130 Genetic Analyzer (Applied Biosystems). The obtained sequences were curated manually if necessary and analyzed using BioEdit software, version 7.0.5.3 [25]. Generated DNA consensus sequences were aligned to appropriate reference sequences using MEGA X software (<http://www.megasoftware.net/> accessed on 20 April 2021) [26], and compared with available sequences retrieved from the NCBI database through the BLAST tool (<http://blast.ncbi.nlm.nih.gov/Blast.cgi>, accessed on 20 February 2021).

*Toxoplasma gondii* strain genotyping analyses were carried out at the Complutense University of Madrid. DNA extracts from SD2 heart, muscle, and brain tissues were subjected to the widely used Mn-PCR restriction fragment length polymorphism (RFLP) method, with the markers *SAG1*, *SAG2* (5′–3′ *SAG2*, and alt. *SAG2*), *SAG3*, *BTUB*, *GRA6*, *c22-8*, *c29-2*, *L358*, *PK1*, *Apico*, and *CS3* [27,28]. ToxoDB RFLP genotype was identified according to <http://toxodb.org/toxo/> accessed on 20 April 2021.

## 3. Results

### 3.1. Naturally Infected Dolphins

Results of *postmortem*, routine investigations, along with anamnestic data, are summarized in Table 1.

### 3.2. Histology and Immunohistochemistry

Significant histopathological lesions detected for SD1 and SD2 are detailed in Table 1. Both SD1 and SD2 were diagnosed with severe and diffuse NS meningoencephalitis in association with the detection of protozoan tissue cysts (a single cyst for SD1 and two cysts for SD2). The cysts were morphologically distinct from *T. gondii*. In addition, SD2 was also diagnosed with *T. gondii*, whereas SD1 samples demonstrated no detectable antibodies for *T. gondii* nor detectable *T. gondii* DNA by PCR. No cysts were observed in the other target tissues investigated: muscle of SD2 and heart of both SD1 and SD2. *Morbillivirus*-specific antigens were detected in brain, urinary bladder, and muscle of SD2 by IHC, while SD1 did not show any specific staining.

All brain cysts observed in both animals stained positive with the polyclonal Ab raised for *T. gondii*. Since these data were not supported by molecular and serological investigations performed in SD1, an antigenic cross-reactivity among genetically related protozoa was hypothesized.



**Table 1.** Stranding data, body condition, most significant findings (gross and microscopic), pathogens detected, and the hypothesis of causa mortis in the two animals under study.

ID	YS	DC	NuS	Age/ Sex	Main Lesions (Gross and Microscopic)	Detected Pathogens	Cause of Death	Reference
SD1	2011	3	Poor	Adult M	Severe granulomatous pneumonia; fibrinous peritonitis; splenomegaly associated to chronic granulomatous splenitis; cholangiohepatitis; generalized lymphadenitis associated to lymphoid depletion; severe NS meningoencephalitis	<i>Photobacterium damsela</i> subsp. <i>damsela</i> (isolated from blowhole and lungs); <i>Campylobacter jejuni</i> (pancreas and liver); <i>Monorygma grimaldi</i> (musculature and peritoneum); <i>Skrjabinalius guevarai</i> (lung); anti-DMV antibodies (1:16) in blood serum (VN)	Infectious disease (parasitic and unknown agent)	[11]
SD2	2017	2	Moderate	Juvenile M	Skin ulcers; ulcerative glossitis; subcutaneous parasitic cysts; bronchointerstitial pneumonia; multifocal necrotizing hepatitis; cholangiohepatitis; splenomegaly and generalized lymphadenomegaly associated to multicentric lymphoid necrosis; interstitial nephritis; lymphadenitis; severe NS meningoencephalitis	<i>Phyllobotrium</i> spp (blubber); <i>Monorygma grimaldii</i> (musculature); <i>Brucella ceti</i> (isolation from CNS, lung, and spleen; PCR from brain, liver, lung spleen, and lymph nodes); DMV (PCR, IHC from CNS, spleen, kidney, tonsils, and lymph nodes, bladder and muscle); <i>Toxoplasma gondii</i> (PCR, IHC from CNS, lymph nodes, spleen, liver, and muscle); anti-DMV antibodies (1:8) in blood serum (VN); anti- <i>T. gondii</i> antibodies (>1:640) in blood serum, (1:160) in CSF, (1:80) in aqueous humor (IFAT). Severe immunosuppression (CAN = 0.688) [18]	Infectious disease (viral, bacterial, and parasitic)	[10]

YS = year of stranding; DC = decomposition code (2, fresh; 3, moderate autolysis); NuS = nutritional status; M = male; NS = nonsuppurative; DMV = *Dolphin morbillivirus*; VN = virus neutralization; CNS = central nervous system; PCR = polymerase chain reaction; IHC = immunohistochemistry; CSF = cerebrospinal fluid; IFAT = indirect fluorescent antibody technique; CAN = canonical variable.

### 3.3. PCR and Sequence Analysis

No biomolecular evidence of DMV, HV, *T. gondii* or *Brucella* spp. was found in SD1.

A systemic DMV infection was demonstrated in SD2, through PCR, in brain, lung, laryngeal tonsils, tracheobronchial lymph node, spleen, kidney, and bladder, and subsequently confirmed through amplicon sequencing and BLAST analysis.

However, in SD2, molecular data supported a coinfection with both *T. gondii*, in brain, liver, muscle, spleen, and tracheobronchial and pulmonary lymph nodes, and *Brucella* sp., by PCR detection, in brain, liver, lung, spleen, and tracheobronchial, pulmonary, and prescapular lymph nodes. The HV analysis was negative for SD2.

### 3.4. Serological, Toxicological, and Microbiological Analyses

Anti-Morbillivirus antibodies (1:16) were detected in serum of SD1, while anti-Morbillivirus (1:8 serum) and anti-*T. gondii* antibodies (>1:640 serum; 1:160 CSF; 1:80 aqueous humor) were detected in SD2. No evidence of anti-*Brucella* spp. antibodies was demonstrated in sera, cerebrospinal fluid, or aqueous humor samples from either of the dolphins.

For SD2, the levels of PCBs, HCB, and DDTs, expressed in  $\text{ng}\cdot\text{g}^{-1}$  on a lipid weight basis (PCBs: 136810.3; DDTs: 69866.92; HCB: 153.6; canonical variable value (CAN) = 0.688), confirmed the presence of immunotoxic levels of OC pollutants (CAN > 0.47).

*Photobacterium damsela* subsp. *damsela* was isolated by microaerobic bacterial culture from blowhole and lungs of SD1; no other significant bacteria, including *Salmonella* spp., *Listeria* spp., and *Brucella* spp., were isolated. *Brucella ceti* was isolated from CNS, spleen, and lung of SD2; no other significant bacteria, including *Listeria* spp. and *Salmonella* spp., were isolated.

### 3.5. Light Microscopy Re-Examination: Histology and Immunohistochemistry

For both SD1 and SD2, several non-*Toxoplasma* protozoal tissue cysts were observed in all the CNS areas studied, with major involvement of the brain cortical areas. Overall, neural tissue cysts were round to oval in shape, from 27 to 119.3  $\mu\text{m}$  in diameter, presented with a distinguishable, apparently smooth outer wall, and they were filled with mild basophilic bradyzoites (Figure 2). Within the range of the available magnifications, neither internal septations nor villous protrusions were visible by light microscopy. Moreover, it was not possible to detect the presence of free schizonts or merozoites in any of the brain sections examined. The histomorphological appearance was consistent with that of other apicomplexan coccidia, with most features resembling the genus *Sarcocystis*. No other cysts were observed in the heart of either case, while, in the skeletal muscle from SD2, only one tissue cyst morphologically resembling *T. gondii* was observed.

*Sarcocystis*-like tissue cysts in the brains of both SD1 and SD2 stained immunopositive with the anti-*S. neurona* polyclonal antiserum. Similar results were obtained with the anti-*S. falcatula* polyclonal antiserum whereas MAb 2G5 failed in labeling protozoal antigens. Overall, the application of the polyclonal antisera resulted in a negative staining of the cyst wall and in a sparse labeling of the enclosed bradyzoites (Figure 2).

### 3.6. Ultrastructural Description of Tissue Cysts

After processing of samples, no tissue cysts could be observed from the SD1 specimen-derived blocks, but a mature thin-walled (400 nm) cyst resembling *T. gondii* (Figure 3) was examined in dolphin SD2. Typical morphology with simple wall structure presenting vesicles, absence of septae, and small bradyzoites of  $5.3 \times 1.4 \mu\text{m}$  in size ( $n = 10$ ) were observed.

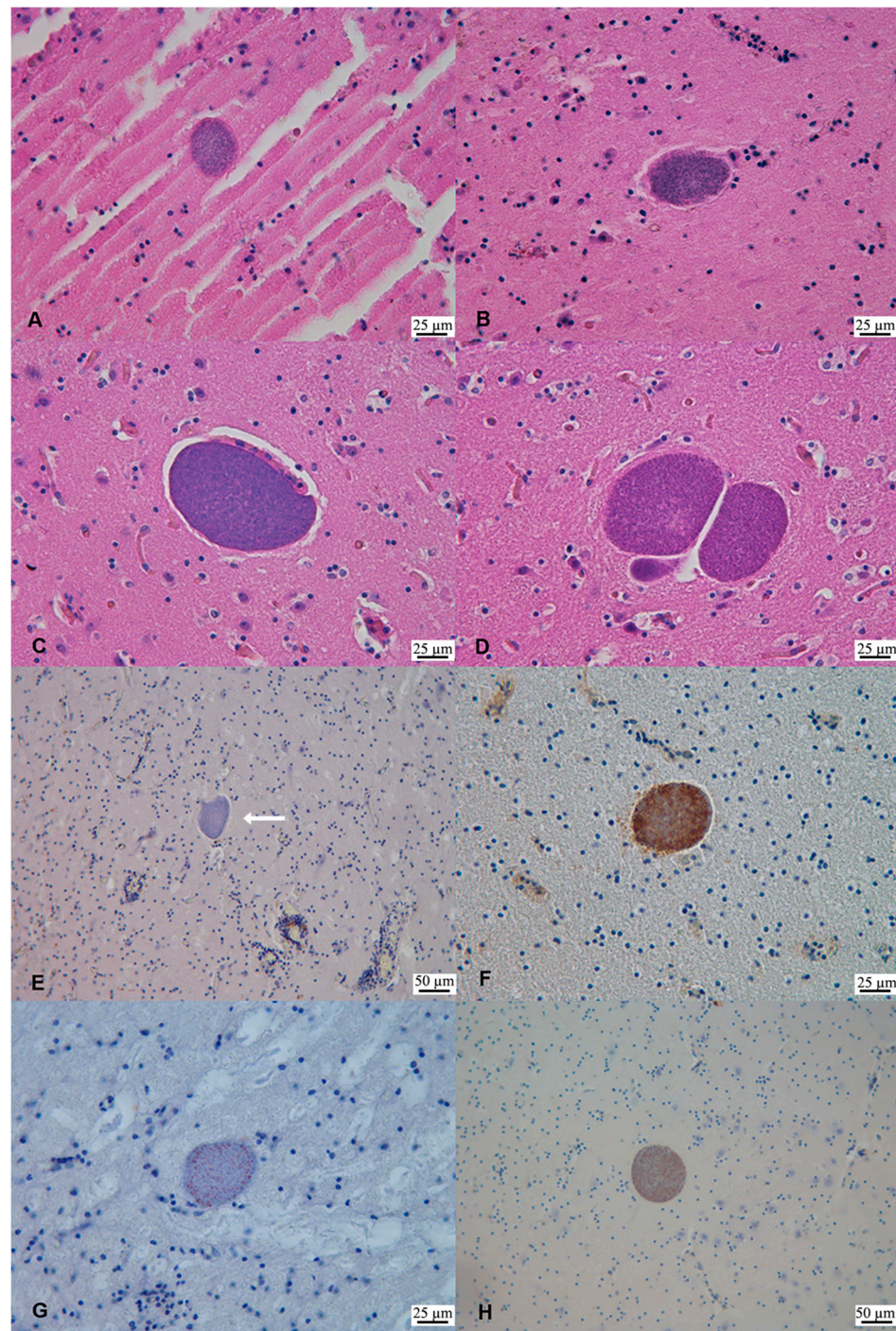


**Figure 2.** *Sarcocystis*-like tissue cysts in the brain of striped dolphins (*Stenella coeruleoalba*) SD1 and SD2 from Liguria, Italy. (A) Parietal cortex (SD1). Protozoan tissue cyst measuring  $70 \times 50 \mu\text{m}$ . H&E. (B) Occipital cortex (SD1). Protozoan tissue cyst measuring  $44.6 \times 58.1 \mu\text{m}$ . H&E. (C) Frontal cortex (SD2). Protozoan tissue cyst measuring  $72.83 \times 116.34 \mu\text{m}$ . H&E. (D) Basal ganglia (SD2). Protozoan tissue cysts measuring (left-right reading)  $110 \times 119.3 \mu\text{m}$ ,  $40 \times 19.8 \mu\text{m}$  and  $50 \times 99.1 \mu\text{m}$ . H&E. (E) Mesencephalon (SD1). Negative immunostaining of a protozoan tissue cyst (arrow). Monoclonal Ab anti-*S. neurona*. (F) Cerebellum (SD1). Positive labeling of *Sarcocystis*-like tissue cyst. Polyclonal Ab anti-*S. falcatula*. (G) Mesencephalon (SD1). Positive labeling of a protozoan tissue cyst bradyzoites. Polyclonal Ab anti-*S. neurona*. (H) Parietal cortex (SD2). Positive immunostaining of a protozoan tissue cyst bradyzoites. Polyclonal Ab anti-*S. neurona*.



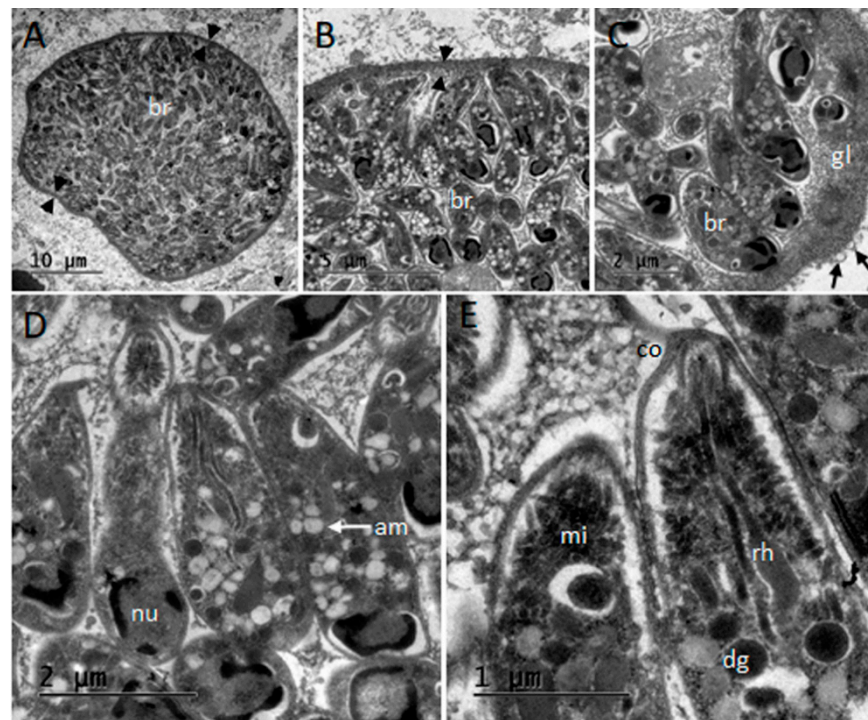


**Figure 3.** Transmission electron microscopy micrographs of the *Toxoplasma gondii* tissue cyst studied from central nervous system of striped dolphin (*Stenella coeruleoalba*) SD2 in Liguria, Italy. (A) Section of the thin-walled tissue cyst; note the cyst wall (arrowheads) and densely packaged bradyzoites (br). (B,C) Details of the simple and thin cyst wall (arrowheads) and granular layer (gl) presenting vesicles (arrows). (D,E) Ultrastructural details of bradyzoites, note: nucleus (nu), micronemes (mi), dense granules (dg), amylopectin granules (am), conoid (co), and rhoptries (rh).

### 3.7. Molecular Detection and Parasite Identification

The findings on PCR screening for tissue-cyst forming coccidia DNA are summarized in Supplementary material Table S2. PCR n.1 (18S region) and n.9 protocols showed the presence of cyst-forming coccidia DNA in at least one tissue of each animal, in agreement with histological findings. Sequencing of PCR products confirmed the absence of *T. gondii* DNA in SD1 and the presence of *T. gondii* in SD2. PCR n.5 and n.6 protocols showed the presence of *Sarcocystis* sp. DNA in the tissues from both SD1 and SD2. The *Sarcocystis* sp. DNA detection was confirmed by sequencing of the amplicons produced from DNA extracted from SD1 myocardial tissue and SD2 skeletal muscle tissue. BLAST<sup>®</sup> analysis retrieved different homology to *Sarcocystis* species infecting members of the family Bovidae, *S. hirsuta* (99.4%), and *S. buffalonis* (97.8%), respectively. These sequences were deposited in GenBank<sup>®</sup> with the following accession numbers: MW151248 (*Sarcocystis* sp.) and MW151249 (*Sarcocystis* sp.).

PCR n.7 and n.8 protocols resulted in the detection of Sarcocystidae-unspecific products in heart and brain tissues from SD2 followed by PCR n.8, and DNA sequencing which was used to confirm the presence of *T. gondii* DNA in SD2 heart and brain tissues. This finding was further documented by PCR n.10 (specific for *T. gondii* amplification). Molecular methods confirmed the presence of *T. gondii* in addition to the detection of *Sarcocystis* DNA. The molecular results suggest a potentially greater distribution of *T. gondii* parasites or higher concentration of DNA from *T. gondii* as compared to the *Sarcocystis* sp.

Phylogenetic analysis of the 18S rRNA *Sarcocystis* sp. sequence from SD2 indicated a *Sarcocystis buffalonis*-like organism (MW151249) when the sequence was compared to genetically similar species and the *Sarcocystis* spp. infecting major livestock species in Mediterranean Europe (Figure 4). The *S. hirsuta*-like sequence (MW151248) was not included in the tree because of its short length (122 bp). PCR n.11 screening for *N. caninum*

DNA resulted in none detected in both cases. All SD2 target organs tested for the presence of *T. gondii* DNA were strongly positive (100% homology with other *T. gondii* sequences deposited such as MH793505). Furthermore, all three DNA samples from SD2 were genotyped by PCR-RFLP method as ToxoDB genotype #3 showing type II alleles for all the markers except *Apico* (type I allele) (Table 2).

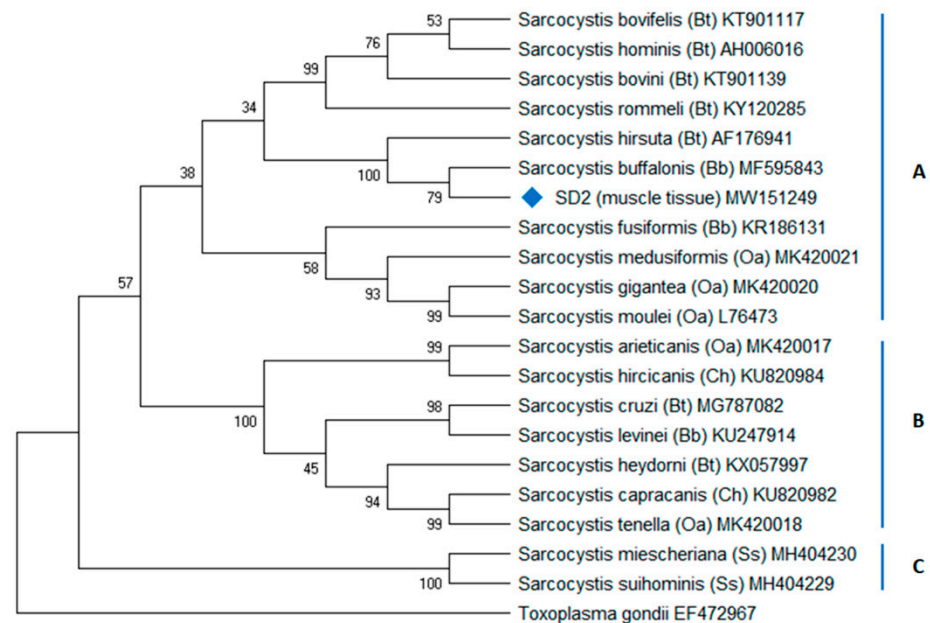


**Figure 4.** Phylogenetic positioning of the *Sarcocystis*-like organism found in muscle of striped dolphin (*Stenella coeruleoalba*) SD2 in Liguria, Italy. The evolutionary history was inferred using the maximum parsimony (MP) method. Tree n.1 out of three most parsimonious trees (length = 1532) is shown. The consistency index is (0.750000), the retention index is (0.820830), and the composite index is 0.689026 (0.615623) for all sites and parsimony-informative sites (in parentheses). The percentage of replicate trees in which the associated taxa clustered together in the bootstrap test (1000 replicates) is shown next to the branches [29]. The MP tree was obtained using the subtree-pruning-regrafting (SPR) algorithm [30] with search level 1 in which the initial trees were obtained by the random addition of sequences (10 replicates). This analysis involved 21 nucleotide sequences from *Sarcocystis* species infecting domestic hosts that are raised in Europe (Bt, *Bos taurus*; Bb, *Bubalus bubalis*, Ch, *Capra hircus*; Oa, *Ovis aries*; Ss, *Sus scrofa*). In cluster B and C, a high or moderate bootstrap (BP) value at each node supported each group containing closely related *Sarcocystis* species with canids as the definitive host, respectively, whereas, in cluster A, some low BP values indicated that the phylogenetic position of *Sarcocystis* species with felids as definitive hosts is not conclusive (BP = 34–38%). These results are probably due to the fact that the 18S rRNA locus is not the most appropriate to infer phylogenetic relationships; moreover, the short length of the SD2 sequence obtained is a limitation identified here. Nonetheless, it should be noted that neighbor-joining and maximum-likelihood methods also resulted in phylogenetic trees in which *S. hirsuta*, *S. buffalonis*, and SD2 *Sarcocystis* sp. grouped together (data not shown). There were a total of 1974 positions in the final dataset. Evolutionary analyses were conducted in MEGA X [26].

**Table 2.** Results of genotyping analysis carried out on *Toxoplasma gondii* strain identified in dolphin SD2.

Isolate/ Sample	SAG1	3'-SAG2	5'-SAG2	Alt. SAG2	SAG3	BTUB	GRA6	c22-8	C29-2	L358	PK1	Apico	ToxoDB PCR-RFLP Genotype #
RH (ref. type I)	I	I/III	I/II	I	I	I	I	I	I	I	I	I	#1
Me-49 (ref. type II)	II/III	II	I/II	II	II	II	II	II	II	II	II	II	#1
NED (ref. type III)	II/III	I/III	III	III	III	III	III	III	III	III	III	III	#2
SD2 (muscle)	II/III	II	I/II	II	II	II	II	II	II	II	II	I	#3
SD2 (CNS)	II/III	II	I/II	II	II	II	II	II	II	II	II	I	#3
SD2 (Heart)	II/III	II	I/II	II	II	II	II	II	II	II	II	I	#3

#### 4. Discussion

NS meningoencephalitis in dolphins is usually related to *B. ceti* infections, to viruses such as DMV and HV, and to protozoa, especially *T. gondii* [7,31]. In this study, involving two striped dolphins (*Stenella coeruleoalba*) stranded along the Ligurian coast of Italy, samples from SD2 demonstrated the presence of *T. gondii*, DMV, and *B. ceti*. This coinfection, alongside with the toxicological stress detected (CAN > 0.47, [18]), has been considered responsible for the cerebral impairment and the consequential animal's stranding [10]. In contrast, samples from SD1 lacked direct detection of commonly recognized neurotropic agents to explain the observed neuroinflammatory pattern present. SD1 demonstrated serological evidence of DMV infection, evident by a very low titer of antibodies, and suggestive of contact with the virus, rather than the disease, i.e., subclinical infection [32]. Therefore, a closer examination of the tissues for other potential neurotropic agents was undertaken for SD1 and SD2 for comparison.

From the histopathological examination, the morphological appearance of the unusual cysts observed in both animals was highly suggestive of a *Sarcocystis*-like coccidium. Although neither villous protrusions nor internal septations were observed, the protozoan tissue cysts were large (up to 116 µm in diameter), presented with a discernible thin outer wall, and the enclosed bradyzoites stained more basophilic than *T. gondii* ones.

As it is routinely done in suspected cases of toxoplasmosis, an immunohistochemical characterization of the unknown organism was attempted. The obtained results were inconclusive and consistent with the reviewed literature [20–22]. The reactivity of the two polyclonal *Sarcocystis* spp. antisera was mild and failed to label the tissue cyst wall. The absent reactivity of the cyst wall may be related to its maturity, as previously proposed [22]. This similar reactivity of both the anti-*S. neurona* and anti-*S. falcatula* antisera to the cysts is in agreement with what has been previously reported [20,21]. A possible broader spectrum of antigenic cross-reactivity between closely related *Sarcocystis* species and other Apicomplexa has been suggested [20,33].

It should be also noted that, during previous standard investigations, large *Sarcocystis*-like tissue cysts in the CNS of both animals stained positively to the anti-*T. gondii* PoAb, even in the absence of a molecular and serological confirmation of *T. gondii* in SD1. This finding suggests that common epitopes may be shared between these two protozoa and that the commercial anti-*T. gondii* PoAb is not specific in discriminating between these two protozoa, as previously documented by other authors [34], in cases of closely related cyst-forming apicomplexan parasites. The anti-*S. neurona* 2G5 monoclonal antibody did not stain the bradyzoites or the cyst wall of the protozoan tissue cyst in SD1 brain. Although this monoclonal antiserum is directed against a more conserved epitope among *S. neurona* strains and it is suitable to stain FFPE tissues [21], low reactivity was also observed by other authors [35] in the IHC investigations performed on the brains from California Sea otters (*Enhydra lutris nereis*) with PCR-confirmed *S. neurona* infection.

Therefore, the diagnostic value of the IHC staining is questionable and, in this study, could be limited in that both the monoclonal and polyclonal antibodies were raised against merozoite epitopes and may not be suitable to label the cyst wall or the enclosed bradyzoites [35].

As the IHC evaluations were insufficient for parasite identification, in order to have a final confirmation of the parasites detected, 11 different PCR protocols were employed in an attempt to molecularly characterize the tissue-cyst forming protozoa. *Sarcocystis* sp. infections, previously unreported in muscle tissue of Mediterranean cetaceans, were confirmed by PCR means in the myocardium and in the skeletal muscle.

PCR n.1 excluded parasite identification as *S. neurona* or *S. falcatula* in either SD1 or SD2. Moreover, the sequencing of the 18S rDNA amplicon to discern the presence of mixed protozoal infections [35] was nonspecific in SD1, resulting in exclusion of other known tissue cyst-forming coccidia, such as *T. gondii*, *N. caninum*, and *Hammondia hammondi*. *Neospora caninum* infection was also excluded by specific PCR n.11, and the thickness of the observed tissue cyst walls did not correspond to what is expected in such an organism.

The results obtained from SD2 tissues should be carefully interpreted. A majority of the DNA sequencing showed homology to *T. gondii* sequences deposited in GenBank®. SD2 was already proven coinfecting with *T. gondii* by means of PCR [14] and IHC [6] and the massive infection by *T. gondii* could have masked the detection of other pathogens, including *Sarcocystis* sp. Perhaps, in SD2, DNA extraction from purified tissue cyst would be more effective as compared to genomic DNA extracted without isolating tissue cyst from the surrounding tissue [36].

PCR protocol n.6 succeeded in amplifying *Sarcocystis* sp. DNA sequences from target organs. A short sequence (122 bp), showing high BLAST homology with *S. hirsuta*, was obtained from SD1 myocardium, whereas a longer (188 bp), high-quality sequence was obtained from SD2 skeletal muscle showing 97.8% homology with *S. buffalonis* isolates.

To date, *S. hirsuta* and *S. buffalonis* have been reported only in cattle and water buffaloes [33] and seem to be strictly intermediate host-specific, like other livestock *Sarcocystis* species, with no reported infection in non-ruminant intermediate hosts. Furthermore, in the present study, parasite identification was achieved targeting the 18S rRNA gene but other authors [37,38] recommend the analysis of *cox1* gene to molecularly discriminate between *Sarcocystis* species-infecting hosts from the Bovidae family.

Although lacking additional natural cases or experimental infections, the possibility for marine wildlife to share *Sarcocystis* species with domestic animals cannot be ruled out completely, especially when intermediate hosts are phylogenetically related. Specifically, the order Cetacea is a sister-group to the family Hippopotamidae and to the Ruminantia taxa [39] which includes also the Bovidae family.

However, considering the results of the BLAST analysis in relationship to sequence quality and the host specificity of this protozoal family, it is most likely that a previously-undescribed *Sarcocystis*-like protozoa, within the family Sarcocystidae and phylogenetically related to species cycling in livestock, is infecting Mediterranean marine mammals. The lack of reports and of prevalence data on muscular sarcocystosis in the Mediterranean makes it difficult to determine the origin of this pathogen.

Since the highest degree of similarity was observed with bovine and bubaline *Sarcocystis* species, a land-to-sea transfer can be hypothesized for this protozoon even though, in the absence of an exhaustive characterization, a marine cycle cannot be discarded. Being that most *Sarcocystis* species are highly host-specific, the hypothesis of a two-host heteroxenous marine cycle, like the one proposed for *Sarcocystis balaenopteralis* [40], seems unlikely as dolphins are apex predators rather than prey in the Mediterranean food web.

To date, *S. neurona* is commonly reported in cases of muscular and neural sarcocystosis diagnosed in marine mammals in North America [1], but its presence has not yet been reported in Europe. However, a *S. neurona* infection in Mediterranean dolphins is highly improbable due to the lack of the definitive hosts (*D. virginiana* and *D. albiventris*) which are geographically confined to the New World.



In the Mediterranean basin, protozoal meningoencephalitis has been limited to reports associated with *T. gondii* subacute to chronic infections [6,7]. A *T. gondii* infection was also confirmed and fully characterized by means of TEM, IHC, and PCR in the present study. Multilocus RFLP PCR genotyping of the *T. gondii* strain infecting SD2 retrieved a type II PRU variant genotype (ToxoDB#3), which is common in felids, livestock, and wildlife around Europe [41,42]. To date, type II genotypes account for the totality of toxoplasmosis reports in Mediterranean cetaceans [43–45] (reviewed in Table 3). Although a marine cycle for this parasite cannot be precluded, the results from SD1 and SD2 support the role of protozoa as a land-base “pollutant” that have expanded the range of their intermediate hosts to the marine environment.

**Table 3.** Summary of the available literature reporting genotyping data on *Toxoplasma gondii* strains infecting dolphins.

Host	Location	N <sup>o</sup> . of Individuals	Condition	Genotype (n)	Method (Markers)	Isolate ID	Reference
Bottlenose dolphin ( <i>Tursiops truncatus</i> )	South Carolina (USA)	3	Stranded	#1 (2/3); Unique (1/3)	PCR-RFLP (SAG1, SAG2, SAG3, BTUB, GRA6, c22-8, c29-2, L358, PK1, and Apico)	TgDoUs1-3	[46]
	Canada (born in Russia)	1	Captivity	#3 (1/1)	PCR-RFLP (B1, SAG1, SAG2, SAG3, BTUB, GRA6, c22-8, c29-2, L358, PK1, and Apico) +PCR-Seq (B1, SAG1)	TgDoCA1	[47]
Hector’s dolphins ( <i>Cephalorhynchus hectori</i> )	New Zealand	8	By caught/stranded	#3 (7/8); Type II variant (Type I + II at L358 and Type I at Apico)	PCR-RFLP (SAG1, SAG2 (5’ + 3’), SAG3, GRA6, L358, PK1, and Apico)	No isolation	[48]
Striped dolphin ( <i>Stenella coeruleoalba</i> )	Costa Rica	1	Stranded	#1 (1/1)	PCR-RFLP (SAG1, SAG2, SAG3, BTUB, GRA6, c22-8, c29-2, L358, PK1, and Apico)	TgSdCo1	[49]
	Italy	3	Stranded	Type II (2/3); Unique (1/3)	PCR-seq (B1, gra6 and uprt1)	TSL2, TSL3, and TSL6	[43]
	Italy	1	Stranded	#1 (1/1)	RFLP-PCR (SAG1, SAG2 (5’ + 3’), alt SAG2, SAG3, BTUB, GRA6)	No isolation	[45]

Previously, *Sarcocystis* spp. have not been observed in histopathological brain sections of stranded cetaceans. The only documented *Sarcocystis* sp. infection in a wild Mediterranean marine mammal is a hepatic sarcocystosis due to a *S. canis*-like protozoan infecting a striped dolphin stranded along the Spanish coast [8]. *Sarcocystis* spp. have already been reported in other marine mammals [50,51]. In aquatic species, *S. canis*-like infection causes a fatal and acute hepatitis with microscopic lesions confined to the liver [8,24,50]. Mature and immature schizonts are the protozoal stages observed during histopathological and TEM investigations, whereas tissue cysts have not been observed [8,50].

However, sarcocysts in muscle tissue are chronic lesions that have been incidentally observed in mysticetes and odontocetes from other geographical areas without associated pathology [52–56]. In previous reports, protozoal tissue cysts were attributed to *Sarcocystis* spp. only on the basis of light microscopy and TEM findings. In our study, muscular sarcocystosis was evidenced by means of PCR in each stranded dolphin. To the



authors' best knowledge, no other *Sarcocystis* species have been previously observed or isolated in Mediterranean cetaceans. Moreover, the prevalence of muscular sarcocystosis in Mediterranean marine mammals is unknown as such infections are likely overlooked during routine investigations. Therefore, it is not possible to state whether or not tissue cysts are a common finding in muscle tissues and which species of *Sarcocystis* are prevalent in Mediterranean marine mammals.

The most likely hypothesis would be to consider the same protozoa in the muscle tissues as the etiologic agents of the cysts observed in the CNS. Nevertheless, we cannot discard the possibility of two different species infecting the same host. The morphology of the observed neural cysts is highly suggestive of a *Sarcocystis*-like coccidium. It was not feasible to perform a morphological comparison with the muscle tissue cysts because SD1 FFPE skeletal muscle was not available and only *T. gondii* muscular cysts were observed in SD2 skeletal muscle sections (*data not shown*), while no cysts were identified in the heart sections of either SD1 or SD2.

As the biomolecular investigations failed in amplifying specific *Sarcocystis* sequences in the CNS, further investigations are needed to confirm our putative diagnosis.

## 5. Conclusions

The present study represents the first description of a *Sarcocystis*-like infection in muscle tissue of dolphins from the Mediterranean basin along with the first report of *Sarcocystis*-like tissue cysts in the brain of stranded cetaceans.

The *T. gondii* strain detected belongs to a common genotype circulating in Europe, while the unknown organisms were genetically similar to *Sarcocystis* species infecting the Bovidae family. Such results might suggest a land-to-sea cycling of these Apicomplexan parasites and the need for further investigations.

Because of the novelty of these findings, special attention should be reserved for the differential diagnosis of protozoal infections when performing sanitary surveillance on stranded Mediterranean cetaceans, including collection and preservation of tissues to enable a panel of characterization studies.

**Supplementary Materials:** The following are available online at <https://www.mdpi.com/article/10.3390/ani11051201/s1>, Table S1: Selected PCR protocols used in the present study to detect DNA from tissue-cyst forming coccidian, Table S2: Results of the PCR protocols screening for tissue cyst-forming coccidian DNA in target organs.

**Author Contributions:** Conceptualization, F.G., E.S., A.F. and C.C.; formal analysis, F.G., U.R.-C., A.E.M., C.G. and R.C.-B.; funding acquisition, R.C.-B. and C.C.; investigation, B.L., A.P., K.V., E.B., P.G., L.M., C.E.D.F., M.G., F.V., T.A., S.P. and M.F.-E.; methodology, F.G., U.R.-C., A.E.M., C.G. and R.C.-B.; supervision, M.C., R.C.-B. and C.C.; writing—original draft, F.G. and U.R.-C.; writing—review and editing, A.E.M., M.C., R.C.-B. and C.C. All authors have read and agreed to the published version of the manuscript.

**Funding:** This research was funded by the Italian Ministry of Health [Ricerca Corrente 2016 IZS PLV 05/16 RC].

**Institutional Review Board Statement:** Not applicable.

**Data Availability Statement:** The data presented in this study are available within the article and the Supplementary Materials. The sequences generated in the present study were submitted to the GenBank database with the following accession numbers: MW151248-MW151249.

**Acknowledgments:** The authors are grateful to Milena Monnier and Laura Serracca for their support in biomolecular analyses, to Walter Mignone for necropsy investigations and to Agustín Rebollada-Merino (VISAVET Health Surveillance Centre, UCM) for his assistance with microscope images. Rafael Calero-Bernal is part of the TOXOSOURCES consortium supported by the funding from the European Union's Horizon 2020 Research and Innovation Program under the grant agreement No 773830: One Health European Joint Program.

**Conflicts of Interest:** The authors declare no conflict of interest. The funders had no role in the design of the study; in the collection, analyses, or interpretation of data; in the writing of the manuscript, or in the decision to publish the results.

## References

1. Miller, M.A.; Shapiro, K.; Murray, M.J.; Haulena, M.; Raverty, S. Protozoan Parasites of Marine Mammals. In *CRC Handbook of Marine Mammals*; Gulland, F.M.D., Dierauf, L.A., Whitman, K.L., Eds.; CRC Press: New York, NY, USA, 2018; pp. 425–469; ISBN 9781498796873.
2. Gibson, A.K.; Raverty, S.; Lambourn, D.M.; Huggins, J.; Magargal, S.L.; Grigg, M.E. Polyparasitism is associated with increased disease severity in *Toxoplasma gondii*-infected marine sentinel species. *PLoS Negl. Trop. Dis.* **2011**, *5*, 14–16. [[CrossRef](#)]
3. Shapiro, K.; Miller, M.A.; Mazet, J. Temporal Association Between Land-Based Runoff Events and California Sea Otter (*Enhydra lutris nereis*) Protozoal Mortalities. *J. Wildl. Dis.* **2012**, *48*, 394–404. [[CrossRef](#)]
4. Van Bresse, M.; Raga, A.; Di Guardo, G.; Jepson, P.; Duignan, P.; Siebert, U.; Barrett, T.; Santos, M.; Moreno, I.; Siciliano, S.; et al. Emerging infectious diseases in cetaceans worldwide and the possible role of environmental stressors. *Dis. Aquat. Organ.* **2009**, *86*, 143–157. [[CrossRef](#)]
5. Barbosa, L.; Johnson, C.K.; Lambourn, D.M.; Gibson, A.K.; Haman, K.H.; Huggins, J.L.; Sweeny, A.R.; Sundar, N.; Raverty, S.A.; Grigg, M.E. A novel *Sarcocystis neurona* genotype XIII is associated with severe encephalitis in an unexpectedly broad range of marine mammals from the northeastern Pacific Ocean. *Int. J. Parasitol.* **2015**, *45*, 595–603. [[CrossRef](#)]
6. Di Guardo, G.; Proietto, U.; Di Francesco, C.E.; Marsilio, F.; Zaccaroni, A.; Scaravelli, D.; Mignone, W.; Garibaldi, F.; Kennedy, S.; Forster, F.; et al. Cerebral Toxoplasmosis in Striped Dolphins (*Stenella coeruleoalba*) Stranded Along the Ligurian Sea Coast of Italy. *Vet. Pathol.* **2010**, *47*, 245–253. [[CrossRef](#)]
7. Pintore, M.D.; Mignone, W.; Di Guardo, G.; Mazzariol, S.; Ballardini, M.; Florio, C.L.; Gorla, M.; Romano, A.; Caracappa, S.; Giorda, F.; et al. Neuropathologic findings in cetaceans stranded in Italy (2002–2014). *J. Wildl. Dis.* **2018**, *54*. [[CrossRef](#)] [[PubMed](#)]
8. Resendes, A.R.; Juan-Sallés, C.; Almeria, S.; Majó, N.; Domingo, M.; Dubey, J.P. Hepatic sarcocystosis in a striped dolphin (*Stenella coeruleoalba*) from the Spanish Mediterranean coast. *J. Parasitol.* **2002**, *88*, 206–209. [[CrossRef](#)]
9. Geraci, J.R.; Lounsbury, V.J. *Marine Mammals Ashore: A Field Guide for Strandings*, 2nd ed.; National Aquarium: Baltimore, MD, USA, 2005; Volume 486, ISBN 0977460908.
10. Garofolo, G.; Petrella, A.; Lucifora, G.; Di Francesco, G.; Di Guardo, G.; Pautasso, A.; Iulini, B.; Varello, K.; Giorda, F.; Gorla, M.; et al. Occurrence of *Brucella ceti* in striped dolphins from Italian Seas. *PLoS ONE* **2020**, *15*, e0240178. [[CrossRef](#)]
11. Giorda, F.; Ballardini, M.; Di Guardo, G.; Pintore, M.D.; Grattarola, C.; Iulini, B.; Mignone, W.; Gorla, M.; Serracca, L.; Varello, K.; et al. Postmortem findings in cetaceans found stranded in the Pelagos sanctuary, Italy, 2007–2014. *J. Wildl. Dis.* **2017**, *53*, 795–803. [[CrossRef](#)] [[PubMed](#)]
12. Verna, F.; Giorda, F.; Miceli, I.; Rizzo, G.; Pautasso, A.; Romano, A.; Iulini, B.; Pintore, M.D.; Mignone, W.; Grattarola, C.; et al. Detection of morbillivirus infection by RT-PCR RFLP analysis in cetaceans and carnivores. *J. Virol. Methods* **2017**, *247*, 22–27. [[CrossRef](#)]
13. VanDevanter, D.R.; Warren, P.; Bennett, L.; Schultz, E.R.; Coulter, S.; Garber, R.L.; Rose, T.M. Detection and analysis of diverse herpesviral species by consensus primer PCR. *J. Clin. Microbiol.* **1996**, *34*, 1666–1671. [[CrossRef](#)]
14. Vitale, M.; Galluzzo, P.; Currò, V.; Gozdzik, K.; Schillaci, D.; Di Marco Lo Presti, V. A high sensitive nested PCR for *Toxoplasma gondii* detection in animal and food samples. *J. Microb. Biochem. Technol.* **2013**, *05*, 39–41. [[CrossRef](#)]
15. Baily, G.G.; Krahn, J.B.; Drasar, B.S.; Stoker, N.G. Detection of *Brucella melitensis* and *Brucella abortus* by DNA amplification. *J. Trop. Med. Hyg.* **1992**, *95*, 271–275.
16. Hernández-Mora, G.; González-Barrientos, R.; Morales, J.A.; Chaves-Olarte, E.; Guzmán-Verri, C.; Baquero-Calvo, E.; De-Miguel, M.J.; Marín, C.M.; Blasco, J.M.; Moreno, E. Neurobrucellosis in stranded dolphins, Costa Rica. *Emerg. Infect. Dis.* **2008**, *14*, 1430–1433. [[CrossRef](#)]
17. Marsili, L.; Focardi, S. Chlorinated hydrocarbon (HCB, DDTs and PCBs) levels in cetaceans stranded along the Italian coasts: An overview. *Environ. Monit. Assess.* **1997**, *45*, 129–180. [[CrossRef](#)]
18. Marsili, L.; D’Agostino, A.; Bucalossi, D.; Malatesta, T.; Fossi, M.C. Theoretical models to evaluate hazard due to organochlorine compounds (OCs) in Mediterranean striped dolphin (*Stenella coeruleoalba*). *Chemosphere* **2004**, *56*, 791–801. [[CrossRef](#)]
19. World Organisation for Animal Health (OIE). *Manual of Diagnostic Tests and Vaccines for Terrestrial Animals (Terrestrial Manual)*, 8th ed.; World Organisation for Animal Health (OIE): Paris, France, 2018; ISBN 978-92-95108-18-9.
20. Dubey, J.P.; Garner, M.M.; Stetter, M.D.; Marsh, A.E.; Barr, B.C. Acute *Sarcocystis falcatula*-Like Infection in a Carmine Bee-Eater (*Merops nubicus*) and Immunohistochemical Cross Reactivity Between *Sarcocystis falcatula* and *Sarcocystis neurona*. *J. Parasitol.* **2001**, *87*, 824–832. [[CrossRef](#)]
21. Marsh, A.; Hyun, C.; Barr, B.C.; Tindall, R.; Lakritz, J. Characterization of monoclonal antibodies developed against *Sarcocystis neurona*. *Parasitol. Res.* **2002**, *88*, 501–506. [[CrossRef](#)] [[PubMed](#)]
22. Marsh, A.E.; Chaney, S.B.; Howe, D.K.; Saville, W.J.; Reed, S.M. Small sarcocysts can be a feature of experimental infections with *Sarcocystis neurona* merozoites. *Vet. Parasitol.* **2017**, *245*, 116–118. [[CrossRef](#)] [[PubMed](#)]
23. Chaney, S.B.; Marsh, A.E.; Lewis, S.; Carman, M.; Howe, D.K.; Saville, W.J.; Reed, S.M. *Sarcocystis neurona* manipulation using culture-derived merozoites for bradyzoite and sporocyst production. *Vet. Parasitol.* **2017**, *238*, 35–42. [[CrossRef](#)] [[PubMed](#)]

24. Dubey, J.P.; Calero-Bernal, R.; Rosenthal, B.M.; Speer, C.A.; Fayer, R. Unique Multiple-Host Sarcocystis Species. In *Sarcocystosis of Animals and Humans*, 2nd ed.; CRC Press: Boca Raton, FL, USA, 2015; pp. 125–168.
25. Hall, T.A. BIOEDIT: A user-friendly biological sequence alignment editor and analysis program for Windows 95/98/ NT. *Nucleic Acids Symp. Ser.* **1999**, *41*, 95–98. [[CrossRef](#)]
26. Kumar, S.; Stecher, G.; Li, M.; Nnyaz, C.; Tamura, K. MEGA X: Molecular evolutionary genetics analysis across computing platforms. *Mol. Biol. Evol.* **2018**, *35*, 1547–1549. [[CrossRef](#)]
27. Su, C.; Shwab, E.K.; Zhou, P.; Zhu, X.Q.; Dubey, J.P. Moving towards an integrated approach to molecular detection and identification of *Toxoplasma gondii*. *Parasitology* **2010**, *137*, 1–11. [[CrossRef](#)]
28. Pena, H.F.J.; Gennari, S.M.; Dubey, J.P.; Su, C. Population structure and mouse-virulence of *Toxoplasma gondii* in Brazil. *Int. J. Parasitol.* **2008**, *38*, 561–569. [[CrossRef](#)] [[PubMed](#)]
29. Felsenstein, J. Confidence Limits on Phylogenies: An Approach Using the Bootstrap. *Evolution (N. Y.)* **1985**, *39*, 783. [[CrossRef](#)]
30. Masatoshi, N.; Sudhir, K. *Molecular Evolution and Phylogenetics*; Oxford University Press: Oxford, UK, 2000; ISBN 0 19 513584 9.
31. Sierra, E.; Sánchez, S.; Saliki, J.T.; Blas-Machado, U.; Arbelo, M.; Zucca, D.; Fernández, A. Retrospective study of etiologic agents associated with nonsuppurative meningoencephalitis in stranded cetaceans in the canary Islands. *J. Clin. Microbiol.* **2014**, *52*, 2390–2397. [[CrossRef](#)]
32. Van Bresselem, M.-F.; Duignan, P.; Banyard, A.; Barbieri, M.; Colegrove, K.; De Guise, S.; Di Guardo, G.; Dobson, A.; Domingo, M.; Fauquier, D.; et al. Cetacean Morbillivirus: Current Knowledge and Future Directions. *Viruses* **2014**, *6*, 5145–5181. [[CrossRef](#)] [[PubMed](#)]
33. Dubey, J.P.; Calero-Bernal, R.; Rosenthal, B.M.; Speer, C.A.; Fayer, R. *Sarcocystosis of Animals and Humans*, 2nd ed.; CRC Press: Boca Raton, FL, USA, 2015; ISBN 9780429183188.
34. Sundermann, C.A.; Estridge, B.H.; Branton, M.S.; Bridgman, C.R.; Lindsay, D.S. Immunohistochemical diagnosis of *Toxoplasma gondii*: Potential for cross-reactivity with *Neospora caninum*. *J. Parasitol.* **1997**, *83*, 440–443. [[CrossRef](#)]
35. Miller, M.A.; Barr, B.C.; Nordhausen, R.; James, E.R.; Magargal, S.L.; Murray, M.; Conrad, P.A.; Toy-Choutka, S.; Jessup, D.A.; Grigg, M.E. Ultrastructural and molecular confirmation of the development of *Sarcocystis neurona* tissue cysts in the central nervous system of southern sea otters (*Enhydra lutris nereis*). *Int. J. Parasitol.* **2009**, *39*, 1363–1372. [[CrossRef](#)]
36. Dubey, J.P.; Calero-Bernal, R.; Rosenthal, B.M.; Speer, C.A.; Fayer, R. Techniques. In *Sarcocystosis of Animals and Humans*; CRC Press: Boca Raton, FL, USA, 2015; pp. 121–122.
37. Gjerde, B.; Hilali, M.; Abbas, I.E. Molecular differentiation of *Sarcocystis buffalonis* and *Sarcocystis levinei* in water buffaloes (*Bubalus bubalis*) from *Sarcocystis hirsuta* and *Sarcocystis cruzi* in cattle (*Bos taurus*). *Parasitol. Res.* **2016**, *115*, 2459–2471. [[CrossRef](#)]
38. Gjerde, B. Phylogenetic relationships among *Sarcocystis* species in cervids, cattle and sheep inferred from the mitochondrial cytochrome c oxidase subunit I gene. *Int. J. Parasitol.* **2013**, *43*, 579–591. [[CrossRef](#)]
39. Hassanin, A.; Delsuc, F.; Ropiquet, A.; Hammer, C.; Jansen Van Vuuren, B.; Matthee, C.; Ruiz-Garcia, M.; Catzeflis, F.; Areskoug, V.; Nguyen, T.T.; et al. Pattern and timing of diversification of Cetartiodactyla (Mammalia, Laurasiatheria), as revealed by a comprehensive analysis of mitochondrial genomes. *Comptes Rendus Biol.* **2012**, *335*, 32–50. [[CrossRef](#)]
40. Seilacher, A.; Reif, W.-E.; Wenk, P. The parasite connection in ecosystems and macroevolution. *Naturwissenschaften* **2007**, *94*, 155–169. [[CrossRef](#)]
41. Amouei, A.; Sarvi, S.; Sharif, M.; Aghayan, S.A.; Javidnia, J.; Mizani, A.; Moosazadeh, M.; Shams, N.; Hosseini, S.A.; Hosseini, S.A.; Z.; et al. A systematic review of *Toxoplasma gondii* genotypes and feline: Geographical distribution trends. *Transbound. Emerg. Dis.* **2020**, *67*, 46–64. [[CrossRef](#)]
42. Fernández-Escobar, M.; Calero-Bernal, R.; Benavides, J.; Regidor-Cerrillo, J.; Guerrero-Molina, M.C.; Gutiérrez-Expósito, D.; Collantes-Fernández, E.; Ortega-Mora, L.M. Isolation and genetic characterization of *Toxoplasma gondii* in Spanish sheep flocks. *Parasites Vectors* **2020**, *13*, 1–14. [[CrossRef](#)]
43. Di Guardo, G.; Di Cesare, A.; Otranto, D.; Casalone, C.; Iulini, B.; Mignone, W.; Tittarelli, C.; Meloni, S.; Castagna, G.; Forster, F.; et al. Genotyping of *Toxoplasma gondii* isolates in meningo-encephalitis affected striped dolphins (*Stenella coeruleoalba*) from Italy. *Vet. Parasitol.* **2011**, *183*, 31–36. [[CrossRef](#)]
44. Marcer, F.; Marchiori, E.; Centelleghè, C.; Ajzenberg, D.; Gustinelli, A.; Meroni, V.; Mazzariol, S. Parasitological and pathological findings in fin whales *Balaenoptera physalus* stranded along Italian coastlines. *Dis. Aquat. Organ.* **2019**, *133*, 25–37. [[CrossRef](#)] [[PubMed](#)]
45. Terracciano, G.; Fichi, G.; Comentale, A.; Ricci, E.; Mancusi, C.; Perrucci, S. Dolphins stranded along the tuscan coastline (Central Italy) of the “pelagos sanctuary”: A parasitological investigation. *Pathogens* **2020**, *9*, 612. [[CrossRef](#)] [[PubMed](#)]
46. Dubey, J.P.; Fair, P.A.; Sundar, N.; Velmurugan, G.; Kwok, O.C.H.H.; McFee, W.E.; Majumdar, D.; Su, C. Isolation of *Toxoplasma gondii* From Bottlenose Dolphins (*Tursiops truncatus*). *J. Parasitol.* **2008**, *94*, 821–823. [[CrossRef](#)] [[PubMed](#)]
47. Dubey, J.P.; Mergl, J.; Gehring, E.; Sundar, N.; Velmurugan, G.V.; Kwok, O.C.H.H.; Grigg, M.E.; Su, C.; Martineau, D. Toxoplasmosis in captive dolphins (*Tursiops truncatus*) and walrus (*Odobenus rosmarus*). *J. Parasitol.* **2009**, *95*, 82–85. [[CrossRef](#)] [[PubMed](#)]
48. Roe, W.D.; Howe, L.; Baker, E.J.; Burrows, L.; Hunter, S.A. An atypical genotype of *Toxoplasma gondii* as a cause of mortality in Hector’s dolphins (*Cephalorhynchus hectori*). *Vet. Parasitol.* **2013**, *192*, 67–74. [[CrossRef](#)]

49. Dubey, J.P.; Morales, J.A.; Sundar, N.; Velmurugan, G.V.; González-Barrientos, C.R.; Hernández-Mora, G.; Su, C. Isolation and genetic characterization of *Toxoplasma gondii* from striped dolphin (*Stenella coeruleoalba*) from Costa Rica. *J. Parasitol.* **2007**, *93*, 710–711. [[CrossRef](#)]
50. Calero-Bernal, R.; Mauroo, N.F.; Hui, S.W.; Kuiken, T.; van de Bildt, M.W.G.; de Jong, A.W.; Osterhaus, A.D.M.E.; Sims, L.; Gendron-Fitzpatrick, A.; Carmena, D.; et al. Acute fatal sarcocystosis hepatitis in an Indo-Pacific bottlenose dolphin (*Tursiops aduncus*) in Hong Kong. *Vet. Parasitol.* **2017**, *235*, 64–68. [[CrossRef](#)]
51. Dubey, J.P.; Zarnke, R.; Thomas, N.J.; Wong, S.K.; Van Bonn, W.; Briggs, M.; Davis, J.W.; Ewing, R.; Mense, M.; Kwok, O.C.H.; et al. *Toxoplasma gondii*, *Neospora caninum*, *Sarcocystis neurona*, and *Sarcocystis canis*-like infections in marine mammals. *Vet. Parasitol.* **2003**, *116*, 275–296. [[CrossRef](#)]
52. De Guise, S.; Lagacé, A.; Girard, C.; Béland, P. Intramuscular *Sarcocystis* in two beluga whales and an Atlantic white-sided dolphin from the St. Lawrence estuary, Quebec, Canada. *J. VET Diagn. Investig.* **1993**, *5*, 296–300. [[CrossRef](#)] [[PubMed](#)]
53. Akao, S. A New Species of *Sarcocystis* Parasitic in the Whale *Balaenoptera borealis*. *J. Protozool.* **1970**, *17*, 290–294. [[CrossRef](#)]
54. Ewing, R.; Zaias, J.; Stamper, M.A.; Bossart, G.D.; Dubey, J.P. Prevalence of *Sarcocystis* sp. in stranded Atlantic white-sided dolphins (*Lagenorhynchus acutus*). *J. Wildl. Dis.* **2002**, *38*, 291–296. [[CrossRef](#)]
55. Sierra, E.; Espinosa de los Monteros, A.; Fernández, A.; Díaz-Delgado, J.; Suárez-Santana, C.; Arbelo, M.; Sierra, M.A.; Herráez, P. Muscle Pathology in Free-Ranging Stranded Cetaceans. *Vet. Pathol.* **2017**, *54*, 298–311. [[CrossRef](#)]
56. Munday, B.L.; Mason, R.W.; Hartley, W.J.; Presidente, P.J.; Obendorf, D. *Sarcocystis* and related organisms in Australian wildlife: I. Survey findings in mammals. *J. Wildl. Dis.* **1978**, *14*, 417–433. [[CrossRef](#)] [[PubMed](#)]



**Supplementary material Table S1.** Selected PCR protocols used in the present study to detect DNA from tissue-cyst forming coccidia.

Protocol	Organism	Target region (size, bp)	Primers name	Reference
1	Tissue-cyst forming coccidia	18S rDNA (344/396)	18S FwdExt/18S RevExt/18S RevInt	[29]
	<i>S. neurona</i> and <i>S. falcatula</i>	ITS-1 (500)	ITS1 <sub>500</sub> FwdExt/ITS1 <sub>500</sub> RevExt/ITS1 <sub>500</sub> FwdInt/ITS1 <sub>500</sub> ReveInt	
2	<i>Sarcocystis</i> spp.	ITS-1 (1025-1030)	ITS-5/ITS-2	[30]
3	<i>Sarcocystis</i> spp.	ITS-1 (700)	ITS-5/ITS-SmRi	[30]
4	<i>Sarcocystis</i> spp.	ITS-1 (426)	ITS-SmFi/ITS-SmRi	[30]
5	<i>Sarcocystis</i> spp.	<i>Sarcocystis</i> spp. specific product (334)	JNB25/JD396	[31]
6	<i>Sarcocystis</i> spp.	18S rRNA (164/186)	SARf/SARf	[32]
7	<i>Sarcocystis</i> spp.	<i>cox1</i> (1038)	SF1/SR9	[33]
8	<i>Sarcocystis</i> spp.	<i>cox1</i> (1012)	SF1/SR5	[34]
9	<i>Sarcocystis</i> spp.	18S rRNA (950)	2L/2H/3H	[35]
10	<i>T. gondii</i>	ITS-1 (227)	Tg-NN1/Tg-NN2/Tg-NP1/Tg-NP2	[36]
11	<i>N. caninum</i>	Nc5 (350)	Np21+/Np6+	[37]

**Supplementary material Table S2.** Results of the PCR protocols screening for tissue-cyst forming coccidia DNA in target organs.

Case		SD1			SD2		
Target tissue	Heart (FFPE)	Muscle	Brain (FFPE)	Heart	Muscle	Brain	
PCR 1	18S primers	+	+	+	+	+	
	ITS1 <sub>500</sub> primers	–	–	–	–	–	
Seq.	NS	NS	NS	<i>T. gondii</i>	<i>T. gondii</i>	<i>T. gondii</i>	
PCR 2	–	–	–	–	–	–	
PCR 3	–	–	–	–	–	–	
PCR 4	–	–	–	–	–	–	
PCR 5	+	+	+	+	+	+	
Seq.	NS	NS	NS	NS	NS	NS	
PCR 6	+	–	–	–	+	–	
Seq.	<i>S. hirsuta</i> (99.4%)	NA	NA	NA	<i>S. buffalonis</i> (97.8%)	NA	
PCR 7	–	–	–	+	–	+	
Seq	NA	NA	NA	NS	NA	NS	
PCR 8	–	–	–	+	–	+	
Seq.	NA	NA	NA	<i>T. gondii</i>	NA	<i>T. gondii</i>	
PCR 9	–	–	+	+	+	+	
Seq.	NA	NA	NS	<i>T. gondii</i>	<i>T. gondii</i>	<i>T. gondii</i>	
PCR 10	-	-	-	+	+	+	
Seq.	NA	NA	NA	<i>T. gondii</i>	<i>T. gondii</i>	<i>T. gondii</i>	
PCR 11	–	–	–	–	–	–	

Legend: Seq: sequencing; NS: not specific; NP: not performed; NA : not applicable









19  
20

21  
22  
23  
24  
25  
26  
27  
28  
29  
30  
31  
32  
33



## Article

# Neuropathological Characterization of Dolphin Morbillivirus Infection in Cetaceans Stranded in Italy

Federica Giorda <sup>1,2,\*</sup>, Paola Crociara <sup>1,3</sup>, Barbara Iulini <sup>1</sup>, Paola Gazzuola <sup>1</sup>, Alessandra Favole <sup>1</sup>, Maria Gorla <sup>1</sup>, Laura Serracca <sup>1</sup>, Alessandro Dondo <sup>1</sup>, Maria Ines Crescio <sup>1</sup>, Tania Audino <sup>1</sup>, Simone Peletto <sup>1</sup>, Cristina Esmeralda Di Francesco <sup>4</sup>, Maria Caramelli <sup>1</sup>, Eva Sierra <sup>2</sup>, Fabio Di Nocera <sup>5</sup>, Giuseppe Lucifora <sup>5</sup>, Antonio Petrella <sup>6</sup>, Roberto Puleio <sup>7</sup>, Sandro Mazzariol <sup>8</sup>, Giovanni Di Guardo <sup>9</sup>, Cristina Casalone <sup>1</sup> and Carla Grattarola <sup>1</sup>

- <sup>1</sup> Istituto Zooprofilattico Sperimentale del Piemonte, Liguria e Valle d'Aosta, 10154 Torino, Italy; paola.crociara@gmail.com (P.C.); barbara.iulini@izsto.it (B.I.); paola.gazzuola@izsto.it (P.G.); alessandra.favole@izsto.it (A.F.); maria.gorla@izsto.it (M.G.); laura.serracca@izsto.it (L.S.); alessandro.dondo@izsto.it (A.D.); mariaines.crescio@izsto.it (M.I.C.); tania.audino@izsto.it (T.A.); simone.peletto@izsto.it (S.P.); maria.caramelli@izsto.it (M.C.); cristina.casalone@izsto.it (C.C.); carla.grattarola@izsto.it (C.G.)
- <sup>2</sup> Institute for Animal Health and Food Safety (IUSA), Faculty of Veterinary Medicine, University of Las Palmas de Gran Canaria, Las Palmas de Gran Canaria, 35416 Canary Islands, Spain; eva.sierra@ulpgc.es
- <sup>3</sup> Department of Prevention, Local Veterinary Services (ASLTO4), SS Sanità Animale, Piazza Gino Viano Bellandi, Cuorgnè, 10082 Torino, Italy
- <sup>4</sup> Faculty of Veterinary Medicine, University of Teramo, Strada Provinciale 18 Località Piano d'Accio, 64100 Teramo, Italy; cedifrancesco@unite.it
- <sup>5</sup> Istituto Zooprofilattico Sperimentale del Mezzogiorno, Via della Salute, 2, Portici, 80055 Napoli, Italy; fabio.dinocera@izsmpartici.it (F.D.N.); giuseppe.lucifora@izsmpartici.it (G.L.)
- <sup>6</sup> Istituto Zooprofilattico Sperimentale della Puglia e della Basilicata, Via Manfredonia 20, 71121 Foggia, Italy; antonio.petrella@izspb.it
- <sup>7</sup> Istituto Zooprofilattico Sperimentale della Sicilia, Via Gino Marinuzzi, 3, 90129 Palermo, Italy; roberto.puleio@izssicilia.it
- <sup>8</sup> Department of Comparative Biomedicine and Food Science, University of Padua, Legnaro, 35020 Padua, Italy; sandro.mazzariol@unipd.it
- <sup>9</sup> Retired Professor of General Pathology and Veterinary Pathophysiology, Veterinary Medical Faculty, University of Teramo, Località Piano d'Accio, 64100 Teramo, Italy; gdiguardo@unite.it
- \* Correspondence: federica.giorda@izsto.it



**Citation:** Giorda, F.; Crociara, P.; Iulini, B.; Gazzuola, P.; Favole, A.; Gorla, M.; Serracca, L.; Dondo, A.; Crescio, M.I.; Audino, T.; et al. Neuropathological Characterization of Dolphin Morbillivirus Infection in Cetaceans Stranded in Italy. *Animals* **2022**, *12*, 452. <https://doi.org/10.3390/ani12040452>

Academic Editor: Øivind Bergh

Received: 30 December 2021

Accepted: 8 February 2022

Published: 12 February 2022

**Publisher's Note:** MDPI stays neutral with regard to jurisdictional claims in published maps and institutional affiliations.



**Copyright:** © 2022 by the authors. Licensee MDPI, Basel, Switzerland. This article is an open access article distributed under the terms and conditions of the Creative Commons Attribution (CC BY) license (<https://creativecommons.org/licenses/by/4.0/>).

**Simple Summary:** There is abundant literature reporting demyelination in dogs and pinnipeds affected by morbillivirus infection, but myelinopathy is poorly investigated in stranded cetaceans affected with the virus. Also, the neuropathogenesis of cetacean morbillivirus infection has not been fully clarified, leaving questions on cell tropism unanswered. A novel dolphin morbillivirus lineage of Atlantic origin circulating in Italian waters replaced the previous Mediterranean strain in late 2015; however, differences in virulence and pathogenesis between the two strains have not yet been documented. The aims of the present study were to: describe histopathological changes and immunohistochemical findings in the central nervous system of 31 cetaceans which tested positive on molecular investigations for the two dolphin morbillivirus strains; characterize by double indirect immunofluorescence staining the areas of myelin damage. The most frequently observed morbillivirus-associated lesions were astro-microgliosis, neuronal necrosis, spongiosis, malacia, and non-suppurative meningoencephalitis. Demyelination was detected by means of a specific myelin biomarker. Inside and around the demyelinated areas there were morbillivirus antigen-bearing cells of mainly neuronal and microglial origin, associated with marked astro and microglia reactivity. Molecular and immunohistochemical analysis suggested a higher neurotropic affinity of the novel circulating strain.

**Abstract:** Cetacean morbillivirus (CeMV) is responsible for epidemic and endemic fatalities in free-ranging cetaceans. Neuro-inflammation sustained by CeMV is a leading cause of death in stranded cetaceans. A novel dolphin morbillivirus (DMV) strain of Atlantic origin circulating in Italian waters

since early 2016 has caused acute/subacute lesions associated with positive immunolabelling of the virus. To date, myelin damage has not been fully documented and investigated in cetaceans. This study describes neuropathological findings in the brain tissue of 31 cetaceans found stranded along the Italian coastline and positive for DMV infection on molecular testing. Cell changes in the areas of myelinopathy were revealed by double indirect immunofluorescence. The most frequent DMV-associated lesions were astro-microgliosis, neuronal necrosis, spongiosis, malacia, and non-suppurative meningoencephalitis. Myelin reduction and areas of demyelination were revealed by means of a specific myelin biomarker. Morbilliviral antigen immunolabelling was mainly observed in neurons and microglial cells, in association with a marked activation of microglia and astrocytes. These findings extend our knowledge of DMV-associated brain lesions and shed light on their pathogenesis.

**Keywords:** cetacean morbillivirus; cetaceans; meningoencephalitis; demyelination; neuropathology; immunofluorescence

## 1. Introduction

Neuro-inflammation is a leading cause of death in stranded cetaceans, in which the brain is found to be the only organ affected in some cases [1–3]. Viral meningoencephalitis sustained by cetacean morbillivirus (CeMV) is the most frequent form of meningoencephalitis in cetaceans [2,3]. A member of the genus *Morbillivirus* (family Paramyxoviridae, subfamily Orthoparamyxovirinae), CeMV is the natural agent with the greatest impact on cetacean health and conservation worldwide [4]. This non-segmented single-stranded RNA virus includes three well-characterized strains: dolphin morbillivirus (DMV), porpoise morbillivirus, and pilot whale morbillivirus, plus four more strains recently identified in Hawaii and the southern hemisphere [5–8].

Genomic studies on DMV sequences circulating in the Mediterranean basin in the last 30 years show that the strain is generally well conserved [9,10]. In the last 6 years, however, the DMV Mediterranean strain has been substituted by a new variant called DMV northeast (NE)-Atlantic strain originating from the coasts of Galicia and Portugal [10–12]. No difference in virulence and disease severity between the two strains has been confirmed to date [4].

Neuropathological changes due to morbillivirus infection include demyelination, which is largely reported in both marine and terrestrial species and is commonly associated with canine and phocine distemper virus infection [13–16]. Few studies have described myelin changes in cetaceans with CeMV infection to date [12,17–19]. In some cases, infection has been confirmed by Luxol Fast Blue staining, which has not always proven effective in showing demyelination, however [20].

With the present study, we describe the histopathological changes in the central nervous system (CNS) of cetaceans with DMV infection found stranded along the Italian coastline in the period 2008–2020. In addition, we document differences in the virulence of the two strains circulating in the Mediterranean Sea.

To do this, we performed neuropathological characterization of areas of demyelination/hypomyelination by means of double indirect immunofluorescence (IF) staining to reveal cell changes and viral colonization of the neuronal and glial cell populations. Myelinopathy was confirmed by successful IF staining. To the best of our knowledge, this is the first study on neuropathological characterization by means of double IF staining in marine mammals with systemic CeMV infection. In addition, it is the first application of confocal laser-scanning microscopy for in-depth analysis of CeMV infection.



## 2. Materials and Methods

### 2.1. Materials

All animals were stranded cetaceans diagnosed during routine pathological analysis and cause-of-death assessment by the Italian cetacean stranding network, Istituti Zooprofilattici Sperimentali, veterinary public health institutions under the Italian Ministry of Health. The animals were examined and submitted to complete post mortem examination according to standard protocols [21].

Epidemiological (stranding location and date) and biological data (species, sex, age class, nutritional and decomposition status) were recorded. The animals were divided into three age categories (newborn-calf, juvenile-subadult, adult) based on total body length [21,22]. The decomposition condition of the carcasses (DCC) was classified as: code 1 (extremely fresh carcass, just died); code 2 (fresh); code 3 (moderate decomposition); code 4 (advanced decomposition); and code 5 (mummified or skeletal remains) [23]. The nutritional condition state (NCC) was classified as good, moderate or poor based morphologically on anatomical parameters (e.g., convexity of dorsal profile, rib prominence, amount of body fat).

During necropsy, tissue samples from major organs were collected and divided into three aliquots for subsequent analysis: one was kept frozen at  $-20\text{ }^{\circ}\text{C}$  for microbiological analysis, one at  $-80\text{ }^{\circ}\text{C}$  for biomolecular analysis, and the third was preserved for 10 to 14 days in neutral buffered formalin for histological and immunohistochemical (IHC) analysis. When available, ten areas of the CNS were sampled and examined: basal nuclei, thalamus, mesencephalon, pons, obex, spinal cord, and frontal, parietal, occipital, and cerebellar cortex. After fixing in 10% neutral buffered formalin, the tissue samples were embedded in paraffin, cut to  $4 \pm 2\text{ }\mu\text{m}$  thick, stained with haematoxylin and eosin (H&E), and examined under a light microscope.

Serological testing to screen for specific antibodies against morbillivirus and *T. gondii* was performed on serum, cerebrospinal fluid (CSF), and aqueous humour kept frozen at  $-20\text{ }^{\circ}\text{C}$ , when available. The samples were tested by rapid serum agglutination (Rose Bengal plate test, RBT) using RBT antigen produced from *B. abortus* strain S99 [24,25] to detect anti-smooth *Brucella* spp. antibodies.

### 2.2. Neuropathological Investigation

The neuropathological reports of 188 brain samples submitted to the Italian National Reference Center for Diagnostic Activities in Stranded Marine Mammals (Centro di Referenza Nazionale per le Indagini Diagnostiche sui Mammiferi marini spiaggiati, C.Re.Di.Ma.) in the period 2007–2020 (69/188 in 2007–2015 and 119/188 in 2016–2020) were retrieved and further analysed for biomolecular investigation of DMV on the samples.

Morbillivirus IHC was carried out on tissue sections from all 188 CNS samples by means of a monoclonal anti-canine distemper virus (CDV) antibody (VMRD, Pullman, WA, USA) [25]. *T. gondii* IHC was carried out by means of a polyclonal serum of caprine origin (VMRD) on the tissue samples that showed microscopic and/or molecular evidence of protozoan infection [25].

In all, 31 animals had a morphological diagnosis of CNS inflammation or showed neurodegenerative and reactive changes referable to morbillivirus infection; 37 tested positive for DMV on PCR assay (9/37 were positive for the DMV Mediterranean variant and 28/37 for the DMV NE-Atlantic variant) [10]. Six animals were excluded: 3 were not evaluable due to advanced post mortem autolysis and 3 others presented no evidence of microscopic lesions. Only 9/66 animals (13%) resulted positive on molecular testing for DMV (Mediterranean variant) between 2007 and 2015, whereas 28/119 (23%) tested positive for DMV (NE-Atlantic variant) between 2016 and 2020.

Necropsy reports, including biological and epidemiological data, photographic material, and results of ancillary investigations of the 31 animals were retrieved and further analysed for assessment of the cases and determination of co-infection with other bacterial or viral neurotropic agents. A few cases were also previously published [1,10,12,26–30].

For the present study, the cerebral and the cerebellar cortex (because always present in the sample set) were re-examined according to the scheme devised by Sierra and colleagues (2020) [2] and slightly modified according to the description of CNS lesions reported in dogs affected by CDV [14,31]. Two independent pathologists scored the severity of meningitis, perivascular cuffing, astro-microgliosis, malacia, neuronal necrosis, and spongiosis as absent (-), minimal (+), mild (++), moderate (+++), and severe (++++); intranuclear and/or intracytoplasmic inclusion bodies (INCIBs), haemorrhage, and IHC labelling for morbillivirus were scored as absent (-) or present (+). The stage of infection, termed acute (A), subacute (S) or chronic (C), was determined by multiparametric assessment of the type of neuropathological changes, antigen detection, and presence of co-infection [2,20,31,32]. Lesions of other anatomical regions and non-CNS lesions were recorded when present.

Three animals classified as DCC 2 (fresh carcass, well-preserved tissues), without co-infection with other bacterial and viral neurotropic pathogens, but presenting severe myelinopathy (ID 9, ID 10, ID 28) and brain immunolabelling for CDV were selected for further analysis by double staining indirect immunofluorescence (IF). The aim was to reveal myelin changes and characterize the brain cell populations targeted by the virus involved in demyelinated/hypomyelinated areas in DMV infection.

To do this, selected formalin-fixed paraffin-embedded (FFPE) tissues  $4 \pm 2 \mu\text{m}$  thick (cerebral cortex for ID 9; cerebellar cortex for ID 10; cerebral and cerebellar cortex for ID 28) characterized by severe spongiosis in white matter were processed for IF analysis. Negative control tissues consisting of FFPE cerebral and cerebellar cortex samples from a striped dolphin in DCC 2 tested negative on analysis (molecular, IHC, microbiological) for other neurotropic agents, e.g., DMV, herpesvirus (HV), *T. gondii*, and *Brucella* spp., without evidence of neuropathological changes.

In detail, antigen retrieval was performed using 10 mM citrate buffer (pH 6.1) at  $95^\circ\text{C}$  for 20 min. Sections were incubated in blocking buffer (5% normal donkey serum, 0.3% Triton X-100 in 0.01 M PBS, pH 7.4) for 1 h at room temperature, then incubated for 24–48 h at  $4^\circ\text{C}$  in a solution of 0.01 M PBS, pH 7.4, containing 0.1% Triton X-100, 2% normal donkey serum, and the primary antibodies. Commercially available primary antibodies (Abs) were used: murine monoclonal anti-CDV (1:500, VMRD Inc, Pullman, WA, USA), rabbit polyclonal (poAb) anti-GFAP (1:1000; Millipore, Burlington, MA, USA) (astrocytic marker), rabbit poAb anti-Iba 1 (1:1000, Wako Chemicals Corp., Osaka, Japan) (microglia marker), rabbit poAb anti-oligodendrocyte transcription factor (Olig2) (1:250, Millipore) (oligodendrocyte marker), rabbit poAb anti-myelin proteolipid protein (PLP) (1:500, Abcam, Cambridge, MA, USA) (myelin marker), and a rabbit poAb anti-NeuN (1:1000 Abcam) (neuron marker). After several washes, the sections were incubated with appropriate solutions of donkey Alexa 488 or Alexa 555 conjugated secondary antibodies (1:1000, Thermo Fisher Scientific, Waltham, MA, USA). The slides were then washed in PBS, counterstained with 4,6-diamidino-2-phenylindole (DAPI, 1:1000, KPL, Gaithersburg, MD, USA) and mounted with Fluoromount G (SouthernBiotech, Birmingham, AL, USA). As negative internal controls, primary antibodies were eliminated and replaced by nonimmune homologous serum. All fluorescence images were captured on a confocal laser scanning microscope (Leica TCS SP8, Leica Microsystem, Wetzlar, Germany).

Since no results were obtained with the Ab anti-Olig2 in IF (see Results) dual IHC was attempted for simultaneous localization of CDV and Oligo2. Antigen retrieval was obtained using 10 mM citrate buffer (pH 6.1) at  $95^\circ\text{C}$  for 10 min. The sections were immersed in 3% hydrogen peroxide solution in methanol for 20 min to block endogenous peroxidases and subsequently pretreated with 3% normal horse serum in Tris-buffered saline with 0.1% Tween 20 detergent (TBST) for 20 min. CDV immunohistochemistry was performed first using anti-CDV Ab (VMRD Inc, Pullman, WA, USA) diluted 1:500 in TBST at  $4^\circ\text{C}$  overnight. The slides were treated with appropriate secondary antibody conjugated to biotin, then developed using avidin-conjugated horseradish peroxidase (VECTASTAIN<sup>®</sup> ABC-HRP Kit, Peroxidase-Mouse IgG, PK4002, Vector Laboratories, Burlingame, CA, USA) with DAB (K3467, Agilent Dako, Santa Clara, CA, USA) as substrate. The sections were

then submitted to Oligo2 immunohistochemistry for testing the two markers: the rabbit poAb anti-Oligo2 (1:250 Millipore, Burlington, MA, USA) and the rabbit monoclonal anti-Oligo2 Ab (1:100 Abcam, Cambridge, MA, USA) diluted in TBST and incubated at 4 °C overnight. Both anti-Oligo2 antibodies were revealed using the VECTASTAIN® ABC-HRP Kit, Peroxidase -Rabbit IgG (PK4001, Vector Laboratories, Burlingame, CA, USA) with peroxidase substrate VIP (SK-4600, Vector Laboratories, Burlingame, CA, USA). Table 1 presents the abs and their characteristics.

**Table 1.** Primary antibodies for neuropathological characterization in demyelinated/hypomyelinated areas by means of double IF and double IHC.

Antigen	Target	Antibody/ Antiserum	Host	Dilution	Source	Technique(s)
CDV-NP	Infected cells	Mono	Mouse	1:500	VMRD	IF, IHC
GFAP	Astrocyte	Poly	Rabbit	1:1000	Millipore	IF
Iba-1	Microglia	Poly	Rabbit	1:1000	Wako	IF
Myelin-PLP	Myelin	Poly	Rabbit	1:500	Abcam	IF
NeuN	Neuron	Poly	Rabbit	1:1000	Abcam	IF
Olig2	Oligodendrocyte	Poly	Rabbit	1:250	Millipore	IF, IHC
Olig2	Oligodendrocyte	Mono	Rabbit	1:100	Abcam	IHC

Legend: CDV denotes canine distemper virus; NP nucleoprotein; PLP proteolipid protein; poly polyclonal; mono monoclonal; IF immunofluorescence; IHC immunohistochemistry.

Finally, anti-myelin, anti-GFAP, anti-NeuN, and anti-Iba1 abs were validated by means of Western blot assay for their use in striped dolphin brain samples (Supplementary Materials Figure S1).

### 2.3. PCR and Sequence Analysis in CNS

Molecular detection of dolphin morbillivirus (DMV) was achieved from a fresh-frozen sample of CNS (approximately 1 g) consisting of several subsamples from different anatomical areas of the brain and the cerebellum. This was done to increase diagnostic sensitivity—given the multifocal localization of the infection [32]—with an end-point RT-PCR using degenerate primers to amplify 287 bp of the nucleoprotein (N) gene [26].

All CNS samples ( $n = 31$ ) were screened for other common neurotropic pathogens for cetaceans [1,2], including herpesvirus, *T. gondii*, and *Brucella* spp. In detail, herpesvirus detection was performed with a nested PCR using degenerate primers to amplify a region of the DNA polymerase gene [33]. *T. gondii* DNA was detected with a nested-PCR targeting the ITS1 region [34], and *Brucella* spp. with a TaqMan®*Brucella* species detection kit (Applied Biosystems, Foster City, CA, USA) for real-time PCR targeting the IS711 gene.

For DNA and RNA extraction, tissue samples (30–50 mg) were physically disrupted using a TissueLyser II homogenizer (Qiagen, Hilden, Germany) by high-speed shaking in plastic tubes with stainless-steel beads (5 mm diameter). Genomic DNA was then extracted from the disrupted tissues with an All-Prep DNA/RNA Mini kit (Qiagen, Hilden, Germany) according to the manufacturer's instructions.

The PCR products were analysed by electrophoresis on 2% agarose gel containing GelRed (Biotium, Fremont, CA, USA), compared with molecular weight markers, and then photographed on a Gel-Doc UV transilluminator system (Bio-Rad, Hercules, CA, USA).

For the DMV and herpesvirus assays, the amplicons were directly sequenced using PCR primers on a 3130XL Genetic Analyzer (Thermo Fisher Scientific Inc., Waltham, Massachusetts, USA). The sequences were aligned using SeqMan software (Lasergene package. DNASTAR Inc., Madison, WI, USA) to obtain a consensus sequence and compared with available sequences retrieved from the National Center for Biotechnology Information (NCBI) database with the BLAST tool (Available online: <http://blast.ncbi.nlm.nih.gov/Blast.cgi>; accessed on 10 November 2021). Molecular characterization to discriminate between the DMV strains was carried out as described by Bellière and colleagues [35].

#### 2.4. Microbiological Analysis of the CNS: Standard and Specific for *Brucella* Isolation

All CNS samples ( $n = 31$ ) were processed for standard aerobic, anaerobic, and microaerobic (5% CO<sub>2</sub>) bacterial culture and identification by biochemical and/or molecular analysis. Cultures for *Brucella* spp. were performed following international recommendations [36] and using selective and non-selective solid media and enrichment broths to enhance the chance of isolation.

#### 2.5. Statistical Analysis

Statistical analyses were performed using STATA 17.1 (StataCorp College Station, Texas, USA). As most of the variables are ordinal, we performed univariate analysis with the non-parametric Wilcoxon–Mann–Whitney test to compare either the individual variable (sex, age class, species) or the score of the CNS lesions (meningitis, perivascular cuffing, astro-microgliosis, malacia, neuronal necrosis, spongiosis, intranuclear and/or intracytoplasmic inclusion bodies (INCIBs), haemorrhage, and stage of infection) or the molecular or the immunohistochemical findings between the two DMV strains. Statistical significance was set at  $p < 0.05$ . Multivariate analysis was performed by means of multi-level mixed-effect logistic models, including the strain as the dependent variable, age class, and CNS lesion score, the molecular and the immunohistochemical findings as independent variables, and the individual animal as a random effect.

### 3. Results

We analysed 31 cetaceans with a microscopic diagnosis of brain inflammation or showing neurodegenerative and reactive changes associated with molecular confirmation of DMV infection: 29 striped dolphins (*Stenella coeruleoalba* Meyen, 1833) (93.5%) and 2 bottlenose dolphins (*Tursiops truncatus* Montagu, 1821) (6.5%).

History and stranding data are presented in Supplementary Materials Table S1. Males (20/31; 64.5%) outnumbered females (11/31; 35.5%). The majority were juvenile-subadults (17/31; 54.8%) while the others were adults (14/31; 45.2%); no calves/newborns were present.

Only 3/31 carcasses (9.7%) were classified as very fresh (DCC 1), most were fresh (20/31; 64.5%) (DCC 2) and 8/31 (25.8%) were moderately decomposed (DDC 3). With regard to nutritional status, 9/31 (29%) showed good, 6/31 (19.3%) moderate, and 16/31 (51.6%) poor body condition.

The animals were found stranded over a 13-year period (from October 2008 to April 2020) along the Italian coastline [13/31 (41.9%) in Liguria, 7/31 (22.6%) in Calabria, 5/31 (16.1%) in Campania, 3/31 (9.7%) in Apulia, and 3/31 (9.7%) in Sicily]. A map indicating stranding date and location is shown in Figure 1.

Supplementary Materials Table S2 presents the results of molecular, immunohistochemical, microbiological, and serological analysis, along with the type of infection (systemic or localized) based on whether organs other than the CNS tested positive by molecular testing for DMV [32]. The animals found stranded between 2008 and 2015 were diagnosed with the Mediterranean DMV variant, whereas those found between 2016 and 2020 were diagnosed with the DMV NE-Atlantic variant. Except for ID 2, in which the brain was the only organ that tested positive for DMV, all the other animals presented systemic DMV infection of at least two other organs besides the CNS and tested positive for the virus [32] (data not shown).

With regard to common neuropathogens in cetaceans (Sierra et al. 2020), 10/31 animals (32%) presented with cerebral co-infection: *T. gondii* (7/10) (ID 1, 5, 16, 24, 26, 29, 30), *T. gondii* and *Brucella ceti* (1/10) (ID 14),  $\gamma$ HV (1/10) (ID 11) and *T. gondii* and  $\gamma$ HV (1/10) (ID 20). Overall, immunostaining for *T. gondii* abs was positive in 6/9 animals. In addition, microbiological analysis revealed *P. damsela* subsp. *damsela* in 5 animals (ID 11, 14, 21, 30, 31), *Salmonella* 1,4,[5], 12:i: in ID 16, *L. ivanovii* in ID 10, and *L. innocua* in ID 21.

Overall, immunostaining against CDV abs was positive in 24/31 animals. Noteworthy with regard to the strains circulating in the Mediterranean, 3 of the animals were from the



group of 6 (50%) that tested positive on molecular testing for the DMV Mediterranean variant, while 21 were from the group of 25 animals (80%) that tested positive for the DMV NE-Atlantic variant. Anti-*Morbillivirus*, anti-*T. gondii*, and anti-*Brucella* spp. abs were detected in 13 animals. Anti-morbillivirus antibodies were detected in the serum of ID 6 (1:40), ID 11 (1:40), ID 14 (1:8), ID 17 (>1:256) and in the aqueous humour of ID 28 (1:128). Anti-*T. gondii* abs were detected in ID 1 (1:80 serum), ID 3 (>1:160 serum), ID 6 (1:80 serum), ID 11 (>1:40 serum), ID 14 (>1:40 serum, CSF, aqueous humour), ID 15 (>1:40 serum), ID 16 (>1:640 serum and aqueous humour), and ID 30 (>1:40 serum and aqueous humour). No evidence of anti-*Brucella* spp. abs was found in sera, CSF or aqueous humour in the samples from either of the dolphins tested. No results were obtained from ID 21 because of haemolysis.

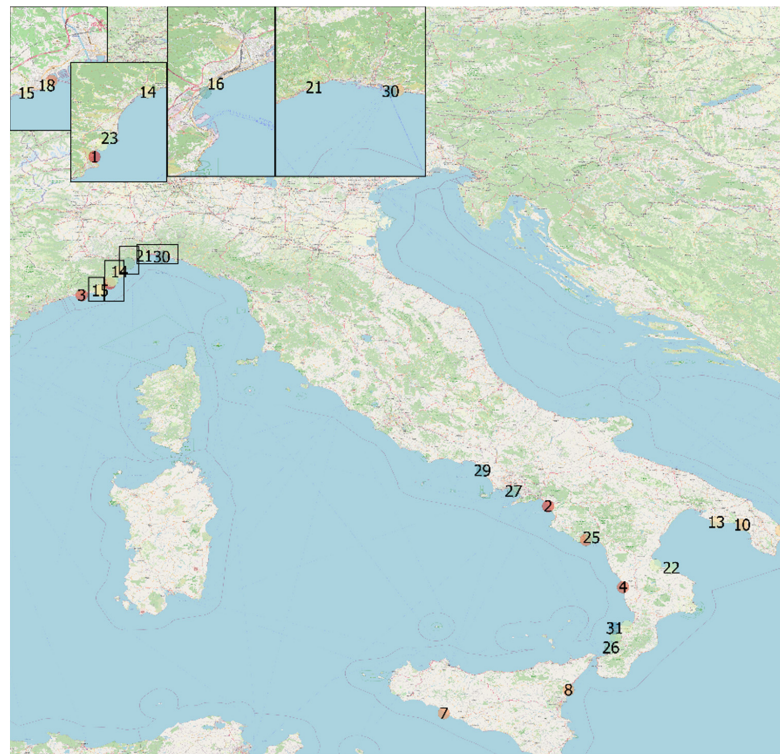


**Figure 1.** Stranding sites of cetaceans infected by dolphin morbillivirus, Italy, 2018–2020. Geographical mapping was created by M.I.C. with QGIS 3 software (QGIS Geographic Information System, QGIS association. [www.QGIS.org](http://www.QGIS.org), accessed on 29 January 2022) using the geographical coordinates found from the strandings.

Table 2 presents a description of CNS DMV-associated lesions and includes inflammatory lesions due to non-suppurative meningoencephalitis, which were classified as subacute or chronic, and acute lesions due to encephalopathy/encephalitis, comprising mainly neurodegenerative and reactive changes with minimal or absent inflammatory components [20,31,32]. In detail, the chronic form was described in only 1 animal (ID 17). Subacute forms were assigned to 17 animals (ID 1, 2, 6, 12, 14, 16, 18–24, 26, 28, 29, 31) presenting meningitis (Figure 2A) and mild to moderate perivascular cuffing (Figure 2A,B) consisting of lymphocytes and plasma cells. Acute forms were found in 13 animals (ID 3–5, 7–11, 13, 15, 25, 27, 30). Minimal to severe astro-microgliosis (Figure 2B,C,E) was present in 24 animals, frequently in those presenting inflammatory forms. Mild to moderate malacia (Figure 2D) was detected in 14 animals presenting inflammatory patterns (severe malacia was observed in 2 animals with acute forms [ID 7 and 8]). Minimal to severe neuronal necrosis (Figure 2B,E) was observed in 23 animals. Mild to severe spongiosis in white matter was a common feature in 27 animals. Three showed severe myelinopathy (ID 9, 10, 28) (Figure 3) and were selected for characterization by double IF and IHC. INCBs

were detected in only one animal (ID 19) (Figure 2G), which presented severe subacute meningoencephalitis. Finally, haemorrhage was present in 16 animals.

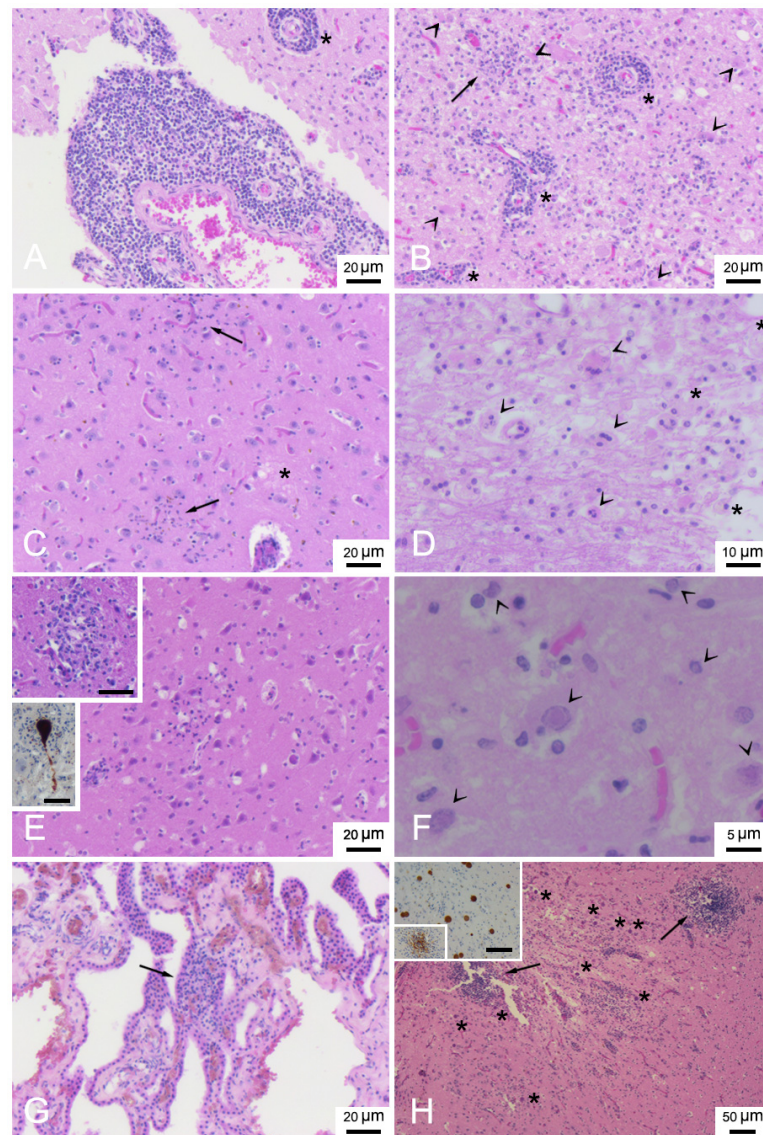


**Figure 2.** Neuropathologic lesions in stranded cetaceans with DMV infection. (A) Frontal cortex (ID 19). Severe non-suppurative meningitis and perivascular cuffing (asterisk). HE. (B) Frontal cortex (ID 19). Severe encephalitis with non-suppurative perivascular cuffing (asterisks), neuronophagic nodule of microglia cells (arrow) and diffuse astro-microgliosis with gemistocytes (arrowheads). HE. (C) Frontal cortex (ID 16). Microgliosis (arrows) and oedema (asterisk), HE. (D) Cerebellum (ID 7). Malacic area with gitter cells (asterisks) and syncytia cells (arrowheads), HE. (E) Parietal cortex (ID 31). Diffuse acute neuronal necrosis (eosinophilic and shrunken neurons) and microgliosis. Upper inset: occipital cortex (ID 24). Neuronophagic nodule of microglia cells. Scale bar = 20 µm. HE. Lower inset: pons (ID 16). Positive labelling of a neuron inside a neuronophagic nodule. Scale bar = 25 µm. IHC for DMV. (F) Occipital cortex (ID 19). Eosinophilic intranuclear inclusion bodies (arrowheads). HE. (G) Plexus choroideus (ID 14). Focal and minimal non-suppurative plexus choroiditis (arrow). HE. (H) Frontal cortex (ID 16). Severe necrotizing granulomatous encephalitis with protozoan cysts (asterisks) and two nodules of microglia and mononuclear inflammatory cells (arrow). HE. Inset: Frontal cortex (ID 16). Positive labelling of a nodule of microglia and mononuclear inflammatory cells and several protozoan cysts. Scale bar = 50 µm. IHC for *Toxoplasma gondii*.

**Table 2.** DMV-associated lesions in CNS, stage of infection, and co-infection in tissue samples from 31 animals.

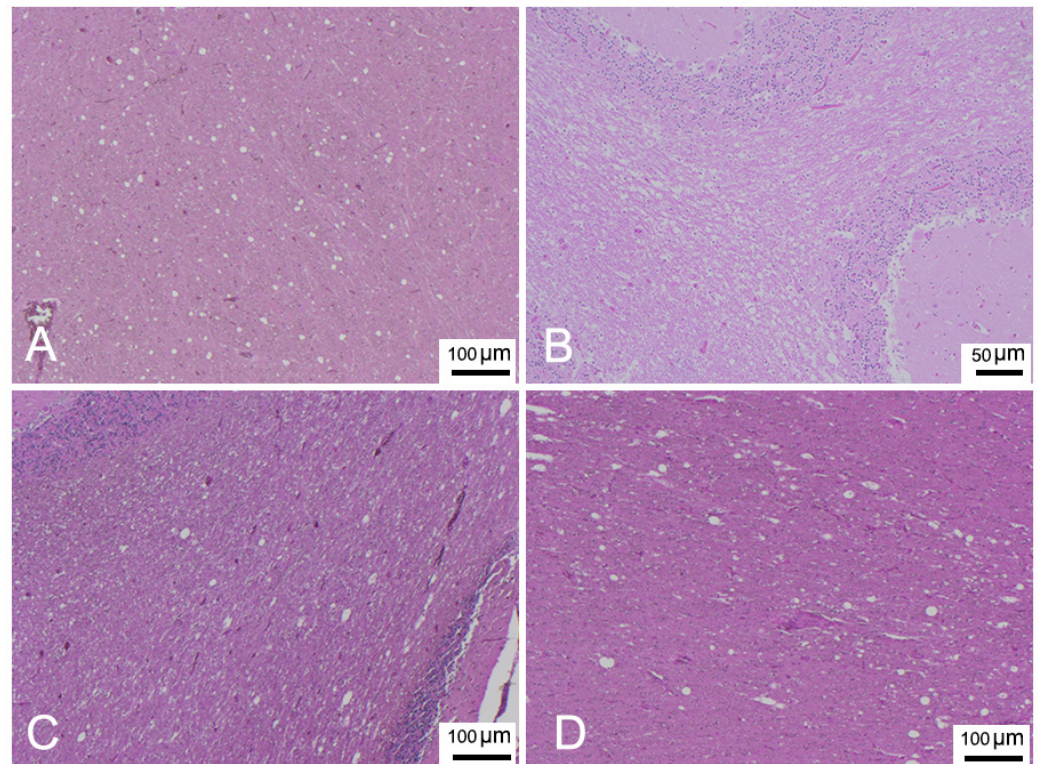
Case No.	Cerebral and Cerebellar Cortex								Lesions in Other Regions	Associated Lesions	SI	Co-Infections	References
	M	PC	Astro-Mg	Malacia	NN	S	INCIBs	H					
1	++	++	+	-	+++	+	-	+	Diffuse and mild NS meningoencephalitis associated with focal and minimal NS plexus choroiditis	Protozoan tissue cysts and syncytia	S	<i>T. gondii</i>	[1,9,10,30,37]
2	+++	+++	+++	+	+++	++	-	+	-	Syncytia	S	-	[1,10]
3	-	+	-	-	-	+++	-	-	Mild NS myelitis	-	A	-	[1,37]
4	-	-	-	-	++	+++	-	+	Multifocal and mild NS plexus choroiditis	-	A	-	[1]
5	-	+	-	-	-	++	-	-	-	-	A	<i>T. gondii</i>	[1]
6	+	++	++++	-	+++	++	-	+	Diffuse and mild NS meningoencephalitis	-	S	-	[10]
7	-	-	+++	++++	++	+++	-	+	-	Syncytia	A	-	
8	-	-	+++	++++	++	+++	-	-	Perivascular oedema	Syncytia	A	-	
9	+	-	+	-	++	++++	-	-	-	-	A	-	
10	-	-	++	++	++++	++++	-	+	-	Purkinje cell loss	A	<i>L. ivanovii</i>	[10,12]
11	-	-	++	-	-	++	-	-	Mild NS plexus choroiditis	-	A	$\gamma$ HV and <i>Photobacterium damsela</i> subsp. <i>damsela</i>	[10,12]
12	+	++	++	++	++++	+++	-	+	-	Suppurative encephalitis characterized by degenerate neutrophils	S	-	[10,12]
13	-	-	-	++	+	+++	-	+	-	-	A	-	[10,12]
14	+++	+++	+++	++	++	+	-	+	Diffuse and moderate NS meningoencephalitis associated with focal and minimal NS plexus choroiditis	Protozoan tissue cysts and syncytia Granulomatous encephalitis	S	<i>Brucella ceti</i> , <i>T. gondii</i> and <i>Photobacterium damsela</i> subsp. <i>damsela</i>	[28,29]
15	-	-	+	+	-	++	-	-	-	-	A	-	[10]
16	++	+++	+++	++	++	++	-	+	Diffuse and moderate NS meningoencephalitis and oedema	Protozoan tissue cysts and syncytia Granulomatous necrotizing encephalitis	S	<i>T. gondii</i> and <i>Salmonella</i> 1,4,[5],12:i:-; .	[10,27]
17	+++	++	-	-	-	++	-	+	Diffuse and moderate NS meningoencephalitis and myelitis	-	C	-	
18	++	-	+	-	++	+++	-	+	-	-	S	-	

Table 2. Cont.

Case No.	Cerebral and Cerebellar Cortex								Lesions in Other Regions	Associated Lesions	SI	Co-Infections	References
	M	PC	Astro-Mg	Malacia	NN	S	INCIBs	H					
19	++++	++++	++++	-	+++	+++	+	+	Multifocal and mild NS plexus choroiditis	Vasculitis, pyogranulomatous encephalitis and syncytia	S	-	
20	++	+	++	++	-	+	-	-	-	Perivascular oedema	S	<sup>γ</sup> HV+ and <i>T. gondii</i>	
21	++	++	++	+++	+++	-	-	+	Diffuse and mild NS meningoencephalitis	Vasculitis, syncytia	S	<i>Photobacterium damsela</i> subsp. <i>damsela</i> , <i>Listeria innocua</i>	
22	++	++	+++	-	+++	++	-	-	Oedema	-	S	-	
23	++	+++	+++	+++	++++	+++	-	-	Diffuse and moderate NS meningoencephalitis	Syncytia	S	-	
24	++	++	+++	-	+++	++	-	+	Focal minimal NS plexus choroiditis	Protozoan tissue cysts, syncytia, and Purkenje cell loss; granulomatous encephalitis	S	<i>T. gondii</i>	
25	-	-	-	-	-	+++	-	-	-	-	A	-	
26	+++	++	-	-	-	++	-	-	-	Protozoan tissue cysts; granulomatous encephalitis	S	<i>T. gondii</i>	
27	-	-	+++	-	++	-	-	-	-	Syncytia	A	-	
28	++	+++	+++	-	+++	++++	-	-	Diffuse and moderate NS meningoencephalitis	-	S	-	
29	+++	+++	+++	++	++	-	-	-	-	-	S	<i>T. gondii</i>	
30	-	-	++	-	+	+++	-	-	-	-	A	<i>T. gondii</i> and <i>Photobacterium damsela</i> subsp. <i>damsela</i>	
31	++	+++	+++	+	+++	-	-	+	-	-	S	<i>Photobacterium damsela</i> subsp. <i>damsela</i>	

Legend: DMV, dolphin morbillivirus; CNS, central nervous system; NS, non suppurative; M, meningitis; PC, perivascular cuffing; Mg, microgliosis; INCIBs, intranuclear and/or intracytoplasmic inclusion bodies; NN, neuronal necrosis; H, haemorrhage; S, spongiosis. Absent (-); minimal (+); mild (++); moderate (+++); severe (++++); SI, stage of infection; A, acute; S, subacute; C, chronic.





**Figure 3.** (A) Parietal cortex (ID 9). Spongiosis in white matter. HE. (B) Cerebellar cortex (ID 10). Severe myelinopathy, HE. (C) Occipital cortex (ID 28). Spongiosis in white matter. HE. (D) Cerebellar cortex (ID 28). Spongiosis in white matter. HE.

Lesions in other anatomical regions included: diffuse non-suppurative meningoencephalitis in all sections examined, along with the cerebellar and the cerebral cortex, in 8 animals (ID 1, 6, 14, 16, 17, 21, 23, 28), non-suppurative plexus choroiditis (Figure 2G) in 6 animals (ID 1, 4, 11, 14, 19, 24), non-suppurative myelitis in 2 animals (ID 3 and 17), oedema (Figure 2C) in 3 animals (ID 8, 16, 22). Associated lesions comprised syncytia (Figure 2D) in 11 animals (ID 1, 2, 7, 8, 14, 16, 19, 21, 23, 24, 27), protozoan tissue cysts associated with granulomatous encephalitis (Figure 2H) in 4 animals (ID 14, 16, 24, 26), protozoan tissue cysts alone in 1 animal (ID 1), Purkinje cell loss in 2 animals (ID 10 and 24), vasculitis in 2 animals (ID 19 and 21), suppurative and pyogranulomatous encephalitis in 1 animal each (ID 12 and 19, respectively). Three animals (ID 5, 20, 29) presented no protozoan cysts, although molecular analysis indicated co-infection with the parasite.

No differences in histopathological features and in stage of infection were found between the two strains (unfortunately, no cases from the 2013 unusual mortality event (UME) were included in the present study). No statistically significant difference between the two strains for any of the parameters was shown by either univariate or multivariate analysis.

IF labelling with anti-myelin ab in areas characterized by myelin damage in 3 animals (ID 9, 10, 28) revealed myelinopathy, with a marked reduction in myelin density and a partial loss of tissue organization (Figure 4B,C) compared to the negative control (Figure 4A), and large areas completely devoid of myelin (Figure 4E). In addition, double staining with CDV indicated viral infection in the demyelinated areas, more pronounced in ID 10 and less so in ID 28 (Figure 4D,F, respectively).



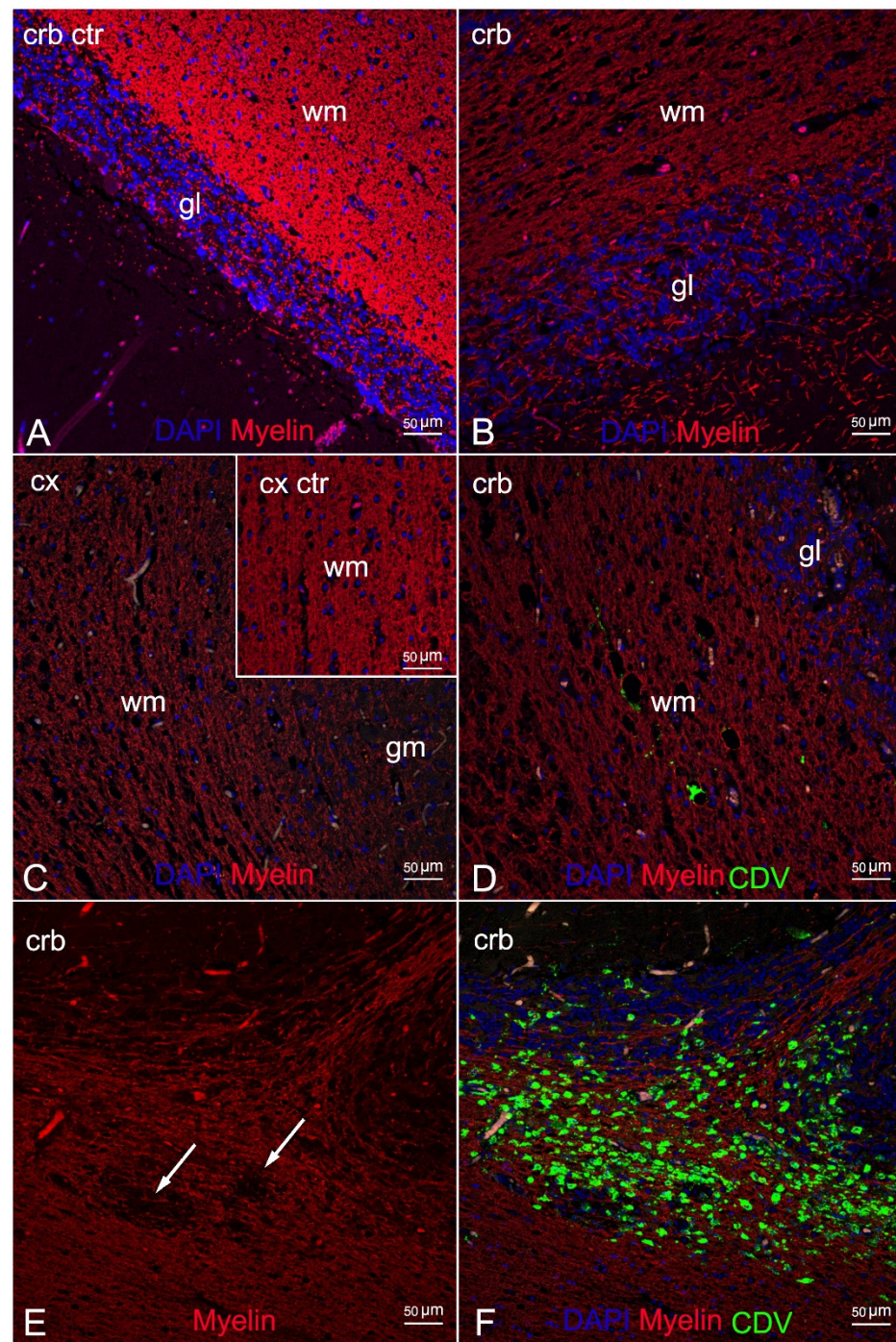


**Figure 4.** Morphological characterization of myelinopathy by means of double IF for myelin and DMV. (A) Cerebellar cortex (negative control). Myelinated white matter. (B) Cerebellar cortex (ID 28). Marked reduction in the myelin density with partial loss of tissue organization. (C) Cerebral cortex (ID 9). Severe reduction of myelin density, 20x. Inset: cortical cortex (negative control). Myelinated white matter. (D) Cerebellar cortex (ID 28). Limited DMV infection of the demyelinated white matter. (E) Cerebellar cortex (ID 10). Demyelinated white matter with complete loss of myelin (arrows). (F) Cerebellar cortex (ID 10). Severe DMV infection of the demyelinated white matter and the granular layer. Legend: wm, white matter; gm, grey matter; gl, granular layer; Cx, cortex; Crb, cerebellum; Ctr, negative control; DAPI, 4,6-diamidino-2-phenylindole; CDV, canine distemper virus.

Comparison of double staining between the anti-GFAP and the anti-CDV abs showed marked astrocytosis, with reactive astrocytes inside and around the demyelinated areas



(Figure 5B,C) but very little viral colonization in these cells, with a single area of overlapping in ID 10 (Figure 5D).

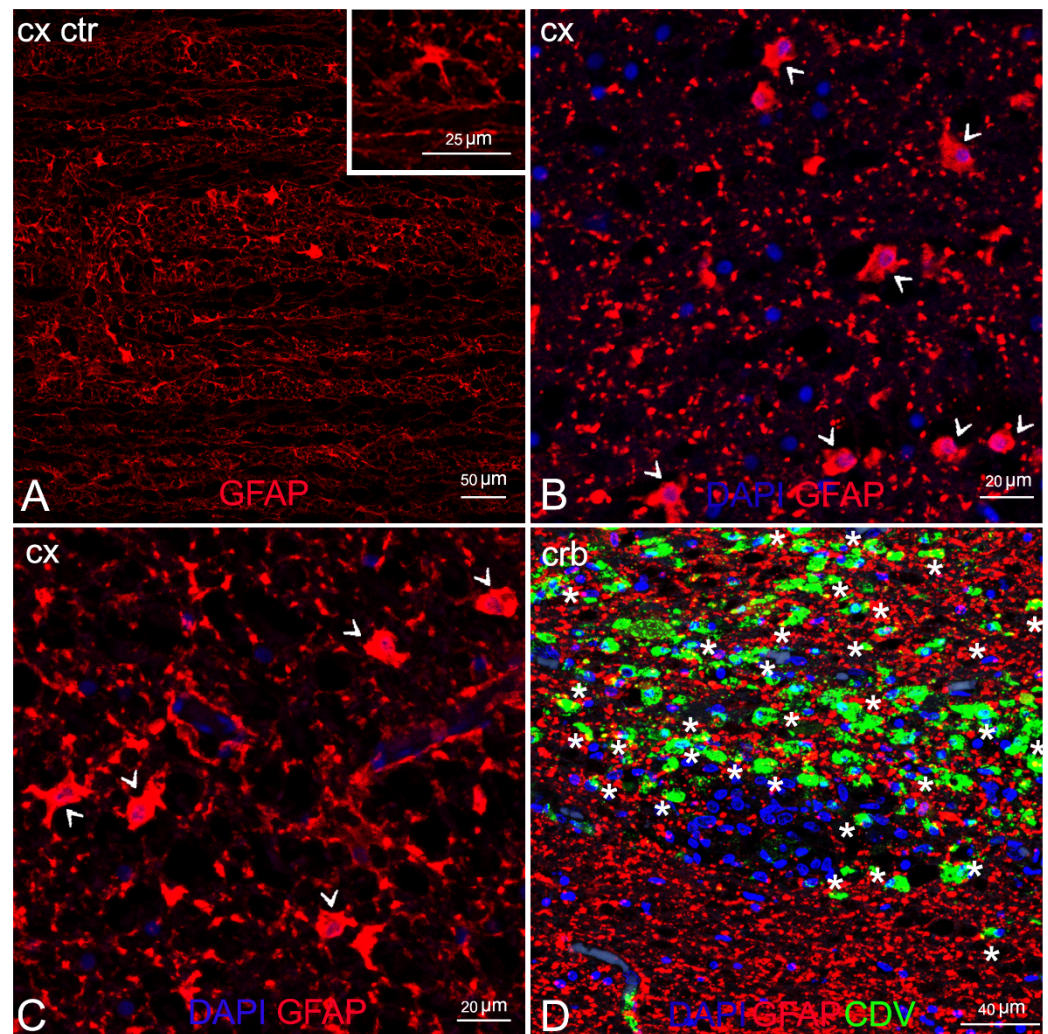


**Figure 5.** Characterization of demyelinated areas by means of double IF for astrocytes and DMV. (A) Cerebral cortex (negative control). Inset: cerebral cortex (negative control). Astrocyte in resting-state. (B) Cerebral cortex (ID 9). Several reactive astrocytes (arrowhead). (C) Cerebral cortex (ID 28). Several reactive astrocytes (arrowhead). (D) Cerebellar cortex (ID 10). Viral infection in astrocytes, co-localization anti-CDV and anti-GFAP visible in yellow (asterisks). Legend: Cx, cortex; Crb, cerebellum; Ctr, negative control; DAPI, 4,6-diamidino-2-phenylindole; CDV, canine distemper virus.

Double IF labelling with anti-CDV, anti-Iba1, and anti-NeuN demonstrated the neuronal and microglial origin of the morbillivirus antigen-bearing cells (Figures 6 and 7). In addition, severe and diffuse microglia activation was observed in all tissue sections (Figure 6B). No oligodendrocyte origin of DMV infection could be found by either double IF or through double IHC, since both anti-Olig2 markers employed failed in staining the oligodendroglia cells.

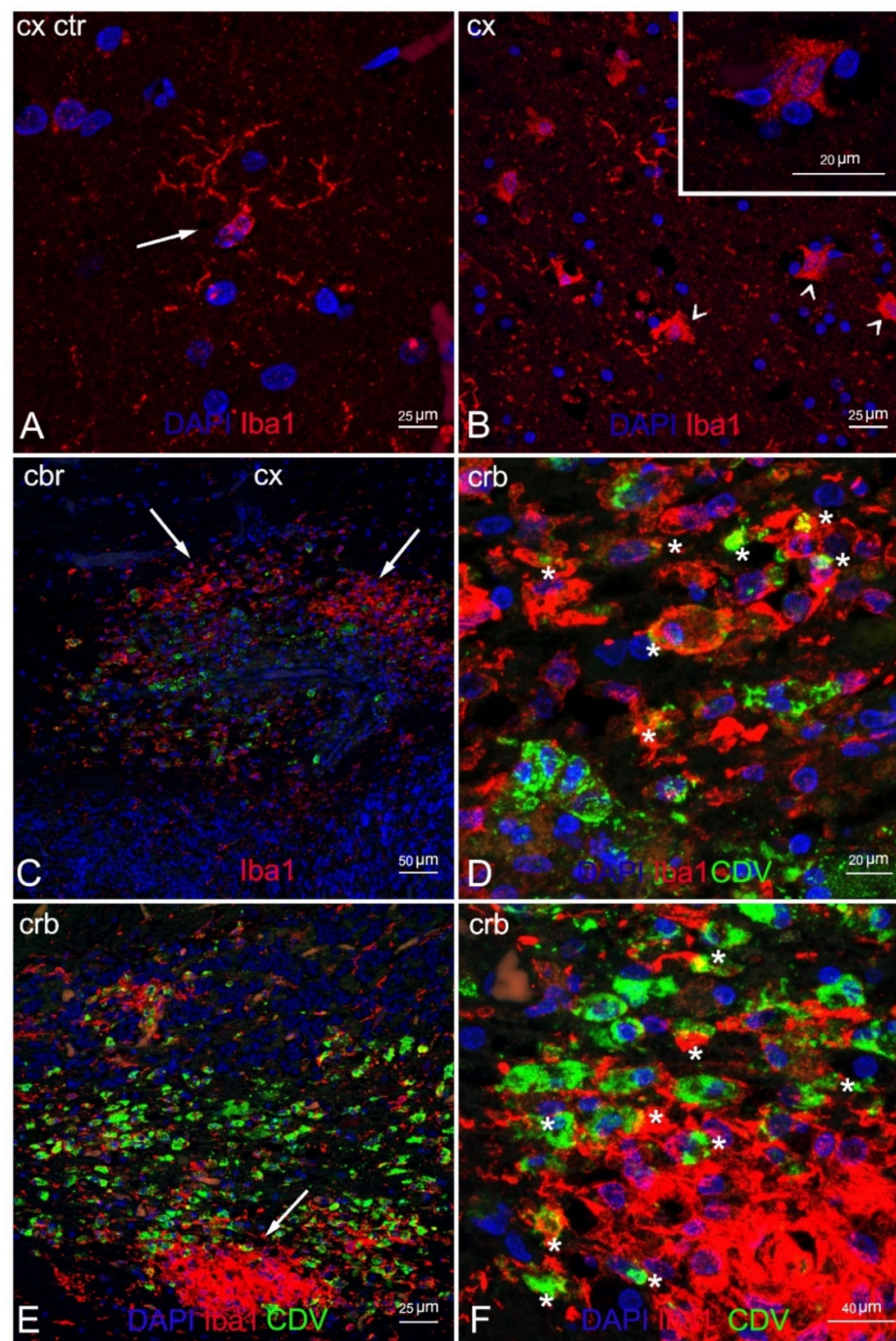


**Figure 6.** Characterization of demyelinated areas by means of double IF for microglia and DMV. (A) Cerebral cortex (negative control). Microglia in normal condition (resting state) (arrow). Note the typical ramified morphology characterizing these cells in healthy tissues. (B) Cerebral cortex (ID 28). Reactive microglia in demyelinated white matter (arrowhead). Inset: magnification of reactive microglia. (C) Cerebellar cortex (ID 10). Microgliosis in white matter (arrow) infected with DMV. (D) Magnification of image 4C. Marked co-localization of microglia and DMV (asterisks). (E) Cerebellar cortex (ID 10). Microglial nodule (arrow) positive for DMV. (F) Magnification of image 6E. Co-localization of microglia and DMV (asterisks) in the periphery of the nodule. Legend: Cx, cortex; Crb, cerebellum; Ctr, negative control; DAPI, 4,6-diamidino-2-phenylindole; CDV, canine distemper virus.



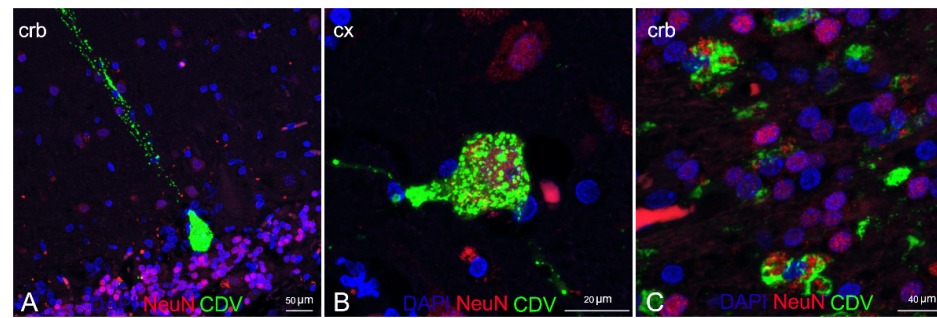


**Figure 7.** Characterization of DMV CNS infection by means of double IF for neurons and DMV. (A) Cerebellar cortex (ID 28) Purkinje cell positive for positive for DMV. (B) Cerebral cortex (ID 28). Cortical neuron positive for DMV. (C) Cerebellar cortex (ID 10). Neurons of granular layer positive for DMV. Legend: Cx, cortex; Crb, cerebellum; DAPI, 4,6-diamidino-2-phenylindole; CDV, canine distemper virus.

#### 4. Discussion

CeMV has been responsible for several outbreaks and inter-epidemic lethal diseases worldwide. Three unusual mortality events (UMEs) associated with DMV infection in the Mediterranean basin were reported for Italy and Spain (2011, 2013, 2016) [12,38,39], in addition to single disease descriptions of DMV infection along the Italian coastline reported by the C.Re.Di.Ma. in standard annual mortality rates [40–44].

Despite high levels of biomolecular positivity to DMV, the majority of the infected animals in the 2011 and 2013 Mediterranean UMEs presented milder lesions and pathological changes not directly referable to the virus but rather indicating chronic systemic DMV infection associated with secondary infection accompanied by scarce or absent immunoreactivity towards the virus [19,32,39]. In contrast, during the 2016 UME, pathological findings suggestive of acute/subacute disease were noted that resembled those reported during the Mediterranean outbreaks of 1990–1992 and 2006–2008 [45], with *Morbillivirus* immunostaining becoming a common feature in tissues testing positive on molecular tests [12].

Recent phylogenetic and phylogeographic analysis [10] on 16 strains that circulated in the last 30 years in the Mediterranean confirmed a general well-conserved homology among the strains, with an overall sequence identity >98%. A novel lineage of Atlantic origin, named NE-Atlantic strain because first detected in animals found stranded along the coasts of Galicia and Portugal in 2011–2013, started to replace the Mediterranean strain by late 2015 in Italian waters [10–12]. The first description of the NE-Atlantic strain in the Mediterranean basin refers to a sperm whale (*Physeter macrocephalus* Linnaeus, 1758) found stranded on the coast of Vasto (CH) in 2014 [10] during a mass stranding episode that involved seven individuals [46]. The animal may have been responsible for the transmission of the new strain in Italian waters, given the role of spillover host of this species [47] and the date of stranding recorded almost 2 years before the first description in small odontocetes inhabiting the same geographical area.

For this study, we retrieved the neuropathological reports on brain tissue samples from 188 cetaceans submitted to the C.Re.Di.Ma. for 2007–2020. Between 2007 and 2015, during which the DMV Mediterranean strain began circulating, 13% (9/69) of the tissue samples tested positive on molecular testing. Differently, between 2016 and 2020, when only the NE-Atlantic strain was known to circulate in Italian waters, 23% (28/119) of the brain samples tested positive for the virus. With reference to antigen detection by IHC analysis, 50% (3/6) of the tissue samples obtained during the first reporting period (DMV Mediterranean strain) showed positive labelling, whereas the percentage of brains with positive immunolabelling was increased by 80% (21/25) for the second reporting period (DMV NE-Atlantic strain). Our data, albeit not statistically significant because of the small number of specimens infected with the DMV Mediterranean strain that precluded analysis, suggest a higher neurotropic potential of the NE-Atlantic strain compared to the

Mediterranean strain. The new variant, because of its higher virulence for the CNS, does not allow the affected animals to survive the acute/subacute stage of infection, different from observations recorded during the UMEs of 2011 [19] and 2013 [39] in which the chronic forms predominated.

Almost half (45.2%) of the animals infected with the new variant were adults. This could mean that the virus was circulating within an immunologically naïve population (unfortunately, the serological analysis did not discriminate between the two variants), and resulted in severe disease. This observation differs from the events reported during the two UMEs which, probably due to a lack of specific antiviral immunity, involved mainly new-born, juveniles, and subadults [38,39].

Further studies would be of paramount importance to confirm our hypothesis for a higher neurotropic potential of the NE-Atlantic strain, with a focus on other target organs (e.g., lungs, spleen, lymph nodes) to better characterize systemic disease severity.

The present study describes the neuropathological findings in cetaceans found stranded along the Italian coastline and which received a morphological diagnosis of CNS inflammation or showed neurodegenerative and reactive changes referable to morbillivirus infection, as confirmed by molecular testing. The neuropathological changes due to DMV infection we noted are shared by previous reports [1,2,18,20,32] and are consistent with an earlier stage of acute and subacute disease: neurodegenerative and reactive alterations accompanied or not by mild-to-severe inflammatory lesions. In many animals (74%) there was minimal-to-severe diffuse neuronal necrosis in both the acute and the subacute/chronic forms, with shrunken eosinophilic neurons and neuronophagic nodules, respectively. This high percentage differs from a recent report by Sierra and colleagues [2] and may be attributable to the stage of infection (chronic forms) described in animals from the Canary Islands. Malacia was commonly observed in acute presentations characterized by gitter cells in almost half of the animals (45%). Syncytia, present in one-third of the animals in our sample, may be considered a characteristic feature of DMV since it was found in brains not co-infected with neurotropic agents (except for ID 1, 14, 16), as reported by Sierra and colleagues [2]. Half of the animals showed haemorrhage, a non-specific lesion observed also in cases of co-infection.

The most common CNS changes were astro-microgliosis and spongiosis of the white matter: astro-microgliosis was noted in 77% of animals, often in moderate and severe form, while spongiosis was seen in nearly all animals (87%) except for four (ID 21, 27, 29, 31). Minimal-to-severe non-suppurative inflammatory infiltrate in the meninges and around the vessels was responsible for a gradual transition to later stages of the disease. It was observed in almost 68% of animals (ID 5 and 9 presented acute infections). Only one animal (ID 19) presented a few neurons and astrocytes with eosinophilic intranuclear inclusion bodies, a typical and rather rare finding in DMV brain infection [2,20]. No co-infection with herpesvirus was reported in this animal. Purkinje cell loss was observed in 6% of the animals; this alteration is considered reliable only in very fresh and fresh cerebellum tissues (DDC 1 and 2). In line with previous data [2,20], vasculitis was seldom present (6%) and not associated with co-infection with common cetacean pathogens in our study. Mild-to-moderate non-suppurative plexus choroiditis was noted in six animals (19%), four of which with co-infection with other neurotropic agents. Of note is that this neuroanatomical region is the initial site of DMV brain invasion by the hematogenous route [48].

The spinal cord was rarely included in the sampling set during necropsy. Spinal cord lesions (non-suppurative myelitis) were observed in only two animals. In addition, diffuse non-suppurative meningoencephalitis was diagnosed in eight animals for which the whole cerebrum was available (exam not limited to only the cerebral and cerebellar cortex). These data highlight the importance of exhaustive sampling during post mortem examination.

In line with a previous description [20], immunostaining for the virus was not consistent for all tissue samples: positive labelling was achieved in 77% of cases (24/31).

We detected cerebral co-infection by common cetacean neurotropic agents [2] in one-third of the animals (10/31, 32%). The most frequent was *T. gondii* (9/10), alone

(7/10) or associated with *Brucella ceti* or  $\gamma$ Herpesvirus (HV) in the other two animals. Moreover,  $\gamma$ HV was also detected in one supplementary case. The activity of these agents in the pathogenesis of lesions cannot be ruled out, since histopathological alterations in co-infection can be a consequence of the overlapping of two or more pathogens [2].

*T. gondii* is a zoonotic coccidian protozoan regarded as a primary pathogen for cetaceans and responsible for toxoplasmosis, a major emerging disease in these species [25,49]. Five out of nine infected animals (ID 1, 14, 16, 24, 26) showed tissues cysts, often associated with moderate-to-severe granulomatous encephalitis, as reported in terrestrial and marine species [2,50]. Tissue cysts and zoites were confirmed by IHC labelling. Three animals tested positive on molecular testing but no cysts could be found in the sections we examined.

Brucellosis is a widespread zoonosis of public health and economic concern in many areas of the world [28]. Meningoencephalomyelitis is one of the most common lesions caused by *B. ceti* in cetaceans, [2], although infections often show subclinical development in these species [51]. The only animal (ID 14) co-infected with *B. ceti* (and *T. gondii*) showed moderate non-suppurative meningitis and focal and minimal plexus choroiditis. Although both lesions are regarded as characteristic for this bacteria [2,28], these features have also been described in animals presenting with DMV infection alone and characterized by a more severe pattern (ID 19).

Herpesvirus infection carries neuropathological significance in cetaceans. CNS damage has been confirmed in association with  $\alpha$ HV [52–54], and lesions typically referable to the infection are consistent with non-suppurative meningoencephalitis. Identifying the pathogenic role of  $\gamma$ HV is more difficult, since the association between encephalitis and meningoencephalitis and  $\gamma$ HV infection was first established in 2021 [55] in 8 animals and in one more with co-infection with  $\alpha$ HV. Since the pathological changes observed in 2 animals with  $\gamma$ HV co-infection (ID 11 and 20) closely matched the lesions characteristic for DMV, a specific role for  $\gamma$ HV in the neuropathogenesis of these lesions cannot be confirmed or ruled out.

Noteworthy with regard to cerebral co-infection with bacterial agents other than *Brucella* spp. is the isolation of *Photobacterium damseale* subs. *damselae* in five animals, of *Salmonella* 1,4,[5],12:i:-, *L. ivanovii*, and *L. innocua* in 1 animal each. *P. damsela* subsp. *damselae* is increasingly found in stranded marine mammals but little is known about its precise etiological responsibility [39,56].

As concerns the pathological significance of *Salmonella* 1,4,[5],12:i:- in cetaceans, very few cases have been documented to date, one of which is ID 16 [27]. The detection of *Salmonella* 1,4,[5],12:i:- in the brain and other tissues and biological fluids, including the blood, was attributed to a septicemic form of infection, with evidence of microscopic intestinal and vascular lesions (intestinal necrosis, vascular embolus in intestinal mesentery) [27].

*Listeria ivanovii*, widely distributed in nature, is a potential cause of listeriosis in ruminants and in immunocompromised humans, which is why it is recognized as a pathogenic agent along with *Listeria monocytogenes* [57], although a neuropathological role has not yet been confirmed [57,58]. The lesions observed in the brain of ID 10 were clearly suggestive of viral infection; a role of the bacteria in the neuropathogenesis of these features was ruled out for this reason.

*L. innocua* is generally considered nonpathogenic. Although two cases of *Listeria innocua* meningoencephalitis were described in domestic animals, one in a ewe (*Ovis aries* Linnaeus, 1758) [59] and the other in a bull (*Bos taurus* Linnaeus, 1758) in northwest Italy [60], no descriptions in marine mammals have been reported to date. Histopathological findings observed in the fatal case involving the bull [60], related to severe vasculitis often associated with large areas of necrosis and haemorrhages, may not exclude a potential role of *L. innocua* in exacerbating the lesions found in ID 21.

Serological analysis in 41% of the animals succeeded in detecting morbillivirus infection in 38% (ID 6, 11, 14, 17, 28). The negative serological findings of DMV-positive cases (ID 1, 3, 15, 16, 30) by PCR, given the simultaneous detection of other abs (anti-*T. gondii*), supports the false-negative results, which are reported to occur in serological tests



performed with heterologous *Morbillivirus* strains [32]. The absence of abs in 23% of the animals (ID 4, 18, 23) could indicate a possible immunocompromised host response or false-negative results, as reported before.

There is abundant literature on demyelinating lesions in morbillivirus infection in pinnipeds and dogs [13–16], probably in relation to the well-documented high phylogenetic correlation between CDV and phocine distemper virus [16]; however, few descriptions of myelin changes have been reported in cetaceans with CeMV infection so far [12,17–19]. In some cases confirmed by Luxol Fast Blue staining, the procedure has not always proven effective in showing demyelination [20].

Here we provide a comprehensive description of neuropathological changes in the cerebral and the cerebellar cortex of three animals characterized by severe spongiosis by means of double IF staining with specific biomarkers targeting the myelin and the brain cell populations (neurons and glial cells) coupled with the anti-CDV ab. The analysis with anti-myelin marker detected severe myelinopathy, with a reduction in myelin density and large areas completely devoid of myelin, confirming demyelination in the animals. In addition, the anti-CDV marker revealed this alteration in the presence and the absence of direct morbillivirus infection in these brain areas. A plausible explanation for the difference is the different stages of infection since demyelination is associated with viral replication in earlier stages of infection [13].

Double IF analysis using anti-GFAP, anti-NeuN, anti-Iba1 abs and coupled with anti-CDV ab showed cellular activation and viral localization of the brain cell populations inside and around the areas affected by myelinopathy. These findings provide new information about the pathogenesis of the infection.

Unlike previous descriptions of demyelinated areas in CDV infection [13], and despite marked astrocytes activation, we found very few astroglial cells infected with the virus. This observation is shared by an ultrastructural description by means of double IF analysis carried out in cetaceans affected by brain only forms of infection (BOFDI) [61]. We noted marked microglial activation, which was evident in all animals with severe viral infection of the cells. This feature is very common in canine brains with CDV infection, in which oligodendrocyte/myelin damage results from virus-induced microglia activation, which releases myelinotoxic reactive oxygen species [13,14,62].

Dual analysis with anti-NeuN and anti-CDV abs confirmed the neuronal origin of the antigen-bearing cells, as largely documented in CeMV infections [1,20,30,32].

Unfortunately, we obtained no information on oligodendrocytes infection or on oligodendrocytes ultrastructural changes as both anti-Olig2 abs failed to target the oligodendroglial cells. Therefore, several questions regarding the pathogenesis of demyelination remain unanswered: is the white matter damage a result of microglial activation induced by the virus, which we successfully documented, or rather a consequence of direct viral infection of this cell population, evaluable by observation of co-localization, as previously reported in CDV infection [13,14,62].

Future studies should be carried out using different oligodendrocyte markers, such as 2′–3′–cyclic nucleotide–3′–phosphatase (CNP) or galactocerebroside (GC), associated with the CeMV marker in dual IF. Another future area of focus is the comparative evaluation of anatomical sections of the entire brain and cerebellum to characterize the variety of cell changes occurring during CeMV brain infection.

To the best of our knowledge, this is the first study to describe myelin damage and microglial changes, as evidenced by IF analysis in cetacean brains affected by CeMV infection. The study provides novel data on ultrastructural pathology and neuropathogenetic alteration in systemic CeMV infection. To date, only one study on BOFDI forms has been published [61]. Finally, this is the first study to use confocal laser-scanning microscopy for in-depth analysis of CeMV infection.

## 5. Conclusions

A novel DMV strain, named NE-Atlantic strain, started to replace the DMV Mediterranean strain circulating in Italian waters by late 2015. Based on molecular and immunohistochemical data, this new strain seems to possess a higher neurotropic potential and to cause more severe acute/subacute disease than previously observed during the 2011 and 2013 UMEs. The most frequently observed DMV-associated lesions were astro-microgliosis, neuronal necrosis, spongiosis, malacia, and non-suppurative meningoencephalitis. Coinfection or secondary infection in one-third of the animals may have been a contributory factor to stranding. A myelin-specific biomarker proved effective in demonstrating myelin damage in cetaceans with DMV infection. Morbillivirus antigen-bearing cells of neuronal and microglia origin inside and around demyelinated areas were associated with marked astro and microglia reactivity. Very little morbillivirus staining was evident in astrocytes. These findings further our understanding of DMV-associated brain lesions, shed light on their pathogenesis, and underscore the importance of CNS examination during forensic analysis.

**Supplementary Materials:** The following are available online at <https://www.mdpi.com/article/10.3390/ani12040452/s1>, Figure S1: Western Blot to evaluate specific reactivity of different polyclonal anti-bodies against *Stenella coeruleoalba*; Table S1: Anamnestic and stranding data of thirty-one animals under study; Table S2: Results of molecular, immunohistochemical, microbiological and serological investigations and type of infection of thirty-one animals under study.

**Author Contributions:** Conceptualization, F.G., C.C., S.M. and G.D.G.; data curation, F.G. and C.G.; formal analysis, F.G., C.C., G.D.G., M.I.C. and C.G.; funding acquisition, C.C.; investigation, F.G., B.I., M.G., P.C., L.S., A.F., P.G., A.D., T.A., S.P., F.D.N., G.L., A.P., C.E.D.F. and R.P.; methodology F.G., C.G. and C.C.; software, M.I.C. and F.G.; supervision, M.C., G.D.G. and C.C.; writing—original draft, F.G., C.G., P.G. and P.C.; writing—review and editing, G.D.G., E.S. and C.G. All authors have read and agreed to the published version of the manuscript.

**Funding:** This research was funded by the Italian Ministry of Health (Ricerca Corrente 2018 IZS PLV 09/18).

**Institutional Review Board Statement:** Not applicable. Ethical review and approval were waived for this study, as neither animals were sacrificed nor experiments were performed with live animals. The permission for the management of dead stranded cetaceans was issued by the Italian Ministry of Health.

**Data Availability Statement:** The data presented in this study are available within the article and the Supplementary Materials.

**Acknowledgments:** The authors are grateful to Milena Monnier, Roberta Battistini, Lucia Florio and Claudia Palmitessa for their assistance with biomolecular, immunohistochemical and Western Blot analyses. Particular thanks are due to Walter Mignone and Enrica Berio for necropsying some of the animals for this study. A special note of thanks goes to the Department of Prevention, Local Veterinary Services (ASL 1 Imperiese) for their assistance.

**Conflicts of Interest:** The authors declare no conflict of interest. The funders had no role in the design of the study, in the collection, analysis or interpretation of data, in the writing of the manuscript or in the decision to publish the results.

## References

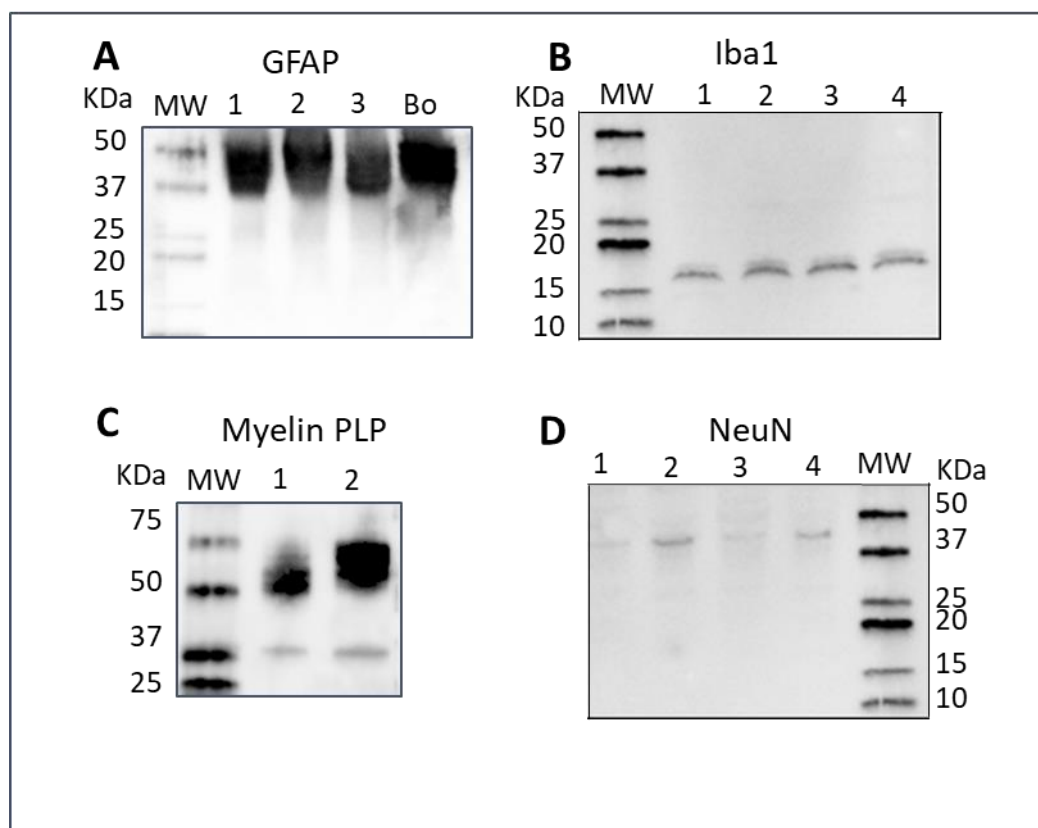
1. Pintore, M.D.; Mignone, W.; Di Guardo, G.; Mazzariol, S.; Ballardini, M.; Florio, C.L.; Gorla, M.; Romano, A.; Caracappa, S.; Giorda, F.; et al. Neuropathologic findings in cetaceans stranded in Italy (2002–14). *J. Wildl. Dis.* **2018**, *54*, 295–303. [[CrossRef](#)]
2. Sierra, E.; Fernández, A.; Felipe-Jiménez, I.; Zucca, D.; Díaz-Delgado, J.; Puig-Lozano, R.; Câmara, N.; Consoli, F.; Díaz-Santana, P.; Suárez-Santana, C.; et al. Histopathological Differential Diagnosis of Meningoencephalitis in Cetaceans: Morbillivirus, Herpesvirus, *Toxoplasma gondii*, *Brucella* sp., and *Nasitrema* sp. *Front. Vet. Sci.* **2020**, *7*, 650. [[CrossRef](#)] [[PubMed](#)]
3. Wessels, M.E.; Deaville, R.; Perkins, M.W.; Jepson, P.D.; Penrose, R.; Rocchi, M.S.; Maley, M.; Ballingall, K.T.; Dagleish, M.P. Novel Presentation of DMV-Associated Encephalitis in a Long-Finned Pilot Whale (*Globicephala melas*). *J. Comp. Pathol.* **2021**, *133*, 51–56. [[CrossRef](#)] [[PubMed](#)]

4. Zinzula, L.; Mazzariol, S.; Di Guardo, G. Molecular signatures in cetacean morbillivirus and host species proteomes: Unveiling the evolutionary dynamics of an enigmatic pathogen? *Microbiol. Immunol.* **2021**, *66*, 52–58. [[CrossRef](#)]
5. Groch, K.R.; Colosio, A.C.; Marcondes, M.C.C.; Zucca, D.; Díaz-Delgado, J.; Niemeyer, C.; Marigo, J.; Brandão, P.E.; Fernández, A.; Catão-Dias, J.L. Novel cetacean morbillivirus in Guiana Dolphin, Brazil. *Emerg. Infect. Dis.* **2014**, *20*, 511–513. [[CrossRef](#)] [[PubMed](#)]
6. West, K.L.; Sanchez, S.; Rotstein, D.; Robertson, K.M.; Dennison, S.; Levine, G.; Davis, N.; Schofield, D.; Potter, C.W.; Jensen, B. A Longman's beaked whale (*Indopacetus pacificus*) strands in Maui, Hawaii, with first case of morbillivirus in the central Pacific. *Mar. Mammal Sci.* **2013**, *29*, 767–776. [[CrossRef](#)]
7. Stephens, N.; Duignan, P.J.; Wang, J.; Bingham, J.; Finn, H.; Bejder, L.; Patterson, I.A.P.; Holyoake, C. Cetacean morbillivirus in coastal indo-pacific bottlenose dolphins, Western Australia. *Emerg. Infect. Dis.* **2014**, *20*, 666–670. [[CrossRef](#)] [[PubMed](#)]
8. West, K.L.; Silva-Krott, I.; Landrau-Giovanetti, N.; Rotstein, D.; Saliki, J.; Raverty, S.; Nielsen, O.; Popov, V.L.; Davis, N.; Walker, W.A.; et al. Novel cetacean morbillivirus in a rare Fraser's dolphin (*Lagenodelphis hosei*) stranding from Maui, Hawai'i. *Sci. Rep.* **2021**, *11*, 15986. [[CrossRef](#)]
9. Peletto, S.; Caruso, C.; Cerutti, F.; Modesto, P.; Biolatti, C.; Pautasso, A.; Grattarola, C.; Giorda, F.; Mazzariol, S.; Mignone, W.; et al. Efficient isolation on Vero.DogSLAMtag cells and full genome characterization of Dolphin Morbillivirus (DMV) by next generation sequencing. *Sci. Rep.* **2018**, *8*, 860. [[CrossRef](#)]
10. Cerutti, F.; Giorda, F.; Grattarola, C.; Mignone, W.; Beltramo, C.; Keck, N.; Lorusso, A.; Di Francesco, G.; Di Renzo, L.; Di Guardo, G.; et al. Specific capture and whole-genome phylogeography of Dolphin morbillivirus. *Sci. Rep.* **2020**, *10*, 20831. [[CrossRef](#)]
11. Mira, F.; Rubio-Guerri, C.; Purpari, G.; Puleio, R.; Caracappa, G.; Gucciardi, F.; Russotto, L.; Loria, G.R.; Guercio, A. Circulation of a novel strain of dolphin morbillivirus (DMV) in stranded cetaceans in the Mediterranean Sea. *Sci. Rep.* **2019**, *9*, 9792. [[CrossRef](#)]
12. Pautasso, A.; Iulini, B.; Grattarola, C.; Giorda, F.; Gorla, M.; Peletto, S.; Masoero, L.; Mignone, W.; Varello, K.; Petrella, A.; et al. Novel dolphin morbillivirus (DMV) outbreak among Mediterranean striped dolphins *Stenella coeruleoalba* in Italian waters. *Dis. Aquat. Organ.* **2019**, *132*, 215–220. [[CrossRef](#)]
13. Vandeveld, M.; Zurbriggen, A. Demyelination in canine distemper virus infection: A review. *Acta Neuropathol.* **2005**, *109*, 56–68. [[CrossRef](#)]
14. Ulrich, R.; Puff, C.; Wewetzer, K.; Kalkuhl, A.; Deschl, U.; Baumgärtner, W. Transcriptional changes in canine distemper virus-induced demyelinating leukoencephalitis favor a biphasic mode of demyelination. *PLoS ONE* **2014**, *9*. [[CrossRef](#)] [[PubMed](#)]
15. Mazzariol, S.; Peletto, S.; Mondin, A.; Centellegh, C.; Di Guardo, G.; Di Francesco, C.E.; Casalone, C.; Acutis, P.L. Dolphin morbillivirus infection in a captive harbor seal (*phoca vitulina*). *J. Clin. Microbiol.* **2013**, *51*, 708–711. [[CrossRef](#)] [[PubMed](#)]
16. Duignan, P.J.; Van Bresse, M.F.; Baker, J.D.; Barbieri, M.; Colegrove, K.M.; de Guise, S.; de Swart, R.L.; di Guardo, G.; Dobson, A.; Duprex, W.P.; et al. Phocine distemper Virus: Current knowledge and future directions. *Viruses* **2014**, *6*, 5093–5134. [[CrossRef](#)]
17. Duignan, P.J.; Geraci, J.R.; Raga, J.A.; Calzada, N. Pathology of morbillivirus infection in striped dolphins (*Stenella coeruleoalba*) from Valencia and Murcia, Spain. *Can. J. Vet. Res.* **1992**, *56*, 242–248. [[PubMed](#)]
18. Domingo, M.; Vilafranca, M.; Visa, J.; Prats, N.; Trudgett, A.; Visser, I. Evidence for chronic morbillivirus infection in the Mediterranean striped dolphin (*Stenella coeruleoalba*). *Vet. Microbiol.* **1995**, *44*, 229–239. [[CrossRef](#)]
19. Soto, S.; Alba, A.; Ganges, L.; Vidal, E.; Raga, J.A.; Alegre, F.; González, B.; Medina, P.; Zorrilla, I.; Martínez, J.; et al. Post-epizootic chronic dolphin morbillivirus infection in Mediterranean striped dolphins *Stenella coeruleoalba*. *Dis. Aquat. Organ.* **2011**, *96*, 187–194. [[CrossRef](#)]
20. Díaz-Delgado, J.; Groch, K.R.; Sierra, E.; Sacchini, S.; Zucca, D.; Quesada-Canales, Ó.; Arbelo, M.; Fernández, A.; Santos, E.; Ikeda, J.; et al. Comparative histopathologic and viral immunohistochemical studies on CeMV infection among Western Mediterranean, Northeast-Central, and Southwestern Atlantic cetaceans. *PLoS ONE* **2019**, *14*, e0213363. [[CrossRef](#)]
21. Geraci, J.R.; Lounsbury, V.J.; Texas A & M University. Sea Grant College Program. In *Marine Mammals Ashore: A Field Guide for Strandings*, 2nd ed.; National Aquarium in Baltimore: Baltimore, MD, USA, 2005; Volume 486, ISBN 9780977460908.
22. Carlini, R.; de Francesco, M.C.; Libera, S. Della Biometric measures indicating sexual dimorphism in *Stenella coeruleoalba* (Meyen, 1833) (Delphinidae) in the north-central Tyrrhenian sea. *Aquat. Mamm.* **2014**, *40*, 59–68. [[CrossRef](#)]
23. IJsseldijk, L.L.; Brownlow, A.C.; Mazzariol, S. (Eds.) Best Practice on Cetacean Post Mortem Investigation and Tissue Sampling. ACCOBAMS ASCOBANS, Ed. In Proceedings of the 25th Meeting of the Advisory Committee, Stralsund, Germany, 17–19 September 2019; p. 73.
24. Hernández-Mora, G.; González-Barrientos, R.; Morales, J.A.; Chaves-Olarte, E.; Guzmán-Verri, C.; Baquero-Calvo, E.; De-Miguel, M.J.; Marín, C.M.; Blasco, J.M.; Moreno, E. Neurobrucellosis in stranded dolphins, Costa Rica. *Emerg. Infect. Dis.* **2008**, *14*, 1430–1433. [[CrossRef](#)]
25. Di Guardo, G.; Proietto, U.; Di Francesco, C.E.; Marsilio, F.; Zaccaroni, A.; Scaravelli, D.; Mignone, W.; Garibaldi, F.; Kennedy, S.; Forster, F.; et al. Cerebral toxoplasmosis in striped dolphins (*Stenella coeruleoalba*) stranded along the Ligurian sea coast of Italy. *Vet. Pathol.* **2010**, *47*, 245–253. [[CrossRef](#)] [[PubMed](#)]
26. Verna, F.; Giorda, F.; Miceli, I.; Rizzo, G.; Pautasso, A.; Romano, A.; Iulini, B.; Pintore, M.D.; Mignone, W.; Grattarola, C.; et al. Detection of morbillivirus infection by RT-PCR RFLP analysis in cetaceans and carnivores. *J. Virol. Methods* **2017**, *247*, 22–27. [[CrossRef](#)] [[PubMed](#)]

27. Grattarola, C.; Gallina, S.; Giorda, F.; Pautasso, A.; Ballardini, M.; Iulini, B.; Varello, K.; Gorla, M.; Peletto, S.; Masoero, L.; et al. First report of Salmonella 1,4,[5],12:i:- in free-ranging striped dolphins (*Stenella coeruleoalba*), Italy. *Sci. Rep.* **2019**, *9*, 6061. [[CrossRef](#)] [[PubMed](#)]
28. Garofolo, G.; Petrella, A.; Lucifora, G.; Di Francesco, G.; Di Guardo, G.; Pautasso, A.; Iulini, B.; Varello, K.; Giorda, F.; Gorla, M.; et al. Occurrence of Brucella ceti in striped dolphins from Italian Seas. *PLoS ONE* **2020**, *15*, e0240178. [[CrossRef](#)] [[PubMed](#)]
29. Giorda, F.; Romani-Cremaschi, U.; Marsh, A.E.; Grattarola, C.; Iulini, B.; Pautasso, A.; Varello, K.; Berio, E.; Gazzuola, P.; Marsili, L.; et al. Evidence for Unknown Sarcocystis-Like Infection in Stranded Striped Dolphins (*Stenella coeruleoalba*) from the Ligurian Sea, Italy. *Animals* **2021**, *11*, 1201. [[CrossRef](#)]
30. Giorda, F.; Di Guardo, G.; Varello, K.; Pautasso, A.; Sierra, E.; Pintore, M.D.; Grattarola, C.; Colella, E.M.; Berio, E.; Gorla, M.; et al. Retrospective immunohistochemical investigation on dolphin morbillivirus infection by comparing the performance of heterologous monoclonal and polyclonal antibodies—Short communication. *Acta Vet. Hung.* **2021**, *69*, 204–210. [[CrossRef](#)]
31. Alldinger, S.; Baumgärtner, W.; Örvell, C. Restricted expression of viral surface proteins in canine distemper encephalitis. *Acta Neuropathol.* **1993**, *85*, 635–645. [[CrossRef](#)]
32. Van Bresseem, M.F.; Duignan, P.J.; Banyard, A.; Barbieri, M.; Colegrove, K.M.; de Guise, S.; di Guardo, G.; Dobson, A.; Domingo, M.; Fauquier, D.; et al. Cetacean morbillivirus: Current knowledge and future directions. *Viruses* **2014**, *6*, 5145–5181. [[CrossRef](#)]
33. VanDevanter, D.R.; Warrener, P.; Bennett, L.; Schultz, E.R.; Coulter, S.; Garber, R.L.; Rose, T.M. Detection and analysis of diverse herpesviral species by consensus primer PCR. *J. Clin. Microbiol.* **1996**, *34*, 1666–1671. [[CrossRef](#)]
34. Vitale, M.; Galluzzo, P.; Currò, V.; Gozdzik, K.; Schillaci, D.; Di Marco Lo Presti, V. A high sensitive nested PCR for *Toxoplasma gondii* detection in animal and food samples. *J. Microb. Biochem. Technol.* **2013**, *5*, 39–41. [[CrossRef](#)]
35. Bellière, E.N.; Esperón, F.; Fernández, A.; Arbelo, M.; Muñoz, M.J.; Sánchez-Vizcaíno, J.M. Phylogenetic analysis of a new Cetacean morbillivirus from a short-finned pilot whale stranded in the Canary Islands. *Res. Vet. Sci.* **2011**, *90*, 324–328. [[CrossRef](#)]
36. World Organisation for Animal Health (OIE). *Manual of Diagnostic Tests and Vaccines for Terrestrial Animals*, 8th ed.; World Organisation for Animal Health (OIE), Ed.; World Organisation for Animal Health: Paris, France, 2018; ISBN 978-92-95108-18-9.
37. Giorda, F.; Ballardini, M.; Di Guardo, G.; Pintore, M.D.; Grattarola, C.; Iulini, B.; Mignone, W.; Gorla, M.; Serracca, L.; Varello, K.; et al. Postmortem findings in cetaceans found stranded in the pelagos sanctuary, Italy, 2007–2014. *J. Wildl. Dis.* **2017**, *53*. [[CrossRef](#)] [[PubMed](#)]
38. Rubio-Guerri, C.; Melero, M.; Esperón, F.; Bellière, E.N.; Arbelo, M.; Crespo, J.L.; Sierra, E.; García-Párraga, D.; Sánchez-Vizcaíno, J.M. Unusual striped dolphin mass mortality episode related to cetacean morbillivirus in the Spanish Mediterranean sea. *BMC Vet. Res.* **2013**, *9*, 106. [[CrossRef](#)]
39. Casalone, C.; Mazzariol, S.; Pautasso, A.; Di Guardo, G.; Di Nocera, F.; Lucifora, G.; Ligios, C.; Franco, A.; Fichi, G.; Cocumelli, C.; et al. Cetacean strandings in Italy: An unusual mortality event along the Tyrrhenian Sea coast in 2013. *Dis. Aquat. Organ.* **2014**, *109*, 81–86. [[CrossRef](#)] [[PubMed](#)]
40. C.Re.Di.Ma. Italian Diagnostic Report on Stranded Cetaceans (2016). Available online: [https://www.izspltv.it/components/com\\_publiccompetitions/includes/download.php?id=863:report\\_diagnostica\\_spiaggiamenti\\_2016.pdf](https://www.izspltv.it/components/com_publiccompetitions/includes/download.php?id=863:report_diagnostica_spiaggiamenti_2016.pdf) (accessed on 17 December 2021).
41. C.Re.Di.Ma. Italian Diagnostic Report on Stranded Cetaceans (2017). Available online: [https://www.izspltv.it/components/com\\_publiccompetitions/includes/download.php?id=864:report\\_spiaggiamenti\\_2017.pdf](https://www.izspltv.it/components/com_publiccompetitions/includes/download.php?id=864:report_spiaggiamenti_2017.pdf) (accessed on 17 December 2021).
42. C.Re.Di.Ma. Italian Diagnostic Report on Stranded Cetaceans (2018). Available online: [https://www.izspltv.it/components/com\\_publiccompetitions/includes/download.php?id=865:report-senza-tabella-2018-vers-3-ottobre-2019.pdf](https://www.izspltv.it/components/com_publiccompetitions/includes/download.php?id=865:report-senza-tabella-2018-vers-3-ottobre-2019.pdf) (accessed on 17 December 2021).
43. C.Re.Di.Ma. Italian Diagnostic Report on Stranded Cetaceans (2019). Available online: [https://www.izspltv.it/components/com\\_publiccompetitions/includes/download.php?id=866:report-credima-2019.pdf](https://www.izspltv.it/components/com_publiccompetitions/includes/download.php?id=866:report-credima-2019.pdf) (accessed on 17 December 2021).
44. C.Re.Di.Ma. Italian Diagnostic Report on Stranded Cetaceans (2020). Available online: [https://www.izspltv.it/components/com\\_publiccompetitions/includes/download.php?id=1955:report-2020\\_merged.pdf](https://www.izspltv.it/components/com_publiccompetitions/includes/download.php?id=1955:report-2020_merged.pdf) (accessed on 17 December 2021).
45. Di Guardo, G.; Mazzariol, S. Cetacean Morbillivirus—Associated Pathology: Knowns and Unknowns. *Front. Microbiol.* **2016**, *7*, 112. [[CrossRef](#)]
46. Mazzariol, S.; Centelleghè, C.; Cozzi, B.; Povinelli, M.; Marcer, F.; Ferri, N.; Di Francesco, G.; Badagliacca, P.; Profeta, F.; Olivieri, V.; et al. Multidisciplinary studies on a sick-leader syndrome-associated mass stranding of sperm whales (*Physeter macrocephalus*) along the Adriatic coast of Italy. *Sci. Rep.* **2018**, *8*, 11577. [[CrossRef](#)] [[PubMed](#)]
47. Jo, W.K.; Osterhaus, A.D.; Ludlow, M. Transmission of morbilliviruses within and among marine mammal species. *Curr. Opin. Virol.* **2018**, *28*, 133–141. [[CrossRef](#)] [[PubMed](#)]
48. Rudd, P.A.; Cattaneo, R.; von Messling, V. Canine Distemper Virus Uses both the Anterograde and the Hematogenous Pathway for Neuroinvasion. *J. Virol.* **2006**, *80*, 9361–9370. [[CrossRef](#)]
49. Costa-Silva, S.; Sacristán, C.; Gonzales-Viera, O.; Díaz-Delgado, J.; Sánchez-Sarmiento, A.M.; Marigo, J.; Groch, K.R.; Carvalho, V.L.; Ewbank, A.C.; Colosio, A.C.; et al. *Toxoplasma gondii* in cetaceans of Brazil: A histopathological and immunohistochemical survey. *Rev. Bras. Parasitol. Vet.* **2019**, *28*, 395–402. [[CrossRef](#)] [[PubMed](#)]
50. Antoniassi, N.A.B.; Boabaid, F.M.; Souza, R.L.; Nakazato, L.; Pimentel, M.F.A.; Filho, J.O.X.; Pescador, C.A.; Driemeier, D.; Colodel, E.M. Granulomatous meningoencephalitis due to *Toxoplasma gondii* in a black-headed night monkey (*Aotus nigriceps*). *J. Zoo Wildl. Med.* **2011**, *42*, 118–120. [[CrossRef](#)] [[PubMed](#)]



51. Hernández-Mora, G.; Palacios-Alfaro, J.D.; González-Barrientes, R. Wildlife reservoirs of brucellosis: Brucella in aquatic environments. *Rev. Sci. Tech.* **2013**, *32*, 89–103. [[CrossRef](#)]
52. Esperón, F.; Fernández, A.; Sánchez-Vizcaíno, J.M. Herpes simplex-like infection in a bottlenose dolphin stranded in the Canary Islands. *Dis. Aquat. Organ.* **2008**, *81*, 73–76. [[CrossRef](#)] [[PubMed](#)]
53. Van Elk, C.E.; Van De Bildt, M.W.G.; De Jong, A.A.W.; Osterhaus, A.D.M.E.; Kuiken, T. Genital herpesvirus in bottlenose dolphins (*Tursiops truncatus*): Cultivation, epidemiology, and associated pathology. *J. Wildl. Dis.* **2009**, *45*, 895–906. [[CrossRef](#)] [[PubMed](#)]
54. Sierra, E.; Sánchez, S.; Saliki, J.T.; Blas-Machado, U.; Arbelo, M.; Zucca, D.; Fernández, A. Retrospective study of etiologic agents associated with nonsuppurative meningoencephalitis in stranded cetaceans in the canary Islands. *J. Clin. Microbiol.* **2014**, *52*, 2390–2397. [[CrossRef](#)]
55. Vargas-Castro, I.; Melero, M.; Crespo-Picazo, J.L.; Jiménez, M.d.l.Á.; Sierra, E.; Rubio-Guerri, C.; Arbelo, M.; Fernández, A.; García-Párraga, D.; Sánchez-Vizcaíno, J.M. Systematic determination of herpesvirus in free-ranging cetaceans stranded in the western mediterranean: Tissue tropism and associated lesions. *Viruses* **2021**, *13*, 2180. [[CrossRef](#)]
56. Di Francesco, G.; Cammà, C.; Curini, V.; Mazzariol, S.; Proietto, U.; Di Francesco, C.E.; Ferri, N.; Di Provido, A.; Di Guardo, G. Coinfection by *Ureaplasma* spp., *Photobacterium damsela* and an *Actinomyces*-like microorganism in a bottlenose dolphin (*Tursiops truncatus*) with pleuropneumonia stranded along the Adriatic coast of Italy. *Res. Vet. Sci.* **2016**, *105*, 111–114. [[CrossRef](#)]
57. Gan, L.; Mao, P.; Jiang, H.; Zhang, L.; Liu, D.; Cao, X.; Wang, Y.; Wang, Y.; Sun, H.; Huang, Y.; et al. Two Prevalent *Listeria ivanovii* subsp. *ivanovii* Clonal Strains With Different Virulence Exist in Wild Rodents and Pikas of China. *Front. Vet. Sci.* **2020**, *7*, 88. [[CrossRef](#)]
58. Disson, O.; Lecuit, M. Targeting of the central nervous system by *Listeria monocytogenes*. *Virulence* **2012**, *3*, 213–221. [[CrossRef](#)] [[PubMed](#)]
59. Walker, J.K.; Morgan, J.H.; McLauchlin, J.; Grant, K.A.; Shallcross, J.A. *Listeria innocua* isolated from a case of ovine meningoencephalitis. *Vet. Microbiol.* **1994**, *42*, 245–253. [[CrossRef](#)]
60. Rocha, P.R.D.A.; Dalmasso, A.; Grattarola, C.; Casalone, C.; Del Piero, F.; Bottero, M.T.; Capucchio, M.T. Atypical cerebral listeriosis associated with *Listeria innocua* in a beef bull. *Res. Vet. Sci.* **2013**, *94*, 111–114. [[CrossRef](#)] [[PubMed](#)]
61. Lucá, R.; Giacomini-Stuffler, R.; Mazzariol, S.; Roperto, S.; Cocumelli, C.; Di Guardo, G. Neuronal and astrocytic involvement in striped dolphins (*Stenella coeruleoalba*) with morbilliviral encephalitis. *Acta Virol.* **2017**, *61*, 495–497. [[CrossRef](#)] [[PubMed](#)]
62. Da Fontoura Budaszewski, R.; von Messling, V. Morbillivirus experimental animal models: Measles virus pathogenesis insights from canine distemper virus. *Viruses* **2016**, *8*, 274. [[CrossRef](#)] [[PubMed](#)]



**Supplementary material Figure S1.** Figure S1. Western Blot to evaluate specific reactivity of different polyclonal antibodies against *Stenella coeruleoalba*.

Central nervous system (CNS) specimens from *Stenella coeruleoalba* (lanes 1, 2, 3 and 4) or *Bos taurus* (lane Bo) were homogenized at 10% weight/volume and subjected to immunoblotting. Twenty to forty  $\mu\text{g}$  of total protein for each sample were reduced, loaded on Mini-PROTEAN TGX 4-20% Gels (#456-1094, Biorad) and separated electrophoretically in XT MES running Buffer 1X (Biorad) for about 50 minutes at 150V using the MiniPROTEANII electrophoretic chamber (Biorad). The proteins transfer was obtained with a voltage of 25 V for 5 minutes using the semi-dry Trans-Blot-Turbo (Biorad) transfer system according to the manufacturer's protocols. Detection of proteins was carried out respectively with: **A)** anti-cow GFAP polyclonal antibody (1:10000 over night, DAKO#Z0334, predicted molecular weight  $\approx$  50 Kda); **B)** anti-Iba1 polyclonal antibody (1:2500 over night, Biocare Med.#CP290, predicted molecular weight  $\approx$  16.7 Kda; **C)** anti-myelin PLP polyclonal antibody (1:2500 over night, abcam#ab28486, predicted molecular weight  $\approx$  35 Kda + isoforms/duplicates from literature); **D)** anti-NeuN polyclonal antibody (1:2500 over night, Abcam#ab104225, predicted molecular weight  $\approx$  48 KDa).

Membranes were incubated with a 1:5000 dilution of the HRP-Goat anti-Rabbit antibody (Invitrogen # 656120) and with 1 ml of the combined 1:1 solution of the Clarity™ Western ECL Substrate detection kit (Biorad). Finally, membranes were acquired in chemiluminescence using the ChemiDoc™ Touch (Biorad), image acquisition system or equivalent system. MW, molecular size markers (in kilodaltons). The data are representative of multiple immunoblots of these specimens.

**Supplementary material Table S1.** Anamnestic and stranding data of thirty-one animals under study

ID Case	Ref. Lab	Species	DCC	NS	Sex	Age	SL	SD
1	123517/08	<i>Stenella coeluleoalba</i>	2	Poor	M	Adult	Laigueglia (SV)	24/10/2008
2	80729/2/11	<i>Stenella coeluleoalba</i>	2	good	M	Juvenile-Subadult	Eboli (SA)	16/07/2011
3	10331/12	<i>Stenella coeluleoalba</i>	3	Good	M	Juvenile-Subadult	Ospedaletti (IM)	24/01/2012
4	42303/13	<i>Stenella coeluleoalba</i>	3	Poor	M	Juvenile-Subadult	S. Lucido (CS)	03/04/2013
5	71891/14	<i>Stenella coeluleoalba</i>	3	Good	M	Juvenile-Subadult	S.Giovanni a Piro (SA)	29/07/2014
6	3908/15	<i>Stenella coeluleoalba</i>	2	Good	F	Adult	Imperia	16/01/2015
7	80677/16	<i>Stenella coeruleoalba</i>	2	Poor	F	Juvenile-Subadult	Eraclea Minoa (AG)	21/08/2016
8	10475/17	<i>Stenella coeruleoalba</i>	3	Good	F	Juvenile-Subadult	Riposto (CT)	19/09/2016
9	10477/17	<i>Stenella coeruleoalba</i>	2	Poor	F	Juvenile-Subadult	Ispica (RG)	30/09/2016
10	92300/16	<i>Stenella coeruleoalba</i>	2	Poor	M	Juvenile-Subadult	Porto Cesareo (LE)	07/10/2016
11	95842/16	<i>Stenella coeruleoalba</i>	2	Poor	M	Juvenile-Subadult	Genova	20/11/2016
12	6023/17	<i>Stenella coeruleoalba</i>	2	Poor	M	Adult	Otranto (LE)	29/11/2016
13	6020/17	<i>Stenella coeruleoalba</i>	2	Poor	M	Juvenile-Subadult	Torricella (TA)	21/12/2016
14	16769/17	<i>Stenella coeruleoalba</i>	2	Moderate	M	Juvenile-Subadult	Savona	16/02/2017
15	26823/17	<i>Stenella coeruleoalba</i>	3	Moderate	F	Juvenile-Subadult	Prino (IM)	09/03/2017
16	78983/17	<i>Stenella coeruleoalba</i>	2	Poor	F	Adult	Savona	14/09/2017
17	106163/17	<i>Stenella coeruleoalba</i>	2	Poor	M	Adult	Alassio (SV)	01/12/2017
18	2926/18	<i>Stenella coeruleoalba</i>	2	Moderate	M	Juvenile-Subadult	Imperia	13/01/2018
19	41779/18	<i>Stenella coeruleoalba</i>	1	Poor	M	Adult	Schiavonea (CZ)	18/04/2018
20	62728/18	<i>Stenella coeruleoalba</i>	2	Poor	M	Adult	Bivona (VV)	27/06/2018



ID Case	Ref. Lab	Species	DCC	NS	Sex	Age	SL	SD
21	87558/18	<i>Stenella coeruleoalba</i>	2	Moderate	F	Juvenile-Subadult	Arenzano (GE)	29/10/2018
22	100927/18	<i>Stenella coeruleoalba</i>	1	Good	M	Adult	Centofontane (CZ)	19/11/2018
23	619/19	<i>Stenella coeruleoalba</i>	2	Poor	M	Adult	Alassio (SV)	03/01/2019
24	9553/19	<i>Stenella coeruleoalba</i>	1	Good	F	Juvenile-Subadult	Nicotera (VV)	09/01/2019
25	23352/19	<i>Stenella coeruleoalba</i>	2	Poor	F	Adult	Ispani (SA)	27/01/2019
26	25089/19	<i>Stenella coeruleoalba</i>	2	Moderate	M	Juvenile-Subadult	Palmi (RC)	29/01/2019
27	23336/19	<i>Stenella coeruleoalba</i>	3	Poor	M	Adult	Torre del Greco (NA)	08/02/2019
28	21724/19	<i>Stenella coeruleoalba</i>	2	Good	F	Adult	Savona	05/03/2019
29	12060/20	<i>Stenella coeruleoalba</i>	3	Good	F	Adult	Mondragone (CE)	03/04/2019
30	59260/19	<i>Tursiops truncatus</i>	2	Moderate	M	Adult	Genova	04/07/2019
31	38375/20	<i>Tursiops truncatus</i>	3	Good	M	Juvenile-Subadult	Parghelia (VV)	22/04/2020

Legend: ID: identification; Ref. lab: Laboratorial reference; DCC: decomposition conservation code; NS: nutritional status; F: female; M: male; SL: stranding location; SD: stranding date.

**Supplementary material Table S2.** Results of molecular, immunohistochemical, microbiological and serological investigations and type of infection of thirty-one animals under study

ID case	DMV strain	Disease type	PCR			IHC		Bacteria	Sierology			References
			<i>T. gondii</i>	HV	<i>Brucella</i> spp.	CDV	<i>T. gondii</i>		CDV	<i>T. gondii</i>	<i>Brucella</i> spp.	
1	Med	Systemic	+	-	-	+	+	negative	-	1:80 (serum)	-	[1,9,10,30,37]
2	Med	NA	-	-	-	+		negative	NP	NP	NP	[1,10]
3	Med	Systemic	-	-	-	-		negative	-	>1:160	-	[1,37]
4	Med	Systemic	-	-	-	-		negative	-	-	-	[1]
5	Med	Systemic	+	-	-	+	-	negative	NP	NP	NP	[1]
6	Med	Systemic	-	-	-	-		negative	1:40 (serum)	1:80 (serum)	-	[10]
7	NE-atlantic	Systemic	-	-	-	+		negative	NP	NP	NP	
8	NE-atlantic	Systemic	-	-	-	+		negative	NP	NP	NP	
9	NE-atlantic	Systemic	-	-	-	+		negative	NP	NP	NP	

ID case	DMV strain	Disease type	PCR		IHC			Bacteria	Sierology			References
			<i>T. gondii</i>	HV	<i>Brucella</i> spp.	CDV	<i>T. gondii</i>		CDV	<i>T. gondii</i>	<i>Brucella</i> spp.	
10	NE-atlantic	Systemic	-	-	-	+		<i>L. ivanovii</i>	NP	NP	NP	[10,12]
11	NE-atlantic	Systemic	-	vHV	-	+		<i>Photobacterium damsela</i>	1:40 (serum)	>1:40 (serum)	-	[10,12]
12	NE-atlantic	Systemic	-	-	-	+		negative	NP	NP	NP	[10,12]
13	NE-atlantic	Systemic	-	-	-	-		negative	NP	NP	NP	[10,12]
14	NE-atlantic	Systemic	+	-	+	+	+	<i>Brucella ceti</i> <i>Photobacterium damsela</i>	1:8 (serum)	>1:40 (serum, CSF and aqueous humor )	-	[28,29]
15	NE-atlantic	Systemic	-	-	-	+		negative	-	>1:40 (serum)	-	[10]
16	NE-atlantic	Systemic	+	-	-	+	+	<i>Salmonella</i> 1,4,[5],12:i:-; .	-	IFAT >1:640 (serum and aqueous humor )	-	[10,27]
17	NE-atlantic	Systemic	-	-	-	-		negative	>1: 256 (serum)	-	-	
18	NE-atlantic	Systemic	-	-	-	-		negative	-	-	-	
19	NE-atlantic	Systemic	-	-	-	+		negative	NP	NP	NP	
20		Systemic	+	vHV	-	+	+	negative	NP	NP	NP	

ID case	DMV strain	Disease type	PCR			IHC		Bacteria	Sierology			References
			<i>T. gondii</i>	HV	<i>Brucella</i> spp.	CDV	<i>T. gondii</i>		CDV	<i>T. gondii</i>	<i>Brucella</i> spp.	
21	NE-atlantic	Systemic	-	-	-	+		<i>Photobacterium damsela</i> , <i>Listeria innocua</i>	NA	NA	NA	
22		Systemic	-	-	-	+		negative	NP	NP	NP	
23	NE-atlantic	Systemic	-	-	-	+		negative	-	-	-	
24	NE-atlantic	Systemic	+	-	-	+	+	negative	NP	NP	NP	
25	NE-atlantic	Systemic	-	-	-	-		negative	NP	NP	NP	
26	NE-atlantic	Systemic	+	-	-	+	+	negative	NP	NP	NP	
27	NE-atlantic	Systemic	-	-	-	+		negative	NP	NP	NP	
28	NE-atlantic	Systemic	-	-	-	+		negative	1:128 (humor aqueous)	-	-	
29	NE-atlantic	Systemic	+	-	-	+	-	negative	NP	NP	NP	
30	NE-atlantic	Systemic	+	-	-	+	-	<i>Photobacterium damsela</i>	-	>1:40 (serum and aqueous humor)	-	
31	NE-atlantic	Systemic	-	-	-	+		<i>Photobacterium damsela</i>	NP	NP	NP	

Legend: ID: identification; PCR: polymerase chain reaction; HV: Herpesvirus; IHC: immunohistochemistry; CDV: canine distemper virus; NE-Atlantic: Northeast Atlantic; Med: Mediterranean.

[1]: 10.7589/2017-02-035

[9]: 10.1038/s41598-018-19269-2

[10]: 10.1038/s41598-020-77835-z

[12]: 10.3354/dao03323

[27]: 10.1038/s41598-019-42474-6

[28]: 10.1371/journal.pone.0240178

[29]: 10.3390/ani11051201

[30]: 10.1556/004.2021.00028

[37]: 10.7589/2016-07-150

### **3. CONCLUSIONS**





- 1) The RT-PCR RFLP method developed, using degenerate primers targeting a 287bp fragment of a conserved portion of the N gene, has proved to be a valuable, reliable, simple and relatively inexpensive diagnostic tool for the diagnosis and identification of several genotypes of morbillivirus, as well as for the discrimination of different DMV variants without the need of sequencing.
  
- 2) The polyclonal antibody against RPV results more efficient in detecting DMV through IHC, compared to the monoclonal antibody raised against CDV, though the staining quality is overall enhanced with the monoclonal antibody. Similar staining location and extent was observed in the brain tissues with the two antibodies.  
 Since the serum against RPV is no longer available due to recent OIE procedures for RPV eradication, future studies should be aimed at evaluating the cross-reactivity of different monoclonal and polyclonal antibodies, raised against additional members of the genus Morbillivirus with DMV-specific epitopes. Finally, producing a monoclonal antibody specific for DMV proteins would be fundamental for increasing the accuracy of diagnostic and pathogenetic investigations.
  
- 3) In the Mediterranean basin cetaceans affected by CeMV can develop opportunistic protozoan infections, caused by agents belonging to the family *Sarcocystiidae* different from *T. gondii*
  
- 4) Based on molecular and immunohistochemical data, the NE-Atlantic strain circulating in the Italian waters seems to possess a higher neurotropic potential and to cause more severe acute/subacute disease than previously observed during the 2011 and 2013 unusual mortality events, referable to the Mediterranean strain
  
- 5) A myelin specific biomarker proved effective in detect severe myelinopathy, with a reduction in myelin density and large areas completely devoid of myelin, confirming demyelination in cetaceans with CeMV infections

- 6) Inside and around the demyelinated areas there are morbillivirus antigen-bearing cells of mainly neuronal and microglial origin, associated with marked astro and microglia reactivity. Very little Morbillivirus staining is evident in astrocytes.

## **4. RESUMEN**



## 4.1. INTRODUCCIÓN Y OBJETIVOS

El morbillivirus de los cetáceos (CeMV) es un miembro del género Morbillivirus (familia *Paramyxoviridae*, orden *Mononegavirales*), constituido por una única molécula lineal de ARN monocatenario de sentido negativo, cuyo genoma está constituido por seis unidades de transcripción que codifican seis proteínas estructurales: la proteína de nucleocápside (N), fosfoproteína (P), proteína de matriz (M), glicoproteína de fusión (F), glicoproteína de hemaglutinina (H) y la ARN polimerasa dependiente de ARN (L), así como dos proteínas del factor de virulencia (C y V).

Está considerado como el agente natural con mayor impacto en la salud y conservación de los cetáceos a nivel mundial (Di Guardo y Mazzariol 2016; Zinzula et al. 2021).

Hasta ahora se han descrito dos linajes de CeMV (Gulland et al. 2018): CeMV-1, que representa las cepas bien caracterizadas del hemisferio norte, que comprende el morbillivirus de los delfines (DMV) (Visser et al. 1993), el morbillivirus de la marsopa (PMV) (Visser et al. 1993), el morbillivirus de los calderones (PWMV) (Taubenberger et al. 2000) y morbillivirus de los zifios (BWMV) (West et al. 2013); y CeMV-2 para tres cepas identificadas más recientemente en el hemisferio sur, precisamente en un delfín de Guayana (*Sotalia guianensis*) de Brasil (Groch et al. 2014), en un delfín mular del Indo-Pacífico (*Tursiops aduncus*) de Australia Occidental (Stephens et al. 2014) y, finalmente, en un delfín de Fraser (*Lagenodelphis hosei*) varado en Hawái y descrito en 2021 (West et al. 2021).

CeMV ha sido responsable de varios brotes y enfermedades letales interepidémicas en todo el mundo (Van Bresse et al. 2014). La primera epizootia de CeMV reconocida ocurrió en 1987–88 en la costa atlántica de los EE. UU., cuando murió aproximadamente el 50% de la población del delfín mular (*Tursiops truncatus*) (Lipscomb et al. 1994).

Durante los últimos 30 años, el virus ha causado dos epizootias en la cuenca mediterránea, la primera reportada en 1990-91 con más de 1000 delfines listados (*Stenella coeruleoalba*) varados (Domingo et al. 1990, 1992), y tres eventos de mortalidad inusual (UMEs) (2011, 2013, 2016) (Rubio-Guerri et al. 2013; Casalone et al. 2014; Pautasso et al. 2019). La segunda reportada a lo largo de las costas italiana a través de descripciones de

enfermedades únicas de infección por DMV informadas por C. Re.Di.Ma. en tasas anuales estándar de mortalidad (CReDiMa 2016, 2017, 2018, 2019, 2020).

Análisis filogenéticos y filogeográficos recientes (Cerutti et al. 2020) de 16 cepas que circularon en los últimos 30 años en el Mediterráneo confirmaron, en general, una homología bien conservada entre las cepas, con una identidad de >98 %. Un nuevo linaje de origen atlántico, denominado cepa NE-Atlántica, llamado así al detectarse por primera vez en animales encontrados varados a lo largo de las costas de Galicia y Portugal en 2011-2013, comenzó a reemplazar a la cepa mediterránea a finales de 2015 en aguas italianas (Pautasso et al. 2019; Cerutti et al. 2020). La primera descripción de la cepa del NE-Atlántico en la cuenca mediterránea se refiere a un cachalote (*Physeter macrocephalus*) hallado varado en la costa de Vasto (Italia, CH) en 2014 (Cerutti et al. 2020) durante un episodio de varamiento masivo (Mazzariol et al. 2018). El animal puede haber sido responsable de la transmisión de la nueva cepa en aguas italianas, dado el rol de “spillover” huésped de esta especie (Jo et al. 2018) y a la fecha de varamiento registrada casi 2 años antes de la primera descripción en pequeños odontocetos que habitan la misma zona geográfica.

Hasta la fecha no se ha confirmado ninguna diferencia en la virulencia y gravedad de la enfermedad entre las dos cepas (Zinzula et al. 2021).

Desde un punto de vista diagnóstico, el aislamiento de DMV en cultivos celulares todavía se considera el "gold standard" para el diagnóstico definitivo de la infección, aunque sigue siendo un desafío cuando se trata de cetáceos varados. De hecho, hay muy pocos informes disponibles sobre el aislamiento exitoso del virus en estas especies (Nielsen et al. 2008; Peletto et al. 2018; West et al. 2021).

La reacción en cadena de la polimerasa con transcripción inversa (RT-PCR) seguida de la secuenciación del producto de la PCR es un método de diagnóstico específico y sensible para obtener una confirmación rápida de la infección, de suma importancia para confirmar rápidamente nuevos brotes en curso, pero también para identificar nuevas cepas y realizar estudios filogenéticos (Van Bresse et al. 2014; Pautasso et al. 2019; Felipe-Jiménez et al. 2022).

Se desarrollaron varios protocolos para discriminar diferentes miembros de Morbillivirus, incluidos PCR tradicionales (Barrett et al. 1993; Frisk et al. 1999; Di Guardo et al. 2010;

Sierra et al. 2014; Van Bresseem et al. 2014) y PCR real time (Grant et al. 2009; Rubio-Guerri et al. 2013; Sacristán et al. 2015; Yang et al. 2016; Groch et al. 2020).

La mayoría de los protocolos mencionados necesitan primer específicos para cada miembro de Morbillivirus y son seguidos por la secuenciación de los productos de reacción como confirmación de la especificidad. Este enfoque requiere instrumentos y kits avanzados y costosos y también una cantidad considerable de tiempo para su realización. Siempre se debe realizar histología e inmunohistoquímica (IHC) para confirmar la infección por morbillivirus (MI) y obtener información sobre el estadio de la enfermedad. El inmunomarcaje de antígeno negativo se obtiene comúnmente en MI de curso subagudo a crónico (Amude y Alfieri 2010; Van Bresseem et al. 2014). Dado que no hay disponibles anticuerpos homólogos comerciales (Ab) contra ningún miembro de CeMV, se han utilizado dos Abs preparados contra otros miembros del género Morbillivirus en todo el mundo en el diagnóstico IHC de MI en todo el mundo. Uno de ellos es un anticuerpo monoclonal (MoAb) contra la proteína N del virus del moquillo canino (CDV) (Giorda et al. 2017; Pintore et al. 2018; Díaz-Delgado et al. 2019; Cuvertoret-Sanz et al. 2020; Sierra et al. 2020). El otro es un Ab poli (policlonal) producido en conejos contra el virus de la peste bovina (RPV) (Yang et al. 2006; Mazzariol et al. 2016).

Las investigaciones serológicas son herramientas muy útiles para estudiar la epidemiología del CeMV, evaluar el estado inmunitario de las poblaciones antes y después de una epidemia y, con suerte, ayudar a predecir nuevos brotes (Van Bresseem et al. 2014; Profeta et al. 2015).

La patología asociada a CeMV es comparable a la observada en otros huéspedes infectados por Morbillivirus, incluidos los humanos (De Vries et al. 2015; da Fontoura Budaszewski y von Messling 2016), con meningoencefalitis no supurativa y neumonía bronco intersticial como principales hallazgos patológicos. Además, un agotamiento severo y generalizado de células linfoides está comúnmente presente en los tejidos linfoides de los animales infectados, demostrando el papel inmunosupresor prominente de este agente. En consecuencia, los individuos afectados tienden a desarrollar un gran número de infecciones secundarias virales, bacterianas, fúngicas, protozoarias y parasitarias (Di Guardo y Mazzariol 2016; Díaz-Delgado et al. 2017; Giorda et al. 2017; Sierra et al. 2018, 2020; Garofolo et al. 2020).



Entre las infecciones por protozoos oportunistas, existe una gran cantidad de literatura que reporta *Toxoplasma gondii* en mamíferos marinos que habitan la cuenca del Mediterráneo (Guardo et al. 2010; Giorda et al. 2017; Pintore et al. 2018), pero hay pocos datos disponibles en esta área geográfica para otros protozoos que se sabe que afectan a estas especies en otros mares (Miller et al. 2009; Gulland et al. 2018).

Los cambios neuropatológicos debidos a MI incluyen desmielinización, que se informa en gran medida tanto en especies marinas como terrestres y que se asocia comúnmente con la infección por el virus del moquillo canino y focino (Vandeveldde y Zurbriggen 2005; Duignan et al. 2014; Ulrich et al. 2014), probablemente debido a la alta correlación filogenética bien documentada entre el CDV y el virus del moquillo focino (Duignan et al. 2014). Hasta el momento se han reportado algunas descripciones de cambios en la mielina en cetáceos afectados por infecciones por CeMV (Duignan et al. 1992; Domingo et al. 1995; Soto et al. 2011; Pautasso et al. 2019), en algunos casos confirmados a través de Luxol Fast Blue que no siempre resultó efectiva para mostrar desmielinización (Díaz-Delgado et al. 2019).

La presente investigación se desarrolló para ampliar el conocimiento disponible sobre CeMV y diseñar nuevas herramientas de diagnóstico para este agente infeccioso. Sus objetivos específicos eran:

1. Desarrollar y proporcionar una nueva técnica RFLP de PCR de punto final para detectar, diferenciar y caracterizar diferentes cepas de Morbillivirus, fácilmente aplicable también en laboratorios con recursos limitados.
2. Comparar los rendimientos diagnósticos de los dos anticuerpos heterólogos utilizados en todo el mundo, MoAb anti-CDV y poli ab anti-RPV, para: detección de positividad, calidad de marcaje y distribución neuroanatómica de la tinción en IHC
3. Profundizar el role inmunosupresor de CeMV a través de la descripción de una nueva infección secundaria por protozoos en la cuenca mediterránea

4. Comparar las dos últimas variantes de DMV que circulan en las aguas italianas, denominadas "Mediterráneo" y "NE-Atlántico", en términos de potencial neurotrópico
5. Confirmar el daño de la mielina, a través de un biomarcador específico aplicado en tinción de inmunofluorescencia indirecta (IF), en cerebros de cetáceos afectados por CeMV sistémico
6. Caracterizar áreas de mielinopatía, revelando cambios celulares y colonización viral mediante doble tinción de inmunofluorescencia.

## 4.2. PUBLICACIONES

Para alcanzar los objetivos de esta tesis de doctorado, se llevaron a cabo las siguientes investigaciones, que dieron como resultado cuatro publicaciones indexadas en el Journal of Citation Reports:

Publicación I:

La transcripción inversa-PCR (RT-PCR) seguida de secuenciación representa una herramienta biomolecular sensible y específica para el diagnóstico de morbillivirus.

La mayoría de los protocolos utilizados para detectar la infección por Morbillivirus necesitan primers específicos para las diferentes especies de Morbillivirus, para amplificar la porción genética diana y secuenciar los productos de reacción, como confirmación de la especificidad. Este enfoque requiere instrumentos y kits avanzados y costosos y también una cantidad considerable de tiempo para su realización.

Se emplearon tejidos congelados de 4 perros (*Canis canis*), 1 zorro (*Vulpes vulpes*) y 3 delfines listados (*Stenella coeruleoalba*) que presentaban evidencias de infección por morbillivirus para desarrollar un ensayo de polimorfismo de longitud de fragmentos de restricción (RFLP) de RT-PCR, utilizando primers degenerados dirigidos a un fragmento de 287 pb de una porción conservada del gen N, para detectar, diferenciar y caracterizar tanto el virus del moquillo canino como el morbillivirus de los delfines, sin necesidad de secuenciación.

Publicación II:

La confirmación y la estadificación de las infecciones por morbillivirus se basan en la histología y la inmunohistoquímica (IHC), después de la detección molecular. Como en la actualidad no se dispone de anticuerpos específicos (Abs) contra el DMV, se han utilizado en todo el mundo dos Abs heterólogos, que se sabe reaccionar de forma cruzada con el DMV, para los exámenes de infecciones por morbillivirus en cetáceos. Uno es un Ab monoclonal (MoAb) preparado contra la proteína N del virus del moquillo canino (CDV), mientras que el otro es un Ab policlonal producido en conejos contra el virus de la peste bovina (RPV).

El objetivo de este estudio fue comparar el rendimiento de estos dos Abs relacionados con: detección de positividad, calidad del inmunomarcaje y distribución neuroanatómica de la tinción.

Se sometieron a IHC secciones en serie de los órganos diana de diez cetáceos de vida libre varados, previamente diagnosticados como infectados con DMV por PCR y/o serología. Se encontró que el cerebro, los pulmones y los ganglios linfáticos de un animal eran positivos con ambos Abs. De otros dos animales, el cerebro y el bazo, respectivamente, dieron positivo solo con el Ab policlonal.

En los tejidos cerebrales positivos, se observó inmunotinción multifocal, con una ubicación y extensión de tinción similares, con los dos anticuerpos probados.

Publicación III:

CeMV es conocido por ser un agente inmunosupresor, capaz de causar también infecciones oportunistas por protozoos. A pesar de que hay una gran cantidad de literatura que reporta *Toxoplasma gondii* en mamíferos marinos que habitan la cuenca del Mediterráneo, hay pocos datos disponibles en esta área geográfica para otros protozoos de la familia *Sarcocystidae* que se sabe que afectan a estas especies en otros mares.

En este estudio presentamos la primera descripción de una infección similar a *Sarcocystis* en tejido muscular de delfines de la cuenca mediterránea junto con el primer informe de quistes de tejido similar a *Sarcocystis* en el cerebro de cetáceos varados. Estos dos animales presentaron una coinfección por CeMV subclínica y sistémica, respectivamente. Los organismos desconocidos eran genéticamente similares a las especies de *Sarcocystis* que infectan a la familia *Bovidae*.

**Publicación IV:**

Un nuevo linaje de morbillivirus de delfines de origen atlántico que circula en aguas italianas reemplazó a la cepa mediterránea anterior a finales de 2015; sin embargo, aún no se han documentado algunas diferencias en cuanto a la virulencia y patogenia entre las dos cepas.

Hay abundante literatura que informa sobre la desmielinización en perros y pinnípedos afectados por la infección por morbillivirus, pero la mielinopatía está poco investigada en los cetáceos varados afectados por este virus. Además, la neuropatogénesis de la infección por morbillivirus de cetáceos no se ha aclarado por completo, dejando sin respuesta preguntas sobre el tropismo celular.

Este estudio describe hallazgos neuropatológicos en el tejido cerebral de 31 cetáceos encontrados varados a lo largo de la costa italiana y positivos para la infección por DMV mediante pruebas moleculares. Los cambios celulares en las áreas de mielinopatía fueron revelados por inmunofluorescencia indirecta doble. Las lesiones asociadas al DMV más frecuentes fueron astromicrogliosis, necrosis neuronal, espongirosis, malacia y meningoencefalitis no supurativa. La reducción de mielina y las áreas de desmielinización se revelaron mediante un biomarcador de mielina específico. El inmunomarcaje de antígenos morbilivirales fue principalmente observado en neuronas y células microgliales, en asociación con una marcada activación de microglia y astrocitos. El análisis molecular e inmunohistoquímico sugirió una mayor afinidad neurotrópica de la nueva cepa circulante.

### 4.3. CONCLUSIONES

- 1- El método RT-PCR RFLP desarrollado, utilizando primers degenerados dirigidos a un fragmento de 287 pb de una porción conservada del gen N, ha demostrado ser una herramienta de diagnóstico valiosa, fiable, simple y relativamente económica para el diagnóstico y la identificación de varios genotipos de morbillivirus, así como para la discriminación de diferentes variantes de DMV sin necesidad de secuenciación.
- 2- El anticuerpo policlonal contra RPV resulta más eficiente en la detección de DMV a través de IHC, en comparación con el anticuerpo monoclonal producido contra CDV, aunque la calidad de la tinción es, en general, mejor con el anticuerpo monoclonal. Se observó una ubicación y extensión de tinción similares en los tejidos cerebrales con los dos anticuerpos. Como el suero contra el RPV ya no está disponible debido a los recientes procedimientos de la OIE para la erradicación del RPV, los estudios futuros deben tener como objetivo de evaluar la reactividad cruzada de diferentes anticuerpos, monoclonales y policlonales, generados contra miembros adicionales del género Morbillivirus con epítomos específicos del DMV. Finalmente, producir un anticuerpo monoclonal específico para las proteínas DMV sería fundamental para aumentar la precisión de las investigaciones diagnósticas y patogenéticas.
- 3- En la cuenca mediterránea los cetáceos afectados por CeMV pueden desarrollar infecciones protozoarias oportunistas, causadas por agentes pertenecientes a la familia Sarcocystiidae distintos de *T. gondii*.
- 4- Según los datos moleculares e inmunohistoquímicos, la cepa del NE-Atlántico que circula en las aguas italianas parece poseer un mayor potencial neurotrópico y causar una enfermedad aguda/subaguda más grave que la observada previamente durante los eventos de mortalidad inusuales de 2011 y 2013, atribuibles a la cepa del Mediterráneo.



- 5- Un biomarcador específico para la mielina demostró ser eficaz para detectar mielinopatía grave, con una reducción en la densidad de mielina y grandes áreas completamente desprovistas de mielina, lo que confirma la desmielinización en cetáceos con infecciones por CeMV.
- 6- Dentro y alrededor de las áreas desmielinizadas hay células portadoras de antígenos de morbillivirus de origen principalmente neuronal y microglial, asociadas con una marcada reactividad de astro y microglia. Muy poca tinción de Morbillivirus es evidente en los astrocitos.

## **5. REFERENCE LIST / LISTA DE REFERENCIAS**



- Amude AM, Alfieri AF, Alfieri AA. 2010. Use of immunohistochemistry and molecular assays such as RT-PCR for precise post mortem diagnosis of distemper-related encephalitis. *Curr Res Technol Educ Top Appl Microbiol Microb Biotechnol* 2:1539–1545.
- Barrett T, Visser IKG, Mamaev L, Goatley L, Van Bresse MF, Osterhaus ADME. 1993. Dolphin and porpoise morbilliviruses are genetically distinct from phocine distemper virus. Elsevier. *Virology* 193:1010–1012.
- Casalone C, Mazzariol S, Pautasso A, Guardo G Di, Nocera F Di, Lucifora G, Ligios C, Franco A, Fichi G, Cocumelli C, et al. 2014. Cetacean strandings in Italy: An unusual mortality event along the Tyrrhenian Sea coast in 2013. *Dis Aquat Organ* 109:81–86.
- Cerutti F, Giorda F, Grattarola C, Mignone W, Beltramo C, Keck N, Lorusso A, Di Francesco G, Di Renzo L, Di Guardo G, et al. 2020. Specific capture and whole-genome phylogeography of Dolphin morbillivirus. Nature Publishing Group UK. *Sci Rep* 10:1–10.
- CRDiMa. 2016. Italian Diagnostic Report on Stranded Cetaceans (2016). [https://www.izspltv.it/components/com\\_publiccompetitions/includes/download.php?id=863:report\\_diagnostica\\_spiaggiamenti\\_2016.pdf](https://www.izspltv.it/components/com_publiccompetitions/includes/download.php?id=863:report_diagnostica_spiaggiamenti_2016.pdf). Accessed December 2021.
- CRDiMa. 2017. Italian Diagnostic Report on Stranded Cetaceans (2017). [https://www.izspltv.it/components/com\\_publiccompetitions/includes/download.php?id=864:report\\_spiaggiamenti\\_2017.pdf](https://www.izspltv.it/components/com_publiccompetitions/includes/download.php?id=864:report_spiaggiamenti_2017.pdf). Accessed December 2021.
- CRDiMa. 2018. Italian Diagnostic Report on Stranded Cetaceans (2018). [https://www.izspltv.it/components/com\\_publiccompetitions/includes/download.php?id=865:report-senza-tabella-2018-vers-3-ottobre-2019.pdf](https://www.izspltv.it/components/com_publiccompetitions/includes/download.php?id=865:report-senza-tabella-2018-vers-3-ottobre-2019.pdf). Accessed December 2021.
- CRDiMa. 2019. Italian Diagnostic Report on Stranded Cetaceans (2019). [https://www.izspltv.it/components/com\\_publiccompetitions/includes/download.php](https://www.izspltv.it/components/com_publiccompetitions/includes/download.php)

- ?id=866:report-credima-2019.pdf. Accessed December 2021.
- CReDiMa. 2020. Italian Diagnostic Report on Stranded Cetaceans (2020).  
[https://www.izspltv.it/components/com\\_publiccompetitions/includes/download.php?id=1955:report-2020\\_merged.pdf](https://www.izspltv.it/components/com_publiccompetitions/includes/download.php?id=1955:report-2020_merged.pdf). Accessed December 2021.
- Cuvertoret-Sanz M, López-Figueroa C, O'Byrne A, Canturri A, Martí-García B, Pintado E, Pérez L, Ganges L, Cobos A, Abarca ML, et al. 2020. Causes of cetacean stranding and death on the Catalan coast (western Mediterranean Sea), 2012-2019. Inter-Research Science Center. *Dis Aquat Organ* 142:239–253.
- De Vries RD, Paul Duprex W, De Swart RL. 2015. Morbillivirus infections: An introduction. *Viruses* 7:699–706.
- Díaz-Delgado J, Groch KR, Sierra E, Sacchini S, Zucca D, Quesada-Canales Ó, Arbelo M, Fernández A, Santos E, Ikeda J, et al. 2019. Comparative histopathologic and viral immunohistochemical studies on CeMV infection among Western Mediterranean, Northeast-Central, and Southwestern Atlantic cetaceans. *PLoS One* 14:1–21.
- Díaz-Delgado J, Sierra E, Vela AI, Arbelo M, Zucca D, Groch KR, Fernández A. 2017. Coinfection by *Streptococcus phocae* and cetacean morbillivirus in a short-beaked common dolphin *Delphinus delphis*. *Dis Aquat Organ* 124:247–252.
- Domingo M, Ferrer L, Pumarola M, Marco A, Plana J, Kennedy S, McAlisey M, Rima BK. 1990. Morbillivirus in dolphins. *Nature* 348:21.
- Domingo M, Visa J, Pumarola M, Marco AJ, Ferrer L, Rabanal R, Kennedy S. 1992. Pathologic and immunocytochemical studies of morbillivirus infection in striped dolphins (*Stenella coeruleoalba*). *Vet Pathol* 29:1–10.
- Domingo M, Vilafranca M, Visa J, Prats N, Trudgett A, Visser I. 1995. Evidence for chronic morbillivirus infection in the Mediterranean striped dolphin (*Stenella coeruleoalba*). *Vet Microbiol* 44:229–239.
- Duignan PJ, Van Bressemer MF, Baker JD, Barbieri M, Colegrove KM, de Guise S, de

- Swart RL, di Guardo G, Dobson A, Duprex WP, et al. 2014. Phocine distemper Virus: Current knowledge and future directions. *Viruses* 6:5093–5134.
- Duignan PJ, Geraci JR, Raga JA, Calzada N. 1992. Pathology of morbillivirus infection in striped dolphins (*Stenella coeruleoalba*) from Valencia and Murcia, Spain. *Can J Vet Res* 56:242–248.
- Felipe-Jiménez I, Fernández A, Arbelo M, Segura-Göthlin S, Colom-Rivero A, Suárez-Santana C, De La Fuente J, Sierra E. 2022. Molecular Diagnosis of Cetacean Morbillivirus in Beaked Whales Stranded in the Canary Islands ( 1999 – 2017 ). *Vet Sci* 121:18.
- da Fontoura Budaszewski R, von Messling V. 2016. Morbillivirus experimental animal models: Measles virus pathogenesis insights from canine distemper virus. *Viruses* 8.
- Frisk AL, König M, Moritz A, Baumgärtner W. 1999. Detection of canine distemper virus nucleoprotein RNA by reverse transcription-PCR using serum, whole blood, and cerebrospinal fluid from dogs with distemper. *J Clin Microbiol* 37:3634–3643.
- Garofolo G, Petrella A, Lucifora G, Di Francesco G, Di Guardo G, Pautasso A, Iulini B, Varello K, Giorda F, Goria M, et al. 2020. Occurrence of *Brucella ceti* in striped dolphins from Italian Seas. *PLoS One* 15.
- Giorda F, Ballardini M, Di Guardo G, Pintore MD, Grattarola C, Iulini B, Mignone W, Goria M, Serracca L, Varello K, et al. 2017. Postmortem findings in cetaceans found stranded in the pelagos sanctuary, Italy, 2007–14. *J Wildl Dis* 53:795–803.
- Grant RJ, Banyard AC, Barrett T, Saliki JT, Romero CH. 2009. Real-time RT-PCR assays for the rapid and differential detection of dolphin and porpoise morbilliviruses. *J Virol Methods* 156:117–123.
- Groch KR, Colosio AC, Marcondes MCC, Zucca D, Díaz-Delgado J, Niemeyer C, Marigo J, Brandão PE, Fernández A, Catão-Dias JL. 2014. Novel cetacean morbillivirus in Guiana Dolphin, Brazil. *Emerg Infect Dis*. 2014;20(3):511-513.

- Groch KR, Taniwaki SA, Favero CM, Brandão PE, Díaz-Delgado J, Fernández A, Catão-Dias JL, Sierra E. 2020. A novel real-time PCR to detect Cetacean morbillivirus in Atlantic cetaceans. *J Virol Methods* 285:113964.
- Guardo G, Proietto U, Di Francesco CE, Marsilio F, Zaccaroni A, Scaravelli D, Mignone W, Garibaldi F, Kennedy S, Forster F, et al. 2010. Cerebral toxoplasmosis in striped dolphins (*Stenella coeruleoalba*) stranded along the Ligurian sea coast of Italy. *Vet Pathol* 47:245–253.
- Di Guardo G, Mazzariol S. 2016. Cetacean Morbillivirus -Associated Pathology : Knowns and Unknowns. *Front Microbiol* 7:1–5.
- Gulland FMD, Dierauf L A, Whitman KL. 2018. *CRC Handbook of Marine Mammal Medicine*, 3rd edition. CRC Press, New York, 1144 pp.
- Jo WK, Osterhaus AD, Ludlow M. 2018. Transmission of morbilliviruses within and among marine mammal species. *Curr Opin Virol* 28:133–141.
- Lipscomb TP, Schulman FY, Moffett D, Kennedy S. 1994. Morbilliviral Disease in Atlantic Bottlenose Dolphins (*Tursiops truncatus*) from the 1987-1988 Epizootic. *J Wildl Dis* 30:567–571.
- Mazzariol S, Centelleghè C, Beffagna G, Povinelli M, Terracciano G, Cocumelli C, Pintore A, Denurra D, Casalone C, Pautasso A, et al. 2016. Mediterranean fin whales (*Balaenoptera physalus*) threatened by dolphin morbillivirus. *Emerg Infect Dis* 22:302–305.
- Mazzariol S, Centelleghè C, Cozzi B, Povinelli M, Marcer F, Ferri N, Di Francesco G, Badagliacca P, Profeta F, Olivieri V, et al. 2018. Multidisciplinary studies on a sick-leader syndrome-associated mass stranding of sperm whales (*Physeter macrocephalus*) along the Adriatic coast of Italy. *Sci Rep* 8:1–18.
- Miller MA, Barr BC, Nordhausen R, James ER, Magargal SL, Murray M, Conrad PA, Toy-Choutka S, Jessup DA, Grigg ME. 2009. Ultrastructural and molecular confirmation of the development of *Sarcocystis neurona* tissue cysts in the central nervous system of southern sea otters (*Enhydra lutris nereis*). *Int J Parasitol*



39:1363–1372.

Nielsen O, Smith G, Weingartl H, Lair S, Measures L. 2008. Use of a slam transfected vero cell line to isolate and characterize marine mammal morbilliviruses using an experimental ferret model. *J Wildl Dis* 44:600–611.

Pautasso A, Iulini B, Grattarola C, Giorda F, Gorla M, Peletto S, Masoero L, Mignone W, Varello K, Petrella A, et al. 2019. Novel dolphin morbillivirus (DMV) outbreak among Mediterranean striped dolphins *Stenella coeruleoalba* in Italian waters. *Dis Aquat Organ* 132(3):215-220.

Peletto S, Caruso C, Cerutti F, Modesto P, Biolatti C, Pautasso A, Grattarola C, Giorda F, Mazzariol S, Mignone W, et al. 2018. Efficient isolation on Vero.DogSLAMtag cells and full genome characterization of Dolphin Morbillivirus (DMV) by next generation sequencing. *Sci Rep* 8, 860.

Pintore MD, Mignone W, Di Guardo G, Mazzariol S, Ballardini M, Florio CL, Gorla M, Romano A, Caracappa S, Giorda F, et al. 2018. Neuropathologic findings in cetaceans stranded in Italy (2002–14). *J Wildl Dis* 12(4): 452.

Profeta F, Di Francesco CE, Marsilio F, Mignone W, Di Nocera F, De Carlo E, Lucifora G, Pietroluongo G, Baffoni M, Cocumelli C, et al. 2015. Retrospective seroepidemiological investigations against Morbillivirus, *Toxoplasma gondii* and *Brucella* spp. in cetaceans stranded along the Italian coastline (1998-2014). *Res Vet Sci* 101:89–92.

Rubio-Guerri C, Melero M, Esperón F, Bellière EN, Arbelo M, Crespo JL, Sierra E, García-Párraga D, Sánchez-Vizcaíno JM. 2013. Unusual striped dolphin mass mortality episode related to cetacean morbillivirus in the Spanish Mediterranean sea. *BMC Vet Res* 9:106. doi: 10.1186/1746-6148-9-106.

Sacristán C, Carballo M, Muñoz MJ, Bellière EN, Neves E, Nogal V, Esperón F. 2015. Diagnosis of Cetacean morbillivirus: A sensitive one step real time RT fast-PCR method based on SYBR® Green. *J Virol Methods* 226:25–30.

Sierra E, Sánchez S, Saliki JT, Blas-Machado U, Arbelo M, Zucca D, Fernández A.

2014. Retrospective study of etiologic agents associated with nonsuppurative meningoencephalitis in stranded cetaceans in the canary Islands. *J Clin Microbiol* 52:2390–2397.
- Sierra E, Fernández A, Felipe-Jiménez I, Zucca D, Díaz-Delgado J, Puig-Lozano R, Câmara N, Consoli F, Díaz-Santana P, Suárez-Santana C, et al. 2020. Histopathological Differential Diagnosis of Meningoencephalitis in Cetaceans: Morbillivirus, Herpesvirus, *Toxoplasma gondii*, *Brucella* sp., and *Nasitrema* sp. *Front Vet Sci* 7:650.
- Sierra E, Fernández A, Zucca D, Câmara N, Felipe-Jiménez I, Suárez-Santana C, Bernaldo de Quirós Y, Díaz-Delgado J, Arbelo M. 2018. Morbillivirus infection in Risso's dolphin *Grampus griseus*: a phylogenetic and pathological study of cases from the Canary Islands. *Inter-Research. Dis Aquat Organ* 129:165–174.
- Soto S, Marco A, Domingo M, González R, Alegre F, González B, Medina P, Raga JA. 2011. Epizootic of dolphin morbillivirus on the Catalanian Mediterranean coast in 2007. *Vet Rec* 169:2011–2013.
- Stephens N, Duignan PJ, Wang J, Bingham J, Finn H, Bejder L, Patterson IAP, Holyoake C. 2014. Cetacean morbillivirus in coastal indo-pacific bottlenose dolphins, Western Australia. *Emerg Infect Dis* 20:666–670.
- Taubenberger JK, Tsai MM, Atkin TJ, Fanning TG, Krafft AE, Moeller RB, Kodosi SE, Mense MG, Lipscomb TP. 2000. Molecular genetic evidence of a novel morbillivirus in a long-finned pilot whale (*Globicephalus melas*). Centers for Disease Control and Prevention (CDC). *Emerg Infect Dis* 6:42–45.
- Ulrich R, Puff C, Wewetzer K, Kalkuhl A, Deschl U, Baumgärtner W. 2014. Transcriptional changes in canine distemper virus-induced demyelinating leukoencephalitis favor a biphasic mode of demyelination. *PLoS One* 9(4): e95917.
- Vandeveldt M, Zurbriggen A. 2005. Demyelination in canine distemper virus infection: a review. *Acta Neuropathol* 109:56–68.

- Van Bresseem MF, Duignan PJ, Banyard A, Barbieri M, Colegrove KM, de Guise S, di Guardo G, Dobson A, Domingo M, Fauquier D, et al. 2014. Cetacean morbillivirus: Current knowledge and future directions. MDPI AG. *Viruses* 6:5145–5181.
- Visser IKG, Van Bresseem MF, De Swart RL, Van de Bildt MWG, Vos HW, Van der Heijden RWJ, Saliki JT, Orvell C, Kitching P, Kuiken T, et al. 1993. Characterization of morbilliviruses isolated from dolphins and porpoises in Europe. *J Gen Virol* 74:631–641.
- West KL, Sanchez S, Rotstein D, Robertson KM, Dennison S, Levine G, Davis N, Schofield D, Potter CW, Jensen B. 2013. A Longman’s beaked whale (*Indopacetus pacificus*) strands in Maui, Hawaii, with first case of morbillivirus in the central Pacific. *Mar Mammal Sci* 29:767–776.
- West KL, Silva-Krott I, Landrau-Giovannetti N, Rotstein D, Saliki J, Raverty S, Nielsen O, Popov VL, Davis N, Walker WA, et al. 2021. Novel cetacean morbillivirus in a rare Fraser’s dolphin (*Lagenodelphis hosei*) stranding from Maui, Hawai‘i. Nature Publishing Group UK. *Sci Rep* 11:1–13.
- Yang WC, Pang VF, Jeng CR, Chou LS, Chueh LL. 2006. Morbilliviral infection in a pygmy sperm whale (*Kogia breviceps*) from Taiwanese waters. *Vet Microbiol* 116:69–76.
- Yang WC, Wu BJ, Sierra E, Fernandez A, Groch KR, Catão-Dias JL, West K, Chan KW. 2016. A simultaneous diagnosis and genotyping method for global surveillance of cetacean morbillivirus. *Sci Rep* 6:30625.
- Zinzula L, Mazzariol S, Di Guardo G. 2021. Molecular signatures in cetacean morbillivirus and host species proteomes: Unveiling the evolutionary dynamics of an enigmatic pathogen? *Microbiol Immunol* 66(2), 52-58.

**6. ACKNOWLEDGMENTS / AGRADECIMIENTOS**



I primi ringraziamenti vanno a Toño, Eva e Cristina che mi hanno sostenuta in questo percorso complicato e non mi hanno mai fatto mancare il loro supporto, anche nei momenti più difficili, in cui le avversità mi parevano a tratti insormontabili.

Un importante grazie va a Carla, che mi ha sollevata da alcune attività lavorative, permettendomi di concentrarmi maggiormente sulle scadenze del dottorato.

Un grazie anche alle nostre ragazze in laboratorio: Lucia, Paola e Giulia che hanno lavorato per rispettare le mie scadenze, riuscendo ad incastrare al meglio queste attività con la routine.

Ritornando alle Canarie, un ringraziamento lo voglio dedicare a Raquel, Kita e Idaira per esserci sempre state quando avevo bisogno di ottenere informazioni su tempi e modalità del dottorato ed a Miguel, senza il cui aiuto non sarei riuscita a districarmi nei meandri della burocrazia.

Un grazie di cuore va a Diego, mio grande amico, per esserci stato sempre e a Francesca, la persona che più di tutte ha compreso con empatia le mie difficoltà e mi ha dato la forza per non mollare, grazie Amica!!

Con il cuore ringrazio anche Giovannino di Guardo, che fin dal principio mi ha sostenuta facendomi sempre pensare che ce l'avrei fatta, che sarei finalmente arrivata a questo punto.

In ultimo, ma non in quanto ad importanza, desidero ringraziare i miei genitori ed il mio compagno per avermi sempre supportata e aiutata in questo lungo percorso, anche accudendo Pietrino durante le mie assenze. Senza di voi non ce l'avrei mai fatta, grazie per aver reso possibile questo traguardo!!!

